FTD-ID(RS)T-0939-81

FOREIGN TECHNOLOGY DIVISION

ANTENNA

(Selected Articles)

Approved for public release;
distribution unlimited.

EDITED TRANSLATION

FTD-ID(RS)T-0939-81 3 December 1981

MICROFICHE NR: FTD-81-C-001080

ANTENNA (Selected Articles)

English pages: 100

Source: Antenny, Nr. 6, 1969, pp. 17-49; 106-162

Country of origin: USSR
Translated by: SCITRAN
F33657-81-D-0263
Requester: FTD/TQFE
Approved for public release; distribution unlimited.

Table of Contents

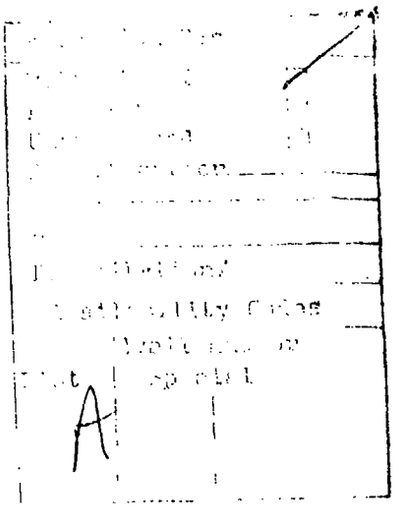

U. S. BOARD ON GEOGRAPHIC NAMES TRANSLITERATION SYSTEM

Block	Italic	Transliteration	Block	Italic	Transliteration
А а	*А а*	A, a	Р р	*Р р*	R, r
Б б	*Б б*	B, b	С с	*С с*	S, s
В в	*В в*	V, v	Т т	*Т т*	T, t
Г г	*Г г*	G, g	У у	*У у*	U, u
Д д	*Д д*	D, d	Ф ф	*Ф ф*	F, f
Е е	*Е е*	Ye, ye; E, e*	Х х	*Х х*	Kh, kh
Ж ж	*Ж ж*	Zh, zh	Ц ц	*Ц ц*	Ts, ts
З з	*З з*	Z, z	Ч ч	*Ч ч*	Ch, ch
И и	*И и*	I, i	Ш ш	*Ш ш*	Sh, sh
Й й	*Й й*	Y, y	Щ щ	*Щ щ*	Shch, shch
К к	*К к*	K, k	Ъ ъ	*Ъ ъ*	"
Л л	*Л л*	L, l	Ы ы	*Ы ы*	Y, y
М м	*М м*	M, m	Ь ь	*Ь ь*	'
Н н	*Н н*	N, n	Э э	*Э э*	E, e
О о	*О о*	O, o	Ю ю	*Ю ю*	Yu, yu
П п	*П п*	P, p	Я я	*Я я*	Ya, ya

*ye initially, after vowels, and after ъ, ь; e elsewhere.
When written as ё in Russian, transliterate as yё or ё.

RUSSIAN AND ENGLISH TRIGONOMETRIC FUNCTIONS

Russian	English	Russian	English	Russian	English
sin	sin	sh	sinh	arc sh	$\sinh^{-1}$
cos	cos	ch	cosh	arc ch	$\cosh^{-1}$
tg	tan	th	tanh	arc th	$\tanh^{-1}$
ctg	cot	cth	coth	arc cth	$\coth^{-1}$
sec	sec	sch	sech	arc sch	sech^{-1}
cosec	csc	csch	csch	arc csch	csch^{-1}

Russian	English
rot	curl
lg	log

SCATTERING OF A SPHERICAL WAVE ON TRUNCATED REVOLUTION BODIES

Yu. A. Yerukhimovich

Summary

A scattering field is analyzed on truncated revolution bodies formed by curves of the second order when they are irradiated from one focus by a source of a spherical wave. The analysis uses the method of curvilinear coordinates [1]. The solution is obtained in the distant zone, in approximation of physical optics. The system of formulas describes the diagram of the scattering field in all space, including the transitional zones between the regions of the angles of the observation point.

Int· duction

'ublication [1] presents a method for solving diffraction problems based on the introduction of a special system of curvilinear coordinates associated with the physical features of the phase structure of the field. In this case, the center of the emitted spherical wave and the observation point serve as the focal points for families of ellipsoids and hyperboloids which form two systems of coordinate surfaces. The third system of coordinate surfaces is half planes passing through a line which connects the focus and the observation point. The integral presentation of the diagram of the scattering field in this case acquires the simplest appearance.

In order to obtain a strict solution, it is necessary to know the exact quantity of the current which flows on both sides of the scattering surface. Since this is usually an indepedent complicated task, different approximate methods are used. This work has employed approximation of the physical optics, or according to the terminology of [2], it has assigned a "uniform" component of the current. By using the findings and technique [2], the next step can be taken to compute the marginal waves with regard for the "nonuniform" current component.

We will compute the diagram of the scattering field from the ideally conducting infinitely thin revolution body whose surface is formed by revolution of a curve of the second order

$$\rho = P_0 : (1 + \varepsilon \cos \psi) \qquad (1)$$

during its revolution around the axis z (fig. 1). Here ε--eccentricity, $P_0=(1+\varepsilon)f$. The revolution body is limited by the plane z= -OO'. The phase center of the source is located in the focal point of the curve of the second order, approaching its apex. The equations which link among themselves the Cartesian (x,y,z), spherical (R,θ,φ) and curvilinear coordinates (u, w, v) are presented in [1]. The mutual arrangement of the curves in the section of the studied surface with plane y=0 is shown in fig. 2a. The boundary curves are characterized by the values ε=0 (circle), ε=1 (parabola) and ε=∞ (straight line). The values ε<1 define the family of ellipses; ε>1 defines the family of hyperbolas.

As the analysis made below shows, the obtained solution can be

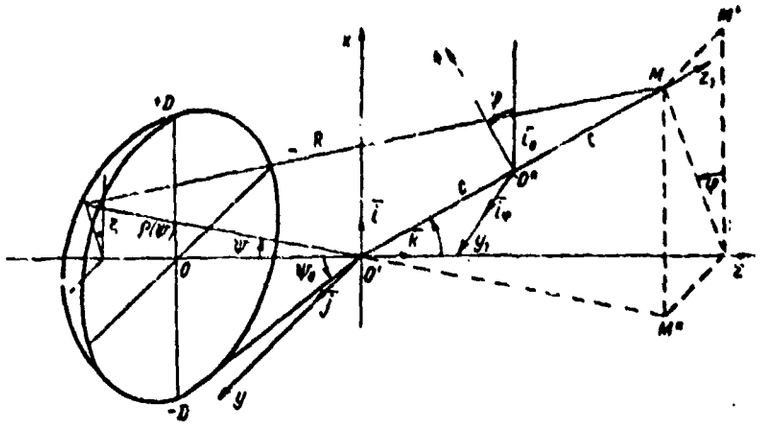

Figure 1.

extended to the case where the source is located in the distant focus of the curve. The changes that are needed in this case in the final expressions are indicated in the appropriate places. Figure 2b gives the mutual arrangement of th curves with the source in the distant focal point.

We will obtain an explicit appearance of the equation for the revolution body with curvilinear coordinates with arbitrary distance between the observation point and the focal point O'. It follows from fig. 1: $\rho\cos\psi = -z$, in relation to (1) this yields $\rho = P_0 + \varepsilon z$.

Publication [1] has obtained the following correlations for arbitrary z and ρ: $z = c[1+ch\ u\cos w)\cos\theta - sh\ u \sin u \sin\theta]$ and $\rho = c(chu+\cos w)$. By using the link between z and ρ by curve (1), we obtain the following appearance of the equation which describes the examined surfaces of the second order:

$$u_0^2 = \frac{P_0}{c}. \qquad (2)$$

For the distant zone of the field, the studied body is always located only in the second or third quadrants of the system of coordinates $z_1 O'' h$. In this case, in the initial relationships, the parameter w should be replaced by $\pi - w$ for the second quadrant and $\pi + w$ for the third [1]. The parameters u and w in the distant zone according to the modulus are much smaller than 1. Accordingly, we replace in (2)

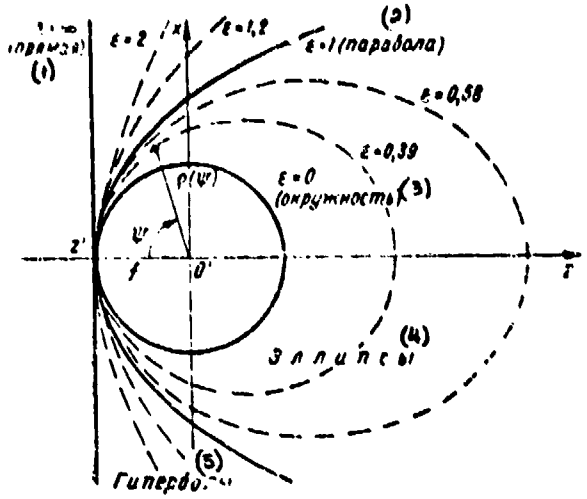

Figure 2a.
1--straight line; 2--parabola; 3--circle; 4--ellipses; 5--hyperbola

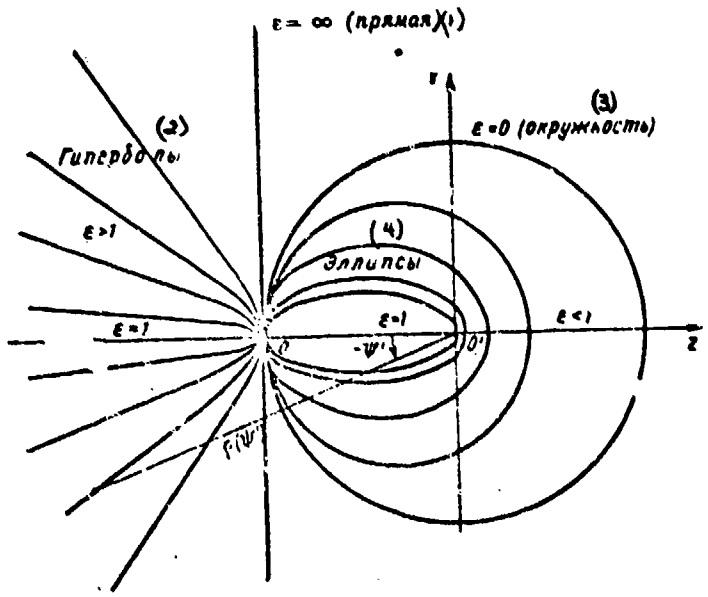

Figure 2b.
1--straight line; 2--hyperbolas; 3--circle; 4--ellipses

the trigonometric and hyperbolic functions with the first terms of their exponential expansions, assuming also that w becomes $\pi+w$. The terms of a higher order of smallness than the others are abandoned.

As a result of the computations we obtain an equation of the studied surfaces

$$F(u,w,v) = 2\varepsilon uw\sin\Theta\sin v + 2u_0^2 - u^2(1+\varepsilon\cos\Theta) - w^2(1-\varepsilon\cos\Theta) = 0, \quad (3)$$

by solving it in relation to u and w, we find:

$$u(1+\varepsilon\cos\Theta) = \varepsilon w\sin\Theta\sin v + \sqrt{2u_0^2(1+\varepsilon\cos\Theta) - w^2(1-\varepsilon^2+\varepsilon^2\sin^2\Theta\cos^2 v)}, \quad (4)$$

$$w(1-\varepsilon\cos\Theta) = \varepsilon u\sin\Theta\sin v \pm \sqrt{2u_0^2(1-\varepsilon\cos\Theta) - u^2(1-\varepsilon^2+\varepsilon^2\sin^2\Theta\cos^2 v)}. \quad (5)$$

The square root sign in (5) is changed in the transition through zero. The root is made equal to zero at the point of contact of the coordinate ellipsoid and the surface of the body. The sign before the root is selected from the condition that w is negative in the second quadrant of the coordinate system $z_1 0''h$ and positive in the third quadrant. The product wsin v always maintains the sign "plus".

The differential parameters of the task equal:

$$p = \frac{\partial w}{\partial u} = [u(1+\varepsilon\cos\Theta) - \varepsilon w\sin\Theta\sin v] : [w(1-\varepsilon\cos\Theta) - \varepsilon u\sin\Theta\sin v], \quad (6)$$

$$q = \frac{\partial w}{\partial v} = -[\varepsilon uw\sin\Theta\cos v] : [w(1-\varepsilon\cos\Theta) - \varepsilon u\sin\Theta\sin v]. \quad (7)$$

From (4)-(7) we find the necessary functional relationships:

$$\sqrt{q^2 + (1+p^2)\frac{u^2w^2}{u^2+w^2}} = uw\sqrt{\frac{4u_0^2}{u^2+w^2} + \varepsilon^2 - 1}\,[2u_0^2(1-\varepsilon\cos\Theta) - u^2(1-\varepsilon^2+\varepsilon^2\sin^2\Theta\cos^2 v)]^{-\frac{1}{2}},$$

$$\cos v = \frac{\sqrt{w^2-a_2^2}\sqrt{a_1^2-w^2}}{w(a_2+a_1)}.$$

The quantities $a_{1,2}$--values of the coordinates w with $v = \pm\frac{\pi}{2}$ equal: $a_{1,2}(1-\varepsilon\cos\Theta) = \varepsilon u\sin\Theta \pm \sqrt{2u_0^2(1-\varepsilon\cos\Theta) - u^2(1-\varepsilon^2)}$. The quantity β is identical to the value w on the edge of the mirror:

$$\beta^2 = \frac{2u_0^2}{1+\varepsilon\cos\psi_0} - u^2, \quad (8)$$

i.e., (8) is the equation for the edge in curvilinear coordinates. The condition $\beta=\alpha_{1,2}$ yields the value u on the edge of the mirror, in the section of it with plane y=0. By solving the corresponding quadratic equation, we find

$$u_{\pm}^2 = 2u_0^2 \frac{\cos^2 \frac{\theta \pm \psi_0}{2}}{1+\varepsilon\cos\psi_0}. \qquad (9)$$

By using (8), we also obtain

$$w_{\pm}^2 = 2u_0^2 \frac{\sin^2 \frac{\theta \pm \psi_0}{2}}{1+\varepsilon\cos\psi_0}.$$

The "plus" index corresponds to the upper point of the mirror edge, the "minus" to the lower.

The integral presentations of the diagram of the scattering field [1] for the given case has a different appearance depending on the combinations of integration variables.

The variables u,v:

$$E^0_{\theta,\varphi} = -i\frac{4kP_0}{\pi u_0^2}\int_{u_-}^{u_+} e^{-ikcu^2}\Psi_0(u)\,u\,du, \qquad (10)$$

where

$$\Psi_0(u) = \int_{v(u)}^{\frac{\pi}{2}} b_{\theta,\varphi}\frac{u\,dv}{\sqrt{2u_0^2(1-\varepsilon\cos\psi)-u^2(1-\varepsilon^2+\varepsilon^2\sin^2\psi\cos^2 v)}}.$$

Variables u,w:

$$E^0_{\theta,\varphi} = -i\frac{4kP_0}{\pi u_0^2}\int_{u_-}^{u_+} e^{-ikcu^2}\Phi_0(u)\,u\,du, \qquad (11)$$

where

$$\Phi_0(u) = \frac{1}{1-\varepsilon\cos\theta}\int_{\alpha(u)}^{\beta(u)} b_{\theta,\varphi}\frac{w\,dw}{\sqrt{w^2-a_2^2}\sqrt{a_1^2-w^2}}.$$

Here $b_{\theta,\varphi} = (\bar{I}_0\bar{i}_{\theta,\varphi})\,2\rho e^{ikp}\sqrt{\frac{4u_0^2}{u^2+w^2}+\varepsilon^2-1}$; $\bar{I}_0$ --uniform current component on the surface of the mirror, i.e., $\bar{I}_0=2[\bar{n}\bar{H}_0]$, $\bar{n}$--unit vector of the perpendicular to the surface of the mirror, $\bar{H}_0$--unperturbed value of the vector of magnetic field intensity of the emitter on the surface of the mirror;

$$\bar{l}_\varphi = -\bar{i}\sin\varphi + \bar{j}\cos\varphi, \quad \bar{l}_\theta = -\bar{i}\cos\theta\cos\varphi + \bar{j}\cos\theta\sin\varphi - \bar{k}\sin\theta.$$

As the emitter we will examine a system made of elementary electric and magnetic dipoles with equal moments, oriented by the x-axis (electric dipole) and the y-axis (magnetic dipole). This emitter is equivalent to the . flare element of the horn emitter. The center of the emitted spherical wave is coincident with the focal point O'. In this case

$$\bar{E}_0 = 2T(\theta, \varphi)\frac{e^{-ikR_0}}{R_0}(\bar{l}_\theta\cos\varphi + \bar{l}_\varphi\sin\varphi),$$

$$T(\theta, \varphi) = T_0(\theta, \varphi)(1-\cos\theta), \quad \bar{E}_0 = \bar{E}^0\frac{e^{-ikR_0}}{R_0}; \qquad (12)$$

$$\bar{H}_0 = 2T(\psi, \xi)\frac{e^{-ik\rho}}{\rho}[\bar{i}(1+\cos\psi)\sin\xi\cos\xi -$$
$$-\bar{j}(\cos^2\xi + \sin^2\xi\cos\psi) - \bar{k}\sin\psi\sin\xi]; \qquad (13)$$

$T_0(\theta,\phi)$--"scalar" diagram of emitter. The vector components perpendicular to the curve of the second order equal:

$$n_x = -\cos\xi\cos\varkappa, \quad n_y = -\sin\xi\cos\varkappa, \quad n_z = \sin\varkappa, \quad \operatorname{tg}\varkappa = \frac{\varepsilon+\cos\psi}{\sin\psi},$$

$\varkappa$--angle compiled by the tangent to the curve with axis z.

After simple but cumbersome computations we find:

$$\bar{I}_0 = 2T(\psi, \xi)\left\{\bar{i}[\sin\varkappa\cos^2\xi + \sin^2\xi\sin(\varkappa+\psi)] - \right.$$
$$\left. -\bar{j}\sin 2\xi\sin\frac{\psi}{2}\cos\left(\varkappa+\frac{\psi}{2}\right) + \bar{k}\cos\xi\cos\varkappa\right\}\frac{e^{-ik\rho}}{\rho}, \qquad (14)$$

$$b_\theta = 2T(\psi, \xi)\left\{\left[(1+\varepsilon)\cos\varphi\cos^2\frac{\psi}{2} - (1-\varepsilon)\sin^2\frac{\psi}{2}\cos(2\xi-\varphi)\right]\times\right.$$
$$\left.\times\cos\theta - \cos\xi\sin\theta\sin\psi\right\}, \qquad (15)$$

$$b_\varphi = -2T(\psi, \xi)\left[(1+\varepsilon)\sin\varphi\cos^2\frac{\psi}{2} + (1-\varepsilon)\sin^2\frac{\psi}{2}\sin(2\xi-\varphi)\right]. \qquad (16)$$

The formulas linking the curvilinear coordinates with the angles ψ and ξ are produced by (8) with replacement of β by w and by the expression

$$\operatorname{tg}\xi = \frac{[(w^2-u^2)\cos\theta + 2uw\sin\theta\sin\upsilon]\sin\varphi + 2uw\cos\upsilon\cos\varphi}{[(w^2-u^2)\cos\theta + 2uw\sin\theta\sin\upsilon]\cos\varphi - 2uw\cos\upsilon\sin\varphi}. \qquad (17)$$

Analysis shows that depending on the position of the observation point in space, the structure of the scattered field changes. For

convenience of the computations it is expedient to divide the space into a number of regions linked to the geometry of the mirror and the position of the observation point. Figures 3 and 4 show the division of the space for curves of hyperbolic and elliptical types respectively. In each of the isolated spaces, the section of the body surface with Fresnel's zones has a different nature. The analytical presentation of the field also differs.

Field in Illuminated Region of Space

In this region, a coordinate ellipsoid is always found which passes through the observation point and touches the surface of the body at a certain point. The contact condition $p^{-1}\Big|_{\theta=\frac{\pi}{2}} = 0$.

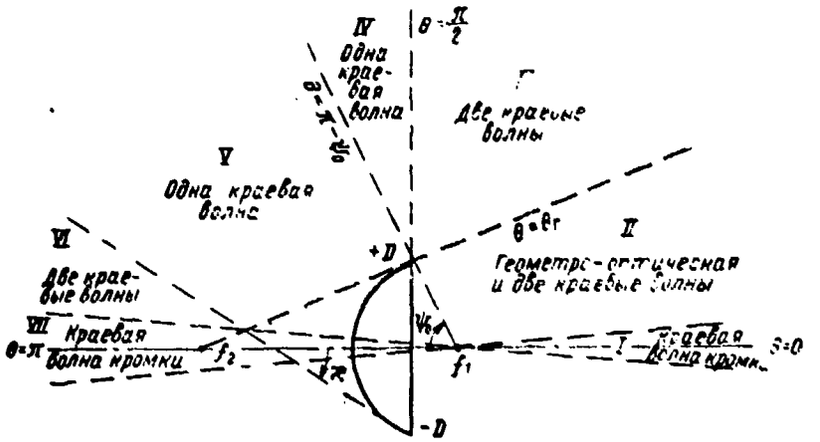

Figure 3.

I--Marginal wave of edge; II--Geometrical-optical and two marginal waves; III--Two marginal waves; IV--One marginal wave; V--One marginal wave; VI--Two marginal waves; VII--Marginal wave of edge.

In addition, at the contact point the square root in the definition of w becomes zero. From here we find

$$\operatorname{ch} u_k = \frac{1}{\varepsilon^2-1}\left[\pm\sqrt{(\varepsilon^2-1)^2+2u_0^2\varepsilon(\varepsilon^2-1)\cos\theta+\varepsilon^2u_0^4}-u_0^2\right], \quad (18)$$

$$\operatorname{tg} w_k = \frac{\varepsilon \operatorname{sh} u_k \sin\theta}{1-\varepsilon \operatorname{ch} u_k \cos\theta}.$$

The "plus" sign corresponds to the curves of the hyperbolic type, the

"minus" to the elliptical. The value $\varepsilon=1$ is boundary. By expanding the square root in (18) into a series and by limiting ourselves to the first terms, we find the following ratio which is correct for all ε:

$$u_k^2 = 2u_0^2 \frac{\varepsilon\cos\theta - 1 + \frac{\varepsilon u_0^2}{\varepsilon+1}}{\varepsilon^2 - 1 + \varepsilon u_0^2},$$

$$w_k^2 = 2u_0^2 \frac{\varepsilon^2\sin^2\theta}{(\varepsilon\cos\theta-1)^3} \frac{\left(\varepsilon\cos\theta - 1 + \frac{\varepsilon u_0^2}{\varepsilon+1}\right)(\varepsilon^2 - 1 + \varepsilon u_0^2)}{[\varepsilon^2 - 1 + \varepsilon u_0^2(1+\cos\theta)]^2}. \quad (19)$$

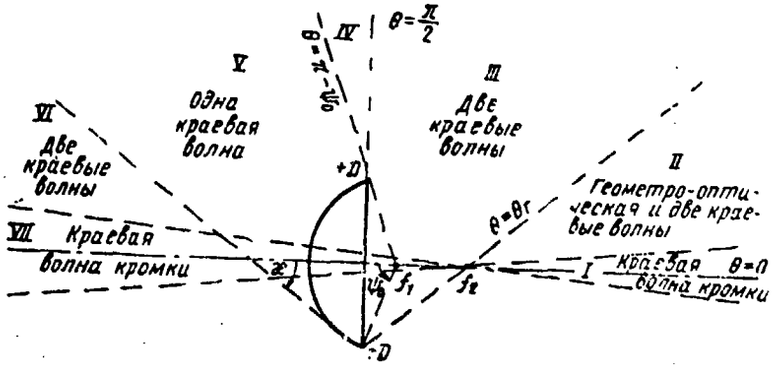

Figure 4.
I--Marginal wave of edge; II--Geometrical-optical and two marginal waves; III--Two marginal waves; V --One marginal wave; VI--Two marginal waves; VII--Marginal wave of edge.

The scattering field with values $\varepsilon\approx1$ (surface of the body is close to a paraboloid) in the narrow region of angles $\theta \sim 0$ must be analyzed separately. This is associated with the fact that with small values of the θ angle, the entire surface of the mirror lies in limits of one-two zones of Fresnel, therefore the contribution to the field from each point of the surface of the mirror is significant. Analysis with $\varepsilon=1$ was made in publication [8]. Accordingly, the case $\varepsilon^2-1\sim u_0^2$ with $\theta\sim0$ is excluded from the examination. For all the other values of the angle of the observation point, the obtained results are correct with $\varepsilon=1$ as well. Then from (8) and (19) for the contact point, we obtain the following relationships:

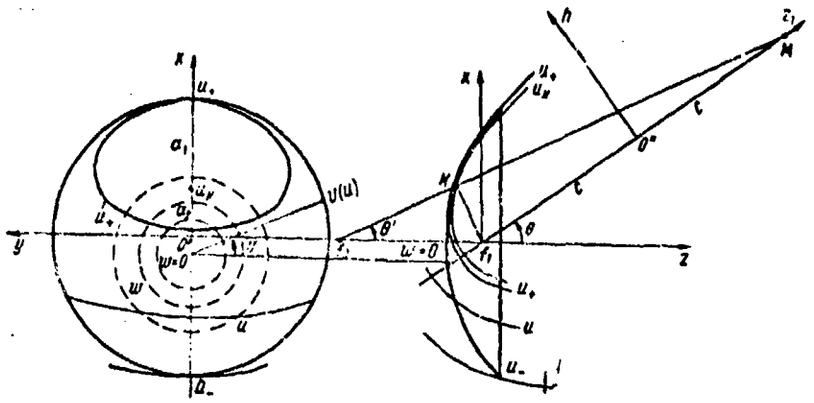

Figure 5.

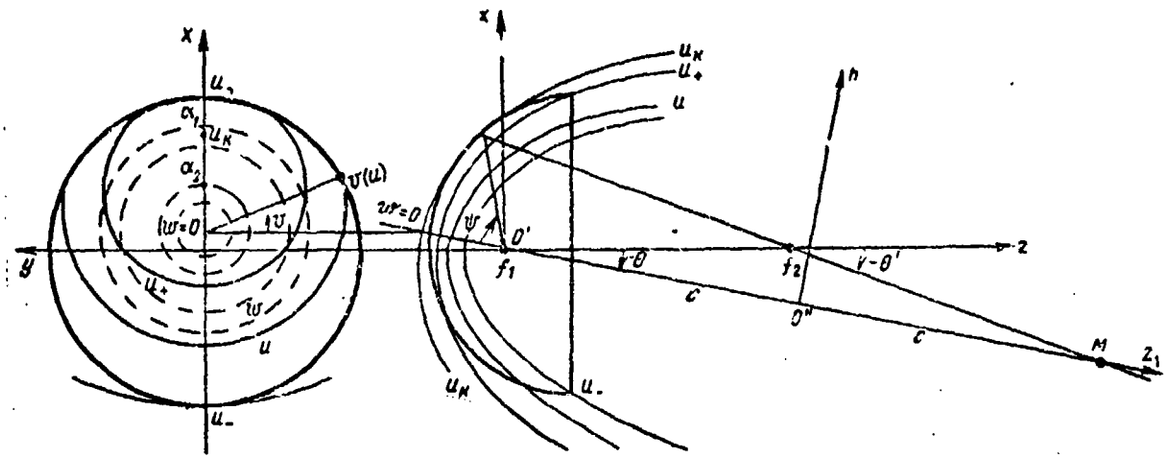

Figure 6.

$$\operatorname{tg}\frac{\theta_k}{2}=\frac{\varepsilon-1}{\varepsilon+1}\operatorname{tg}\frac{\psi_k}{2};\quad \sin\psi_k=\frac{(\varepsilon^2-1)\sin\theta}{\varepsilon^2+1-2\varepsilon\cos\theta};$$

$$\cos\psi_k=\frac{(\varepsilon^2+1)\cos\theta-2\varepsilon}{\varepsilon^2+1-2\varepsilon\cos\theta}.$$

The angle θ' (fig. 5,6) is linked to the angle of observation θ by the correlation $\sin(\theta'-\theta)=u_0^2\frac{\varepsilon\sin\theta}{1-\varepsilon^2}$. In the distant zone of the field, the difference between these angles is negligible.

It is easy to obtain from the geometry of the task, a link between the angles θ' and ψ. This relationship looks like

$$\operatorname{tg}\frac{\theta'}{2}=\frac{\varepsilon-1}{\varepsilon+1}\operatorname{tg}\frac{\psi}{2}, \qquad (20)$$

i.e., is identical to the expression obtained above for the contact point. This identity characterizes the known property of the curves of the second order which can be formulated as follows: if a wave with spherical wave front is emitted from one focal point on the surface formed by a curve of the second order, then after reflection from this surface, a new wave is formed also with spherical front, but with center in the second focal point (real for $\varepsilon<1$ or imaginary for $\varepsilon>1$).

In order to write the integral presentation of the field diagram we will examine figs. 5 and 6. The right side of fig. 5 and 6 shows the pattern of curvilinear coordinates in the xz plane for curves of hyperbolic and elliptical types respectively. On the left side, it is the same in the xy plane. As is apparent from the figures, for values of the parameter u which lie in the intervals u_k-u_+ (hyperbolic curves) or u_+-u_k (elliptical curves), the intersection line of the arbitrary coordinate ellipsoid with the surface of the mirror is a closed curve. Consequently, the Fresnel zones in this case are ring-shaped. The ellipse with the same value of u intersects the x-axis twice: above the point of contact and below it. According to this, the interval of change in the parameter w is α_1-α_2, where $\alpha\equiv w$ on the x-axis with $w\geq w_k$, and $\alpha_2\equiv w$ on the x-axis with $w\leq w_k$.

On the remaining part of the mirror, the lines u=const are not closed. The corresponding Fresnel zones are presented in the form of bands which rest with their edges on the edge of the mirror. The interval of change in the parameter w with fixed u: α_2-β.

The integral presentation of the field diagram is used in the form of (11). In the first interval, the limits of change for u: u_k-u_+, for w: α_1-α_2. In this case $a_{1,2}(1-\varepsilon\cos\theta)=\varepsilon u\sin\theta\pm\sqrt{(1-\varepsilon^2)(a_k^2-u^2)}$. In the second interval, u changes in the interval u_--u_+; w--in the interval α_2-β. As a consequence of the symmetry of the problem, we will do the integration for one half of the mirror (for example, the right in fig. 5,6), then doubling the obtained result. We will introduce the normed variables of integration. In the integral corresponding to the Fresnel zones in the form of rings, we assume: a) curves of the hyperbolic type ($\varepsilon>1$):

$$u^2 = u_k^2 - (u_k^2 - u_+^2)\,s^2 = \frac{2u_0^2[1+\varepsilon\cos\psi_0)(\varepsilon\cos\theta - 1) - a_3 s^2]}{(1+\varepsilon\cos\psi_0)(\varepsilon^2 - 1 + \varepsilon u_0^2)}\ ; \quad (21a)$$

$$w^2 = \alpha_2^2 + (\alpha_2^2 - \alpha_1^2)\,\mu^2,$$

$$a_3 \approx \left(\varepsilon \sin\frac{\psi_0 - \theta}{2} - \sin\frac{\theta + \psi_0}{2}\right)^2;$$

$$\alpha_2^2 - \alpha_1^2 = \frac{4\varepsilon u \sin\theta}{(1-\varepsilon\cos\theta)^2}\sqrt{(1-\varepsilon^2-\varepsilon u_0^2)(u_k^2 - u^2)};$$

b) curves of the elliptical type ($\varepsilon<1$):

$$u^2 = u_k^2 - (u_k^2 - u_+^2)\,s^2 = \frac{2u_0^2}{(1+\varepsilon\cos\psi_0)(1-\varepsilon^2+\varepsilon u_0^2)} \times$$

$$\times [(1+\varepsilon\cos\psi_0)(1-\varepsilon\cos\theta) - a_3 s^2]; \quad (21b)$$

$$w^2 = \alpha_1^2 + (\alpha_2^2 - \alpha_1^2)\,\mu^2; \quad a_3 = \left(\sin\frac{\theta - \psi_0}{2} + \varepsilon\sin\frac{\theta + \psi_0}{2}\right)^2.$$

We note that the transition from curves of the hyperbolic type to curves of the elliptical type in the obtained relationships is made by mutual replacements of $\varepsilon \to 1 \leftarrow 1-\varepsilon$ and $\alpha_2 \rightleftarrows \alpha_3$. Therefore, further analysis is only made for hyperbolic curves. In the integral for the bands, we replace:

$$u^2 = u_+^2 + (u_-^2 - u_+^2)\,t^2 = \frac{2u_0^2}{1+\varepsilon\cos\psi_0}(a + bt^2); \quad w^2 = \alpha_2^2 + (\beta^2 - \alpha_2^2)z^2, \quad (22)$$

$$a = \cos^2\frac{\theta + \psi_0}{2}; \quad b = \sin\theta\sin\psi_0; \quad a + b = \cos^2\frac{\theta - \psi_0}{2}.$$

On the edge of the mirror:

$$\beta^2 = \frac{2u_0^2}{1+\varepsilon\cos\psi_0}(a_1 - bt^2); \quad a_1 = \sin^2\frac{\theta + \psi_0}{2}; \quad a_1 - b = \sin^2\frac{\theta - \psi_0}{2}; \quad (23)$$

$$\cos v(t) = \xi_0(t)\,t\sqrt{1-t^2}; \quad \xi_0(t) = \frac{\sin\psi_0}{\sqrt{a+bt^2}\sqrt{a_1 - bt^2}}.$$

A sample pattern of the introduced normed coordinates in the projection on the xy plane is shown in fig. 7a,b. Now we can write:

$$E^0_{\theta,\varphi} = L_1 + L_2; \; L_1 = i\frac{2}{\pi}\gamma_1 e^{-ikcu_k^2}\int_0^1 e^{i\gamma_1 s^2}\,\Phi(s)\,s\,ds; \quad (24)$$

$$L_2 = -i\frac{2}{\pi}\gamma\, e^{-ikcu_+^2}\int_0^1 e^{-i\gamma t^2}\,\Phi_1(t)\,t\,dt,$$

where

$$\Phi(s)=\frac{1}{1-\varepsilon\cos\theta}\int_0^1 b_{\theta,\varphi}\frac{d\mu}{\sqrt{1-\mu^2}};\quad \Phi_1(t)=\frac{1}{1-\varepsilon\cos\theta}\int_0^1 b_{\theta,\varphi}\frac{x_0\,dz}{\sqrt{1-x_0^2z^2}};$$

$$x_0=\sqrt{\frac{\beta^2-\alpha_1^2}{\alpha_2^2-\alpha_1^2}};\quad \gamma=2kD\sin\theta;\quad \gamma_1=\gamma\frac{n_0}{(\varepsilon^2-1+\varepsilon u_0^2)\,b};$$

$$D=\frac{p_0\sin\psi_0}{1+\varepsilon\cos\psi_0};$$

L_1--contributes to the field from ring-shaped Fresnel's zones, L_2--from the Fresnel zone in the form of bands.

With a value $\theta=\theta_r$, where $\operatorname{tg}\frac{\theta_r}{2}=\frac{\varepsilon+1}{\varepsilon-1}\operatorname{tg}\frac{\psi_0}{2}$, the area of the ring-shaped Fresnel zones is contracted towards zero, and L_1 becomes zero. This circumstance determines the boundaries of action of relationships (24): $0\leq\theta\leq\theta_r$. The interval of applicability of the obtained formulas will further be presented in braces , after the designation of the field component, for example: $E^0_{\theta,\varphi}\{0-\theta_r\}$. We should now compute the integrals included in (24). In this case it is expedient to limit ourselves to terms on the order $\frac{1}{\sqrt{2kP_0}}$ as compared to 1, since the correctness of the terms of higher order of smallness cannot be guaranteed by the initial approximation of the physical optics.

The nature of the dependence of the integrals in (24) on the large parameters of the task is determined by the functions $\Phi(s)$ and $\Phi_1(t)$, therefore, one should first clarify the nature of the change in these functions from the variables s and t.

We will clarify the nature of behavior of the function $\Phi(s)$ depending on the variable s. It is simple to show that

$$\cos v=2\frac{\sqrt{u^2-\alpha_1^2}\sqrt{\alpha_2^2-u^2}}{u(\alpha_2^2-\alpha_1^2)(1-\varepsilon\cos\theta)};\quad (1-\varepsilon^2)(u_2^2-u^2)=2s\gamma\sqrt{1-\mu^2}\sqrt{a_2}\chi,$$

where

$$\chi=\sqrt{\varepsilon^2-1}\{\varepsilon^2\sin^2\theta(\varepsilon\cos\theta-1)(1+\varepsilon\cos\psi_k)-(1-\varepsilon^2+\varepsilon^2\sin^2\theta)a_2s^2-$$

$$-2\sqrt{a_2}s(1-2\varepsilon^2)\varepsilon\sin\theta\sqrt{(\varepsilon^2-1)[(\cos\theta-1)(1+\varepsilon\cos\psi_k)+a_2s^2]}\}^{-\frac{1}{2}}.$$

It follows from here that $\Phi(s)$ is the function of the combination of variables $s\sqrt{a_2}$. This function can be expanded into an exponential

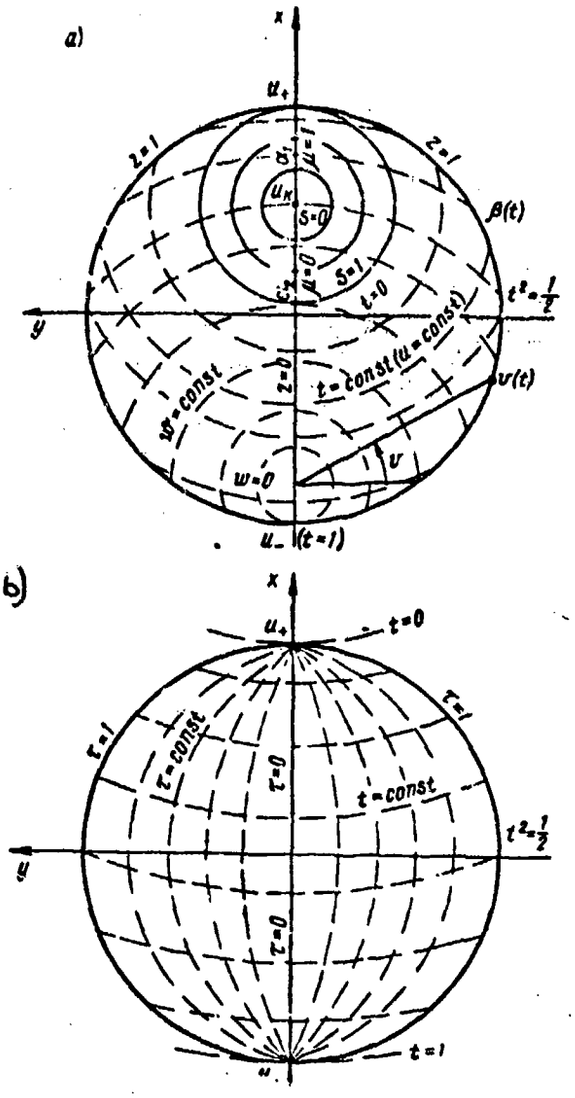

Figure 7.

Taylor series with variable $s\sqrt{a_2}$ close to the value s=0:

$$\Phi(s) = \Phi(0) + s\sqrt{a_2}\Phi'(0) + \ldots \qquad (25)$$

Here

$$\left.\frac{d^n}{dp^n}\left(\frac{1}{\sqrt{1-p^2}}\right)\right|_{p=0} = \frac{2}{\pi}\int_0^{\pi}\frac{\partial}{\partial\alpha}\left(\frac{1}{\sqrt{1-\cos\theta\cos\alpha}}\right)\cos n\alpha\, d\alpha = \Phi(0),$$

$$\left.\frac{d^n}{dp^n}\left(\frac{1}{\sqrt{1-p^2}}\right)\right|_{p=0} = \frac{2}{\pi}\int_0^{\pi}\frac{\cos n\alpha}{\sqrt{1-\cos\theta\cos\alpha}}\,d\alpha = \Phi(0)$$

etc.

The function $b_{\theta,\phi}$ was written above in an explicit form [formulas (15) and (16)] depending on the variables ψ and ξ. These variables are associated with s by the correlations:

$$\cos^2\frac{\psi}{2}=\frac{(\varepsilon-1)(u^2+w^2)+2u_0^2}{2\varepsilon(u^2+w^2)};\quad \cos\xi=\frac{A\cos\varphi-B\sin\varphi}{\sqrt{A^2+B^2}};$$

$$A=\frac{u^2+w^2-2u_0^2}{2\varepsilon};$$

$$B=uw\cos v;$$

$$\cos(2\xi-\varphi)=\frac{(A^2-B^2)\cos\varphi-2AB\sin\varphi}{A^2+B^2};$$

$$\sin(2\xi-\varphi)=\frac{(A^2-B^2)\sin\varphi+2AB\cos\varphi}{A^2+B^2}.$$

At the contact point (s=0) $\psi=\psi_k$, $\xi=\phi$. By substituting these expressions into $\Phi(0)$ and by integrating for μ, we find:

$$\Phi(0)=-\frac{\pi}{2}2T(\psi_k,\varphi)\frac{\varepsilon^2-1}{\varepsilon^2+1-2\varepsilon\cos\theta}l_{\theta,\varphi};\quad l_\theta=\cos\varphi;\quad l_\varphi=-\sin\varphi.$$

Further,

$$\frac{\partial}{\partial s\sqrt{a_s}}b_{\theta,\varphi}\Big|_{s=0}=\frac{\partial b_{\theta,\varphi}}{\partial\psi_k}\left(\frac{\partial\psi}{\partial u}\frac{\partial u}{\partial s\sqrt{a_s}}+\frac{\partial\psi}{\partial w}\frac{\partial w}{\partial s\sqrt{a_s}}\right)_{s=0}+$$

$$+\frac{\partial b_{\theta,\varphi}}{\partial\xi}\left(\frac{\partial\xi}{\partial u}\frac{\partial u}{\partial s\sqrt{a_s}}+\frac{\partial\xi}{\partial\cos v}\frac{\partial\cos v}{\partial s\sqrt{a_s}}\right)_{s=0}.$$

But $\left.\frac{\partial u}{\partial s\sqrt{a_s}}\right|_{s=0}=0$. The terms which are proportional to $\left.\frac{\partial w}{\partial s\sqrt{a_s}}\right|_{s=0}=-2\sqrt{\frac{2u_0^2}{1+\varepsilon\cos\psi_0}}(\varepsilon\cos\theta-1)(1-2\mu^2)$, are also equal to zero. This is associated with the nullification in this case of the integral for the variable μ.

By fulfilling the operations of differentiation, and by assuming in the final expressions s=0, and by integrating for μ, we find as a result

$$\Phi'(0)=-\frac{2}{(\varepsilon^2+1)\cos\theta-2\varepsilon}\sqrt{\frac{(\varepsilon^2-1)(\varepsilon\cos\theta-1)}{1+\varepsilon\cos\psi_0}}\times$$

$$\times\left[2\frac{\partial T(\psi_k,\varphi)}{\partial\varphi}(1+\varepsilon\cos\psi_k)l_{\theta,\varphi}-2T(\psi_k,\varphi)(1-\varepsilon)(1+\cos\psi_k)l_{\varphi,\theta}\right].$$

The intermediate computations which are necessary to obtain the described relationship are omitted here because of their elementary nature.

The derivatives of higher orders can be computed in a similar manner. Further we should substitute (25) into the first integral (24). The integrals for s are expressed through known functions, and each subsequent result of integrating series (25) is an order smaller than the previous. In that case where the "large" parameter of this integral γ_1 proportional to a_2 approaches zero (which occurs on the boundary of the region with $\theta \to \theta_r$), all the terms in series (25) approach zero, except for the first. These features of the obtained expansion $\phi(s)$ show that the greatest contribution to the field is made by the circle of the contact point, and consequently, the expansion into a series near this point is physically justified. In this case there is a possibility of somewhat simplifying further calculations, taking into account that the boundary line $u=u_+$ between both integrals in (24) is common, and the values of the results of integration coincide on it. We will therefore take each of the integrals in (24) once by parts. The values on the line $u=u_+$ are mutually nullified. We obtain:

$$E^0_{\theta,\varphi} = E^{\text{го}}_{\theta,\varphi} + E^{\text{крае}}_{\theta,\varphi};$$

$$E^{\text{го}}_{\theta,\varphi} = \frac{1}{\pi}\Phi(0)\,e^{-i\,kcu_k^2} - \frac{1}{\pi}e^{-i\,kcu_k^2}\int_0^1 e^{-iV_1 s^2}\frac{\partial\Phi(s)}{\partial s}\,ds; \qquad (26)$$

$$E^{\text{крае}}_{\theta,\varphi} = -\frac{1}{\pi}e^{-i\,kcu_+^2}\int_0^{\infty} e^{-iVt^2}\frac{\partial\Phi_1(t)}{\partial t}\,dt. \qquad (27)$$

Here $E^{\text{го}}_{\theta,\phi}$ expresses the field in the "geometro-optical" sense, since with $\lambda \to 0$ in (26) the first term does not disappear and is precisely equal to the "geometro-optical"field [4]. As will be shown below, $E^{\text{крае}}_{\theta,\phi}$ corresponds in nature of the field to the "marginal" waves.

Based on the obtained correlations, it is easy to compute the value $E^{\text{го}}_{\theta,\phi}$. After integration for s with regard for the equality

$$\int_0^1 e^{iV_1 s^2}\,ds = \sqrt{\frac{\pi}{2\gamma_1}}\,[C(\gamma_1) + iS(\gamma_1)],$$

where C(x) and S(x)--corresponding Fresnel integrals [3], we obtain

$$E^{\text{го}}_{\theta,\varphi}(0 \div \theta_r) = (E_1 + E_2)\, e^{-i\,kcu_k^2} I_{\theta,\varphi} + E^{\text{кп}}_{\theta,\varphi}\, e^{-i\,kcu_k^2} I_{\theta,\varphi}. \qquad (28)$$

where

$$E_1 = T(\psi_k, \varphi)\,\frac{\sin\psi_k}{\sin\theta};$$

$$E_2 = 2\,\frac{\partial T(\psi_k, \varphi)}{\partial\varphi}\,\frac{(\varepsilon^2-1)^{3/2}\,(\varepsilon\cos\theta-1)^{3/2}\,[C(\gamma_1)+iS(\gamma_1)]}{\sqrt{\pi\,kP_\theta}\,[(\varepsilon^2+1)\cos\theta-2\varepsilon]^2}.$$

In addition,

$$E^{\text{кп}}_{\theta,\varphi} = -\,\Gamma_\theta(\psi_k, \varphi)\sin\theta\,\frac{(\varepsilon-1)^2\sqrt{(\varepsilon^2-1)(\varepsilon\cos\theta-1)}}{[(\varepsilon^2+1)\cos\theta-2\varepsilon]^2}\,\frac{C(\gamma_1)+iS(\gamma_1)}{\sqrt{\pi\,kP_\theta}}. \qquad (28a)$$

Formula (28) shows that the geometro-optical wave E_1 whose amplitude does not have a frequency relationship, can be viewed as the first approximation. The amplitude of this wave repeats the nature of the diagram of the emitter depending on the angles ψ and ϕ. The component E_2 which has a frequency relationship is a correction for the geometro-optical field. This correction is also linked to the contact point. Its amplitude depends on the degree of nonsymmetry of the emitter diagram for the angle ϕ. The diagram of the emitter may also be nonaxisymmetrical since until now this circumstance was not a restriction on the analysis. The correcting wave has the contact point as its "source."

The quantity $E^k_{\theta,\phi}$ characterizes the cross-polarization component of the field which is also associated with reflection of rays at the contact point. This component has a frequency dependence and becomes zero at $\theta=0$ (as a consequence of symmetry of the mirror) and with $\theta=\theta_r$ (in light of the nullification of L_1). With $\varepsilon=1$ (paraboloid) the cross-correlation component is also missing (the current line does not have a y-component).

To completely characterize the field in the region $0\text{-}\theta_r$ we should also examine the component (27) since precisely this component must "extinguish" the action of the geometro-optical wave on the boundary of the region.

In a similar manner we first determine the explicit form of $\Phi_1(t)$. We expand the function $b_{\theta,\phi}$ into an exponential Taylor series for z^2 near $z=1$ (fig. 7, edge of mirror), after which we integrate the

obtained series for z. We find

$$\Phi_1(t) = \frac{1}{1-\varepsilon\cos\theta}\left[b^{\text{кр}}_{\theta,\varphi}(t)\arcsin x_0 - \frac{x_0 - \arcsin x_0}{2x_0}\frac{\partial}{\partial z^2}b_{\theta,\varphi}\Big|_{z=1} + \ldots\right].$$

Here in order to simplify the analysis, we introduced the restriction that $b^{\text{кр}}_{\theta,\phi}$ does not depend on z. This is equivalent to the hypothesis that the diagram of the emitter $T(\psi,\varphi)$ is axisymmetrical, i.e., depends only on the angle ψ. According to (17) we have on the edge of the mirror:

$$\operatorname{tg}\xi = \frac{(1-2t^2)\sin\varphi + 2t\sqrt{1-t^2}\cos\varphi}{(1-2t^2)\cos\varphi - 2t\sqrt{1-t^2}\sin\varphi};$$

$$e^{-i(2\xi-\varphi)} = (1-8t^2+8t^4+i4t\sqrt{1-t^2})e^{i\varphi}.$$

By substituting this definition of ξ and $\psi=\psi_0$ into (15) and (16), we obtain

$$b^{\text{кр}}_{\theta}(t) = 2T(\psi_0,t)\left\{\cos\varphi\left[\varepsilon\cos\theta + \cos(\theta+\psi_0) + 8(1-\varepsilon)\sin^2\frac{\psi_0}{2}\times\right.\right.$$
$$\left.\times\cos\theta\, t^2(1-t^2) + 2t^2\sin\theta\sin\psi_0\right] + \sin\varphi\left[\sin\theta\sin\psi_0\, 2t\sqrt{1-t^2} +\right.$$
$$\left.\left. + (1-\varepsilon)\sin^2\frac{\psi_0}{2}\cos\theta\, 4t\sqrt{1-t^2}(1-2t^2)\right]\right\};$$

$$b^{\text{кр}}_{\varphi}(t) = -2T(\psi_0,t)\left\{\sin\varphi\left[1+\varepsilon\cos\psi_0 - (1-\varepsilon)\sin^2\frac{\psi_0}{2}8t^2(1-t^2)\right] +\right.$$
$$\left. + 4(1-\varepsilon)\sin^2\frac{\psi_0}{2}t\sqrt{1-t^2}(1-2t^2)\cos\varphi\right\}. \qquad (29)$$

Since

$$\frac{\partial b_{\theta,\varphi}}{\partial z^2}\Big|_{z=1} = \frac{x_0^2(a_1^2-a_2^2)(1+\varepsilon\cos\psi_0)}{2a_0^2\varepsilon b}\left\{\frac{1+\varepsilon\cos\psi_0}{\sin\psi_0}\frac{\partial b_{\theta,\varphi}}{\partial\psi} -\right.$$
$$\left. - \sqrt{\frac{a+bt^2}{a_1-bt^2}}\frac{2(a_1-bt^2)+\varepsilon\cos\psi_0}{\cos^2\psi_0 + 4(a+bt^2)(a_1-bt^2)\cos\vartheta(t)}\frac{\partial b_{\theta,\varphi}}{\partial\xi}\right]_{\text{кр}},$$

then one can find the following term of the expansion $\Phi_1(t)$ etc. in the explicit form. The quantity x_0 that is included here equals:

$$x_0^2 = \frac{\sqrt{a+bt^2}\sqrt{a_2+b't^2} + \sqrt{a_2-t^2\sin^2\psi_0}(\varepsilon-\cos\vartheta)}{2\sqrt{a+bt^2}\sqrt{a_2+b't^2}};$$
$$b' = (\varepsilon^2-1)b;\quad x_0(0)=1;\quad x_0(1)=0.$$

Now (26) adopts the appearance

$$E^{\text{кр}}_{\theta,\varphi} = -\frac{1}{\pi}\frac{e^{-i\,kcu^2_+}}{1-\varepsilon\cos\theta_0}\int_0^1 e^{-i\gamma t^2}\frac{\partial}{\partial t}\left[b^{\text{кр}}_{\theta,\varphi}\arcsin x_0 - \right.$$

$$\left. - \frac{x_0 - \arcsin x_0}{2x_0}\left(b^{\text{кр}}_{\theta,\varphi}\right)'_t + \ldots\right]dt.$$

It is sufficient to be limited only to the first term in the brackets. The following terms of the expansion provide a correction for the negigible order of smallness, of which we can be convinced by direct integration by parts. For similar considerations we should abandon the term $\frac{\partial b^{\text{кр}}_{\theta,\varphi}}{\partial t}\arcsin x_0$ (we recall that $\partial/\partial t$ must be fulfilled with regard for the dependence of $b_{\theta,\phi}$ on $\psi(t)$ and $\xi(t)$, direct application of this operator to $b^{\text{кр}}_{\theta,\phi}$ is unlawful). By differentiating, we also find

$$\frac{\partial}{\partial t}\arcsin x_0 = \frac{\sin\psi_0(1-\varepsilon\cos\theta)}{\sqrt{1-t^2}}\left(\frac{A'\sqrt{a}}{a+bt^2} - \frac{A''\sqrt{a_2}}{a_2+b't^2}\right). \qquad (30)$$

In this case,

$$A' = \sqrt{a+b}:\left[\sqrt{a(a_2+b')} - \sqrt{a_2(a+b)}\right];$$

$$A'' = \sqrt{a_2+b'}:\left[\sqrt{a(a_2+b')} - \sqrt{a_2(a+b)}\right].$$

With regard for what has been said, we obtain

$$E^{\text{крест}}_{\theta,\varphi} = \frac{2}{\pi}\sin\psi_0 e^{-i\,kcu^2_+}\int_0^1 e^{-i\gamma t^2} b^{\text{кр}}_{\theta,\varphi}\left(\frac{A'\sqrt{a}}{a+bt^2} - \frac{A''\sqrt{a_2}}{a_2+b't^2}\right)\frac{dt}{\sqrt{1-t^2}} + 0\left(\frac{1}{\gamma}\right). \qquad (31)$$

With $\gamma >> 1$, the terms of the required order are obtained when only the first term is kept in $b^{\text{кр}}_{\theta,\phi}$

$$b^{\text{кр}}_{\theta,\varphi} \simeq 2T(\psi_0)\, b^0_{\theta,\varphi}\, l_{\theta,\varphi},$$

where

$$b^0_\theta = \varepsilon\cos\theta + \cos(\theta+\psi_0);\quad b^0_\varphi = 1 + \varepsilon\cos\psi_0.$$

In the portion of the region of the observation point angles, in which the parameter $\gamma >> 1$ we obtain

$$E^{\text{крест}}_{\theta,\varphi} = \frac{2}{\pi}e^{-i\,kcu^2_+}\sin\psi_0\, T(\psi_0)\, b^0_{\theta,\varphi}\, l_{\theta,\varphi}\left[A'\sqrt{a}\, I(a,b) - A''\sqrt{a_2} I(a_2,b')\right]$$

Here

$$I(a,b)=\int_0^1 e^{-i\gamma t^2}\frac{dt}{(a+bt^2)\sqrt{1-t^2}}.$$

We use the obvious correlations $\frac{e^{-i\gamma t^2}}{a+bt^2}=\frac{i}{b}e^{i\frac{\gamma a}{b}}\times\int_\gamma^\infty e^{-i\frac{x}{b}\gamma(a+bt^2)}dx.$

By substituting it into the original integral and by integrating for t [3] we find

$$I(a,b)=\frac{i\pi\gamma}{2b}e^{i\frac{\gamma a}{b}}\int_\gamma^\infty e^{-i\frac{x}{2b}\gamma(2a+b)}J_0\left(\frac{x\gamma}{2}\right)dx.$$

This integral is expressed through the cylindrical functions from two actual variables (Lommel functi.n) $U_0(c,x)$ and $U_1(c,x)$--first and second order respectively [5]. These functions have been tabulated and well studied [6,7]. We can write:

$$I(a,b)=\frac{\pi e^{-i\frac{\gamma}{2}}}{|\sqrt{a(a+b)}|}\left[U_0\left(c_0\frac{\gamma}{2},\frac{\gamma}{2}\right)+iU_1\left(c_0\frac{\gamma}{2},\frac{\gamma}{2}\right)-\frac{1}{2}J_0\left(\frac{\gamma}{2}\right)\right];$$

$$c_0=\frac{(\sqrt{a+b}-\sqrt{a})^2}{b}. \qquad (32)$$

By using the asymptotic presentation of Lommel's functions in the form given in [7], we obtain in our designations

$$I(a,b)=\frac{\pi}{2(a+b)}\left\{\frac{1}{2}e^{-i\frac{\gamma}{2}}J_0\left(\frac{\gamma}{2}\right)+ie^{i\frac{\gamma a}{b}-i\frac{\pi}{4}}\sqrt{\frac{2b}{a}}\times\right.$$
$$\left.\times\left[\frac{1}{2}-C\left(\frac{\gamma a}{b}\right)-\frac{i}{2}+iS\left(\frac{\gamma a}{b}\right)\right]\right\}.$$

For $\gamma>>1$

$$I(a,b)\approx\frac{\pi}{2\sqrt{\pi\gamma}}\left[\frac{e^{-i\gamma+i\frac{\pi}{4}}}{a+b}+\frac{F\left(\frac{\gamma a}{b}\right)}{\sqrt{a}}e^{-i\frac{\pi}{4}}\right],$$

where

$$F\left(\frac{\gamma a}{b}\right)=\frac{1}{a+b}\left\{|1\ \overline{a}|+ie^{i\frac{\gamma a}{b}}|\sqrt{2b\pi\gamma}\left[C_1\left(\frac{\gamma a}{b}\right)-\right.\right.$$
$$\left.\left.-iS_1\left(\frac{\gamma a}{b}\right)\right]\operatorname{sign}|\ \overline{a}.\right.$$
$$C_1(x)=\frac{1}{2}-C(x);\quad S_1(x)=\frac{1}{2}-S(x).$$

Now for the unknown component of the field, we can write:

$$E^{\text{краев}}_{\theta,\varphi}(0 \div \theta_r) = a_0 \left[P_{(-)} e^{-i\left(ku_-^2 + i\frac{\pi}{4}\right)} + P_{(+)} e^{-i\left(ku_+^2 - i\frac{\pi}{4}\right)} \right], \quad (33)$$

where

$$a_0 = \frac{T(\psi_0)}{\sqrt{\pi\gamma}} b^0_{\theta,\varphi} \sin\psi_0 l_{\theta,\varphi};$$

$$P_{(-)} = \frac{1}{\sqrt{a+b}\sqrt{a_0+b'}};$$

$$P_{(+)} = A' F\left(\frac{\gamma a}{b}\right) - A'' F\left(\frac{\gamma a_0}{b'}\right).$$

The phase multipliers in the first and second terms (33) show that the "source" of the first wave should be considered the edge of the mirror -D, since the coordinate ellipsoid which is determined by the parameter u_-^2 passes through it, while the "source" for the second wave is the edge +D for a similar reason. Thus, (33) characterizes the known marginal waves in approximation of the physical optics. The amplitudes of these waves, in contrast to other asymptotic methods, are continuous everywhere and do not have peculiarities near caustic curve surfaces. The nature of the change in the diagram of the field near the special points is determined by the F functions. By using the asymptotics of Fresnel's integrals with large values of the argument, we obtain

$$F\left(\frac{\gamma a}{b}\right) \approx \frac{1}{\sqrt{a}} \quad \text{with} \quad \frac{\gamma a}{b} \gg 1;$$

$$F\left(\frac{\gamma a_0}{b'}\right) \approx \frac{1}{\sqrt{a_0}} \quad \text{with} \quad \frac{\gamma a_0}{b'} \gg 1.$$

Accordingly, in that part of the examined region of angles of the observation point where the indicated parameters are fairly great, we have

$$P_{(+)} = \frac{1}{\sqrt{aa_0}}. \quad (34)$$

Below (see fig. 15) is the course for the actual and imaginary parts of the F function and its asymptotic presentation for a certain critical case. It is apparent from the figure that the narrow region of angles θ which adjoin θ_r is transitional. In this transitional region of angles, the marginal wave changes the order of dependence on the large parameter. The "flash" of the marginal wave that is observed in this case partially "extinguishes" the geometrical-optical wave near the

boundary of the region.

By uniting the obtained results, we can write for the scattered field with $0< \theta \leq \theta_r$:

$$E^0_{\theta,\varphi}(0 \div \theta_r) = \left\{ T(\psi_h, \varphi) \frac{\sin\psi_h}{\sin\theta} + \frac{2\frac{\partial T(\psi_h, \varphi)}{\partial \varphi}}{\sqrt{\pi k P_\theta}} \times \right.$$

$$\times \left. \frac{(\varepsilon^2-1)^{3/2}(\varepsilon\cos\theta-1)^{3/2}(C_1(\gamma_1)+iS_1(\gamma_1))}{[(\varepsilon^2+1)\cos\theta-2\varepsilon]^2} \right\} e^{-i k a u_k^2} I_{\theta,\varphi} +$$

$$+ a_\theta \left[P_{(-)} e^{-i k a u_-^2 + i\frac{\pi}{4}} + P_{(+)} e^{-i k a u_+^2 - i\frac{\pi}{4}} \right]. \qquad (35)$$

The cross-polarization component of the field provides expression (28a). The complete field is obtained by adding to (35) the field of the emitter. The scattered field is the sum of the geometrical-optical wave and the two marginal waves. Althought the marginal waves which are computed only for the uniform current component generally inaccurately describe the actual picture of scattering, neverthless, in the examined region of observation point angles in which a geometrical-optical field exists which is dominant in value, (35) apparently yields a satisfactory approximation (naturally, for kD>>1). In the direction of the boundary of the region ($\theta=\theta_r$), it follows from (33)

$$E^{\text{прием}}_{\theta,\varphi}(\theta_r) = -T(\psi_0)\frac{\varepsilon^2-1}{\varepsilon^2+1-2\varepsilon\cos\theta_r} I_{\theta,\varphi} e^{-i k a u_k^2} +$$

$$+ \frac{T(\psi_0)}{\sqrt{\pi\gamma}} \frac{\sin\psi_0}{\sin\theta_r} \left[\frac{1+\varepsilon\cos\psi_0}{\varepsilon+\cos\psi_0} e^{-i k a u_-^2 + i\frac{\pi}{4}} + \frac{\varepsilon+\cos\psi_0}{1+\varepsilon\cos\psi_0} e^{-i k a u_+^2 - i\frac{\pi}{4}} \right]. \qquad (36)$$

It is obvious from here that the marginal wave extinguishes the geometro-optical.

The obtained relationship (35) is incorrect near $\theta \sim 0$ since when the expression is derived for the marginal waves, it was assumed $\frac{\gamma}{2} \gg 1$. With θ close to zero, the marginal waves are transformed into toroidal waves of the edge of the mirror which in this case is excited by the source in-phase. To clarify the characteristics of the wave of the edge in the integral presentation of the field diagram (31), all the terms in $b_{\theta,\phi}$ have to be taken into account. The integrals obtained in this case are known [3]. By omitting the intermediate computations and by only entering those terms which are significant even with $\varepsilon \sim 1$,

we can write the following expressions for the wave diagram which is "emitted" by the mirror edge:

$$E^{\text{кромки}}_{b_{\theta,\varphi}}(0 < \vartheta) = \frac{T(\psi_0)\sin\psi_0}{2\sqrt{aa_2}}\, l_{\theta,\varphi}\left[b_0\Lambda_0\left(\frac{\gamma}{2}\right) - b_1^{\theta}\sqrt{aa_2}\,\Lambda_1\left(\frac{\gamma}{2}\right) - ib_2 J_1\left(\frac{\gamma}{2}\right)\right] e^{-ikau_+^2 - i\frac{\gamma}{2}}; \quad (37)$$

$$E^{\text{кп}}_{b_{\theta,\varphi}}(0 \leqslant \vartheta) = T(\psi_0)\, b_2^{\theta,\varphi}\frac{\sin\psi_0}{\sqrt{aa_2}}\, l_{\theta,\varphi}\,\frac{\sin\frac{\gamma}{2} - \frac{\gamma}{2}\cos\frac{\gamma}{2}}{\left(\frac{\gamma}{2}\right)^2} e^{-ikau_+^2 - i\frac{\gamma}{2}}, \quad (38)$$

where

$$b_0 = b^0_{\theta,\varphi}\left[1 - \sqrt{aa_2} - (\varepsilon + \cos\psi_0)\sin\vartheta\right];\quad b_1^{\theta} = (1-\varepsilon)\sin^2\frac{\psi_0}{2}\cos\vartheta;$$
$$b_1^{\varphi} = -(1-\varepsilon)\sin^2\frac{\psi_0}{2};\quad b_2 = \sin\vartheta\left[\varepsilon + \cos\psi_0 + \frac{a_2 + (\varepsilon^2 - 1)\,a}{1 + \sqrt{aa_2}}\right].$$

Here $\Lambda_0(x)$ and $\Lambda_1(x)$ --lambda-functions of Bessel [3]. In computing the field near $\theta \sim 0$, the marginal waves in (35) must be replaced by a wave which is defined by expression (37). A similar component (38) must be added to the cross-correlation component (28a). It characterizes the action of the mirror edge. We note that with $\varepsilon \to 1$, formula (37) reflects the effect of amplification which is inherent to the parabolic mirror.

In this case we obtain

$$E^{\text{кромки}}_{b_{\theta,\varphi}}(\varepsilon = 1) = -iT(\psi_0)\,\frac{2\operatorname{tg}\frac{\psi_0}{2}}{\sin\vartheta}\, J_1\left(\frac{\gamma}{2}\right) e^{-ikau_+^2 - i\frac{\gamma}{2}}. \quad (39)$$

As already indicated, the case $\varepsilon = 1$, in light of its practical importance, was analyzed separately.

We will now write formulas which determine the field diagram in the remaining space. In light of the fact that the nature of the computations is similar to that already given, and in this area of space, the field is only created by marginal waves which in the approximation of physical optics can be viewed only as auxiliary material for approximate calculations, the calculation details are given in the appendix.

For the part of the illuminated region in space that is included between the boundary of the geometrical-optical field ($\theta = \theta_r$) and the line of the boundary of light and darkness ($\theta = \pi - \psi_0$), we find the

following analytical presentation of the diagram of the scattered field [formula (A.5)]:

$$E^{\text{краев}}_{\theta,\varphi}(\theta_r \div \pi - \psi_0) = -a_0\left[P_{(-)}\, e^{-ikcu_-^2 + i\frac{\pi}{4}} + P_{(+)}\, e^{-ikcu_+^2 - i\frac{\pi}{4}}\right], \quad (40)$$

where $P_{(-)}$ and $P_{(+)}$ are defined as already known functions.

In the middle part of the region where the arguments of both F functions are fairly great, according to (34) we have $P_{(+)} \approx \frac{1}{\sqrt{aa_0}}$. In this interval of angles, shading of one edge of the mirror by the other is possible. The changes that develop in this case in the diagram of the field are not taken into account in the approximation of the physical optics. However, one can draw definite conclusions from the results of a series of numerical calculations which are presented below.

It is easy to verify that substitution of the values $\theta = \theta_r$ in (40) turns this formula into (36).

The obtained relationships (35), (37) and (40) completely characterize the diagram of the scattered field in the adopted approximation for the part of space illuminated by the sources. On the line of the boundary of light and darkness we obtain: $E^0_{\theta,\varphi}(\pi - \psi_0) \approx -\frac{1}{2}E^0 + 0(\frac{1}{\sqrt{\pi\gamma}})$.

Field in the Shaded Region of Space $(\pi - \psi_0 \leqslant \theta \leqslant \pi)$.

In the shaded region, the characteristic division of the mirror surface into Fresnel's zones has the appearance shown in fig. 8. The line u=0 intersects the surface of the scattering body. Part of Fresnel's zones is ring-shaped, part has the appearance of a band. The picture of Fresnel's zones on the surface of the body is similar to the examined case $0 \leq \theta \leq \theta_r$. We therefore make an analysis in the same way. The integral presentation of the scattered field is written in the form

$$E^0_{\theta,\varphi} = -i\frac{4kP_0}{\pi u_0^2}\left[\int_{u_+}^{0} e^{-ikcu^2}\Psi_0(u)\,u\,du + \int_{u_-}^{u_+} e^{-ikcu^2}\Phi_2(u)\,u\,du\right].$$

Here in $\Psi_0(u)$ the limits of integration for v are constant: $-\frac{\pi}{2}$ - $\frac{\pi}{2}$. We will take the entered integrals once by parts. As shown in [1], the field with u=0 equals the field that is created by the emitter at the observation point, but with the opposite sign. The values of the

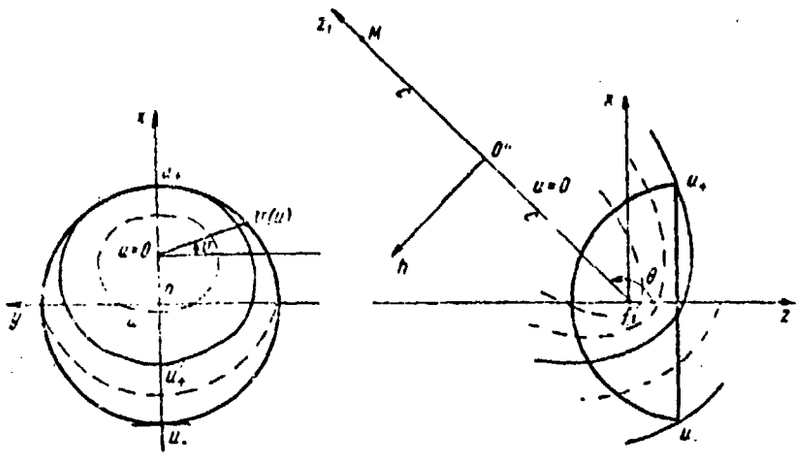

Figure 8.

results for integration by parts for both integrals on the line $u=u_+$ are mutually nullified. The integral presentation of the diagram is written in the variables t and z which are introduced according to formulas (22) with mutual replacements of α_1 and α_2:

$$E^0_{\theta,\varphi} = -\frac{e^{-i k c u_+^2}}{\pi}\int_0^1 e^{-i\gamma t^2}\frac{\partial}{\partial t}\Phi_2(t)\,dt - E^{\cdot}; \qquad (41)$$

$$w^2 = x_1^2 + (\beta^2 - x_2^2)z^2;\ \Phi_2(t) = \frac{x_1^2}{1-\varepsilon\cos v}\int_0^1 b_{\eta,\varepsilon}\frac{dz}{\sqrt{1-x_1^2 z^2}}.$$

The replacement of α_1 and α_2 is caused by the fact that the upper and lower edge of the mirror now fall in the third and second quadrants of the coordinate system ho"z_1 respectively, and not in the second and third, as occurred in the illuminated region. The parameter

$$x_1^2 = \frac{\sqrt{a+bt^2}\sqrt{a_2+b't^2} - \sqrt{aa_2}+t^2(\varepsilon-\cos\delta)\sin\psi_0}{2\sqrt{a+bt^2}\sqrt{a_2+b't^2}}. \qquad (42)$$

By analogy with the previous calculations, we can write:

$$E^{\text{полн}}_{\theta,\varphi} = E^0_{\theta,\varphi} + E^0;$$

$$E^{\text{полн}}_{\theta,\varphi} = -\frac{e^{-i k c u_+^2}}{\pi(1-\varepsilon\cos\delta)}\int_0^1 e^{-i\gamma t^2} b^{\text{кр}}_{\theta,\varphi}\frac{\partial}{\partial t}\arcsin x_1\,dt + O\left(\frac{1}{\gamma}\right).$$

It is easy to obtain $\sin x_1 = \cos x_0$, and consequently $\frac{\partial}{\partial t} \arcsin x_1 = -\frac{\partial}{\partial t} \arcsin x_0$. It follows from here that the final results can be written in the form of (33), but with a change in the sign in front of the formula:

$$E^{\text{полн}}_{\theta,\varphi}\{(\pi-\psi_0)\div\pi\} = -a_0\left[P_{(-)}\, e^{-ikcu_-^2+i\frac{\pi}{4}} + P_{(+)}\, e^{-ikcu_+^2-i\frac{\pi}{4}}\right]. \quad (43)$$

Formula (43) is inapplicable directly near the line of the shading axis $\theta=\pi$ since the hypothesis $\gamma>>1$ is violated which is the basis for its derivation. In this case we should act in the same way as in the derivation of formula (37), i.e., take into consideration the main terms $b_{\theta,\phi}$. By abandoning those terms which are not important with $\theta\sim\pi$, we find

$$E^{\text{полн}}_{\theta,\varphi}\{0\leqslant\pi\} = -T(\psi_0)\frac{\sin\psi_0}{2\sqrt{aa_2}} I_{\theta,\varphi}\left[b^0_{\theta,\varphi}\Lambda_0\left(\frac{\gamma}{2}\right) + b^1_{\theta,\varphi}\Lambda\left(\frac{\gamma}{2}\right)\right] e^{-ikcu_+^2-i\frac{\gamma}{2}}. \quad (44)$$

Expression (44) characterizes the toroidal marginal wave of the in-phase excited edge. The field amplitude of this wave is an order higher than the amplitude of the normal marginal wave. Consequently, in a strictly "backwards" direction, the field diagram has a maximum which is comparable, and in other cases, larger in size, than the field amplitude during emission "forwards." This is the so-called Poisson's loop in the field diagram.

Extension of the Solution Results to the Case of the Source Located in the Distant Focus

The geometry of the problem and the employed coordinate systems when the source is located in the distant focus 0' of the curve generatrix are shown in fig. 9 (as an example, the generatrix is taken in the form of a hyperbola). The equation for the surface of the scattering body in this case is described in the form

$$\rho = P'_0 : (1-\varepsilon\cos\psi'); \; P'_0 = (1-\varepsilon)F; \; F = \frac{1+\varepsilon}{1-\varepsilon}f. \quad (45)$$

The center of the cylindrical coordinate system is taken at the point 0', the angle ψ' is counted from the z-axis. The parameter ε

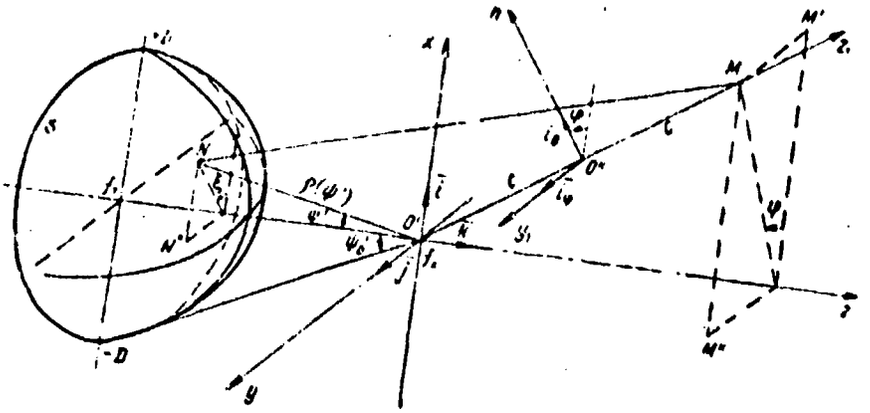

Figure 9.

--eccentricity of the curve; f--distance between the focus and the nearest apex of the curve; F--distance between the focus and the distant apex of the curve. We recall that the mutual arrangement of the curves in this case is shown in fig. 2b. By comparing (1) and (45), we note their identity with replacements of $f \rightleftarrows F$, $\varepsilon \rightleftarrows -\varepsilon$. The angle ψ' is the angle at which the current point N of the body surface is visible from the distant focus of the curve, at angle θ, the angle is elevated at which the observation point M is visible from this focal point. The angles ψ and ψ' are associated by the relationship

$$\operatorname{tg}\frac{\psi'}{2} = \frac{\varepsilon - 1}{\varepsilon + 1}\operatorname{tg}\frac{\psi}{2}.$$

Figure 10 presents the designations of the employed parameters of elliptical and hyperbolic curves with arrangement of the source in one of the foci. Comparison of the nature of division of the body surface into Fresnel zones in both cases, both for the illuminated part of the space (fig. 5 and correspondingly fig. 11), and for the shaded (fig. 8 and correspondingly fig. 12), shows their basic identity.

Taking into consideration that the listed factors are definitive in deriving formulas for the field diagram, one can draw the following conclusion: all the relationships obtained in the previous sections maintain their meaning and transmit the characteristics of the diagram of the scattering field when the body surface is irradiated from the distant focus of the curve with the replacements:

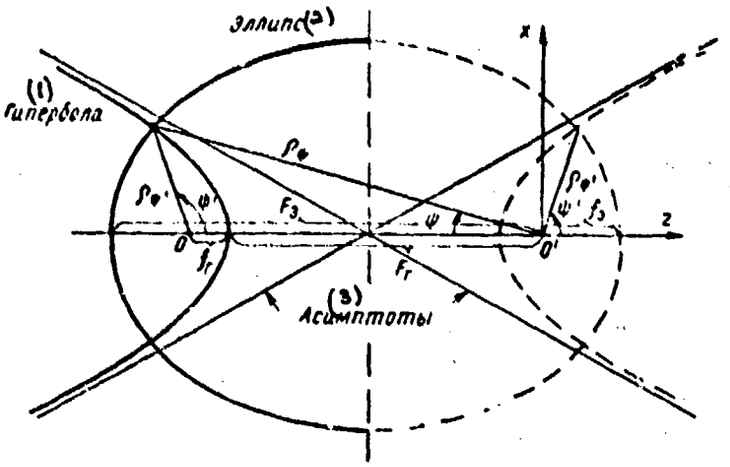

Figure 10. 1--Hyperbola; 2--Ellipse; 3--Asymptotes.

$$f \longleftrightarrow F;\quad \varepsilon \longleftrightarrow -\varepsilon;\quad P_0 \longleftrightarrow P_0' \qquad (46)$$

and with counting of the angles ψ and θ from the distant focal point of the curve. We recall that the previously obtained formulas were written for curves of the hyperbolic type. In the transition to curves of the elliptical type, as before, additional permutations should be made in them

$$\varepsilon + 1 \to 1 - \varepsilon \quad a_3 \to a_3.$$

For economy of space, the corresponding finite expressions are not written.

Certain Solution Results

Analysis of the solution shows that in different regions of space, the problem has different parameter characteristics. The quantities γ, γ/b and $\frac{\gamma a_2}{b'}$ can be isolated as these parameters with "large" parameter of the problem kP_0. On the boundaries between the isolated regions $(0;\ \theta_r\ \pi-\psi_0;\pi)$ one of these parameters is nullified. The order of the dependence of the field amplitude on the main large parameter of the problem kP_0 changes correspondingly. The boundary lines of the regions correspond to the caustic curves of the field. At a sufficient distance from the boundary lines, all the characteristic parameters

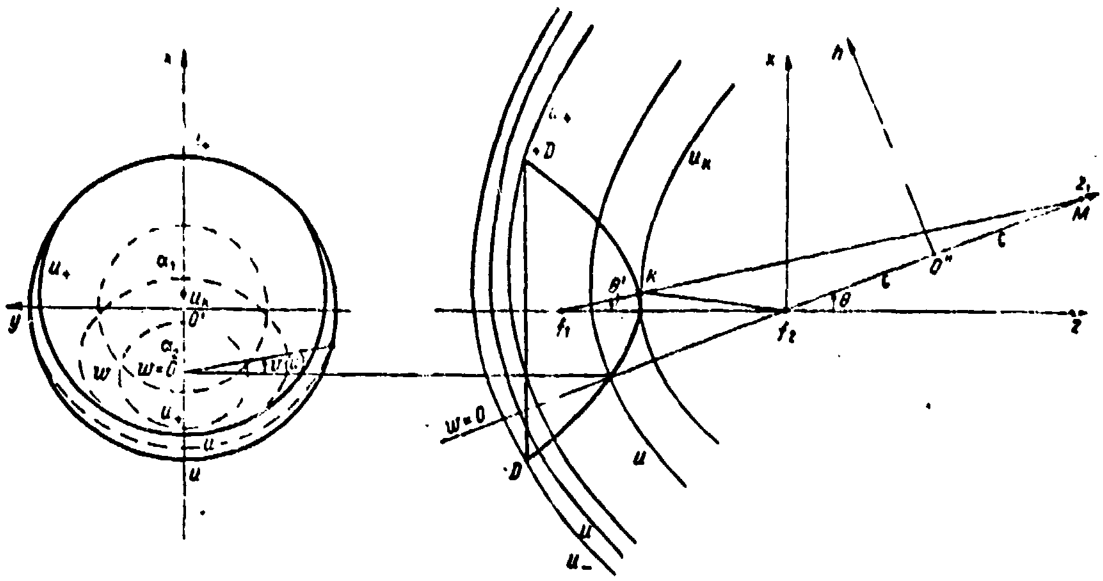

Figure 11.

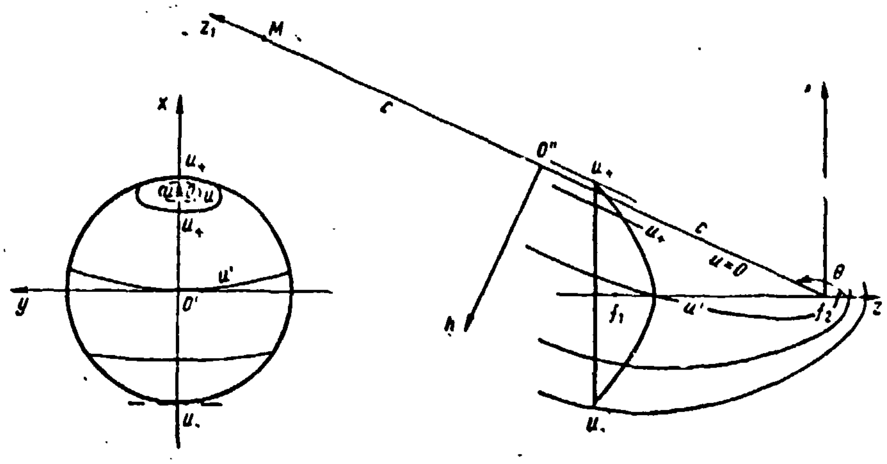

Figure 12.

are "large."

The findings confirm the principle of locality: the scattering field has that phase structure as if it had been created by locally reflected rays of the source from the corresponding points on the mirror surface. The directions near the axis of body symmetry are an exception.

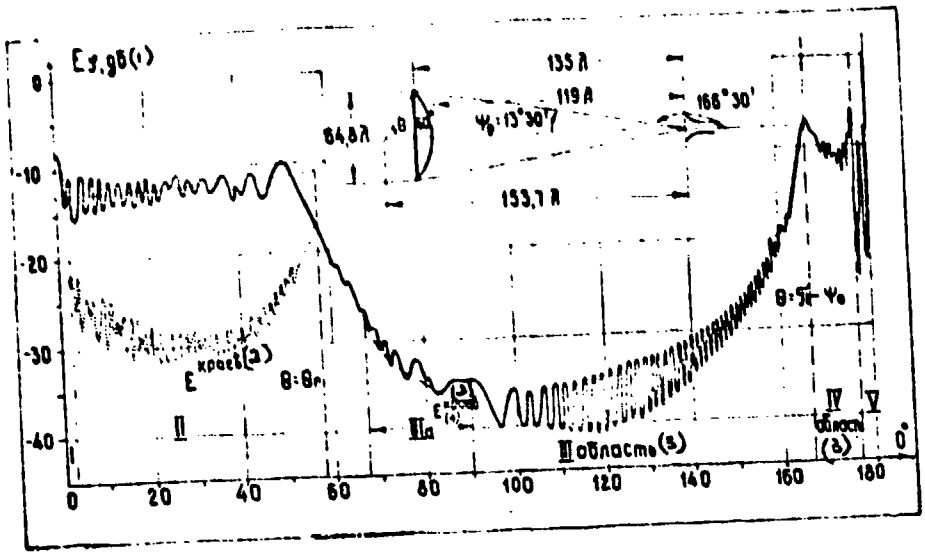

Figure 13.
1--db; 2--marginal; 3--region

The obtained system of formulas makes it possible to compute the scattering field in all the space, including the transitional regions, in the framework of the adopted approximation of physical optics. The formulas guarantee a continual transition from one region of space to another

It is expedient to use the main results of the work for approximate calculations of the scattering field from hyperbolic and elliptical auxiliary mirrors used in standard two-mirror antennas, as well as to compute the radiation field from the main parabolic mirror.

Calculations of the scattering field diagram were made for a number of examples. In publication [4], the initial integrals were computed by the methods of numerical integration. Figures 13 and 14 present the diagram of the scattering field which is computed from the derived formulas from the hyperbolic reflector. Its comparison with analogous curves [4] shows that the general nature of the curves is roughly the same. The main difference appears between the planes E(ϕ=0) and H($\phi=\frac{\pi}{2}$). In the E plane, a dip appears in the diagram which could be explained by the corresponding orientation of current elements flowing on the edge of the mirror in this plane. For certain directions in which the current vector is directed towards the observation point, the current flowing perpendicularly to the edge "emits" weakly.

In publication [4], the diagrams in both planes are practically the same, since the gap in the field in the plane E "is filled" by a field whose order is $1/\gamma$. However, this "correction", to all appearances,

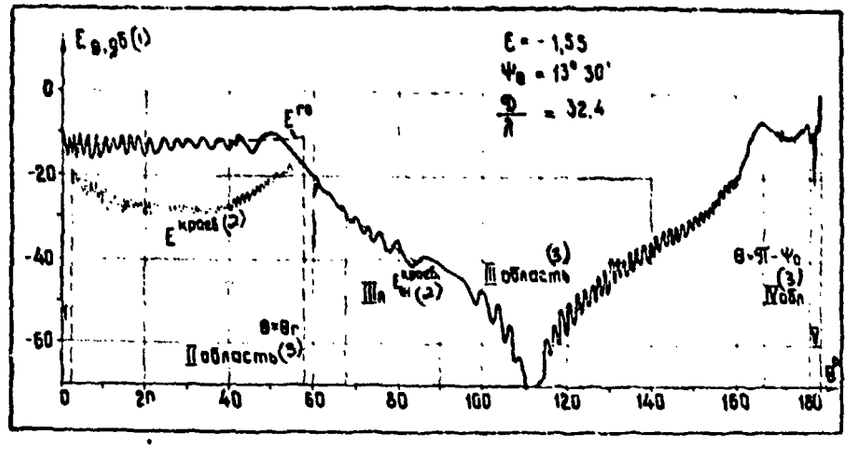

Figure 14.
1--db; 2--marginal; 3--region

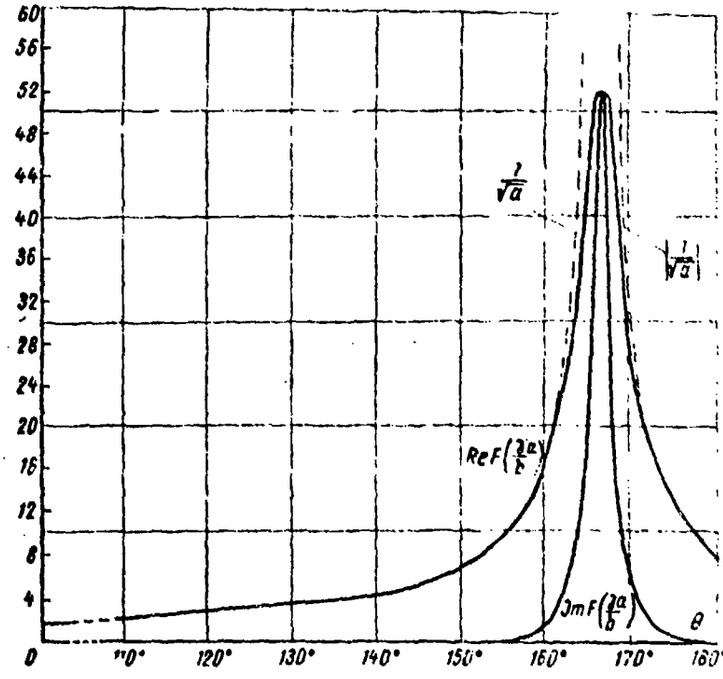

Figure 15.

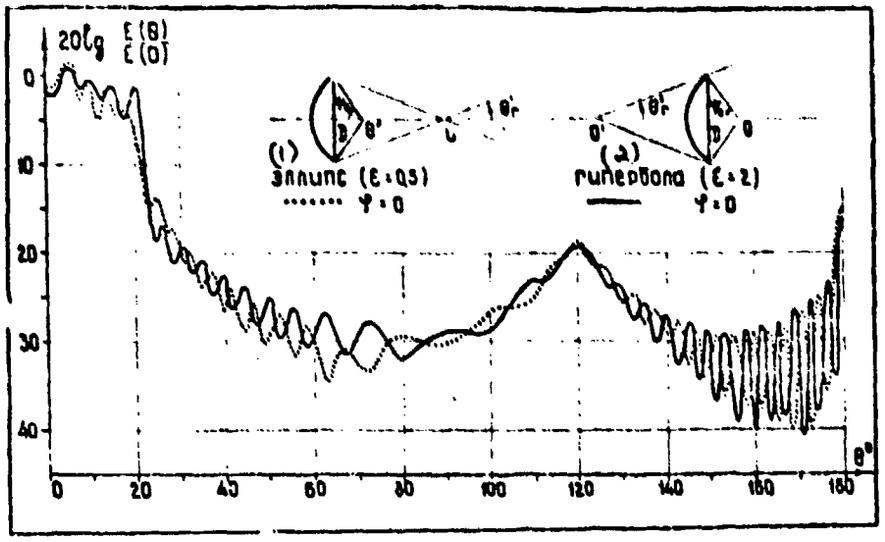

Figure 16.
1--ellipse; 2--hyperbola.

lies beyond the limitis of accuracy which can be guaranteed by the approximation of physical optics. Figures 13 and 14 also give different components of the field which were computed separately from formulas (28), (33), (37) and (40). This separation of the contribution of each component makes it possible to orient oneself in the methods of controlling undesirable radiation in the selected directions. These same figures illustrate by the dotted line (in the region IIIa) the field from one, unshaded edge of the mirror. As is apparent, the difference between the interference field of the "light" edge and the shaded, as compared to the field of one "light" edge, is not great, and may not be taken into consideration in practical orienting calculations. One can draw the conclusion from here that although in the approximation of physical optics in the field, rays are present which "puncture" the mirror metal, their amplitude is significantly lower than the amplitude of the actually "shining" edge.

Figure 15 presents the nature of the change in the function $F\left(\frac{\gamma a}{b}\right)$ for the examined example. The dotted line shows the value of the analog of this function of the quantity $\left|\frac{1}{1'a}\right|$, which follows from the method of the stationary phase. With $\theta_0 \to \theta_r \left|\frac{1}{1'a}\right| \to \infty$.

Figure 16 presents examples of computing the field diagram for a number of specific values of parameters e and kD. It is apparent that the "conjugated" ellipse and hyperbola ($e_1 e_2 = 1$) have practically the same scattering diagrams.

Conclusions

A system of formulas has been obtained which makes it possible in the approximation of physical optics to find at any point in space the characteristics of the scattering field of a spherical wave on finite revolution bodies formed by curves of the second order. The found solution can be used to make the next step in computing the nonuniform component of the current.

The analysis made shows the effectiveness of the method of physical coordinates in solving scattering problems.

The results of the work may be used in different areas of antenna engineering, for example. in computing the scattering field from mirror antennas or re-emitters of the appropriate shape.

Appendix 1.

We will clarify the nature of the relationships that determine the field in the region of angles $\theta_r \leq \theta \leq \pi - \Psi_0$. In this region, there are no rays that are reflected from the mirror according to the laws of geometric optics. The integral presentation of the field is written in the variables u and v. Expression (10)with replacemert of u and v by normed variables t and τ (fig. 7b) according to the formulas

$$u^2 = u_+^2 + (u_-^2 - u_+^2) t^2 \quad \text{и} \quad v = \frac{\pi}{2} + \left| v(t) - \frac{\pi}{2} \right| \tau,$$

adopts the appearance

$$E^0_{\theta,\varphi} = -i \frac{2}{\pi} \gamma e^{-ikau_+^2} \int_0^1 e^{-ik\gamma\tau^2} \xi(t) q(t) t dt.$$

where

$$\xi(t) = \arcsin [\xi_0(t)] \sqrt{1 - t^2} t \Big|; \quad \sin \xi(t) = \cos v(t);$$

$$k(t) = s \sin \theta \frac{\sqrt{a + bt^2}}{\sqrt{a_2 + b' t^2}};$$

$$q(t) = \int_0^1 b_{\theta,\varphi} [2u_0^2 (1 - s \cos \theta) - u^2 (1 - s^2 + s^2 \sin^2 \theta \sin^2 \xi\tau)]^{-\frac{1}{2}} u d\tau.$$

We assume $y = k(t)\sin\xi(t)\tau$, then

$$q(t) = \frac{1}{(1-\varepsilon\cos\eta)\,\xi(t)} \int_0^{k(t)\sin\xi(t)} b_{\theta,\varphi}\left[\frac{1}{\sqrt{1-y^2}} - \frac{1}{\sqrt{k^2(t)-y^2}}\right] dy. \qquad \text{(A.2)}$$

Similarily to the analysis given above, we expand $b_{\theta,\phi}$ into a Taylor series for the exponents y near the edge of the mirror $[y = k(t)\sin\xi(t)]$. It follows from the previously obtained correlations

$$\frac{\partial}{\partial y} b_{\theta,\varphi}\Big|_{\text{кр}} = \frac{2t\sqrt{1-t^2}}{k(t)\left[(1-2t^2)\,\xi_0(t) + t(1-t^2)\dfrac{\partial \xi_0(t)}{\partial t}\right]} \frac{\partial b_{\theta,\varphi}}{\partial t^2}\Big|_{\text{кр}}.$$

After integration for y we determine

$$q(t) = \frac{1}{\xi(t)(1-\varepsilon\cos\eta)}\left\{ b^{\text{кр}}_{\theta,\varphi}\left[\arcsin k(t)\sin\xi(t) - \right.\right.$$
$$\left.\left. - \frac{\partial b_{\theta,\varphi}}{\partial t^2}\Big|_{\text{кр}}\left[1 - \sqrt{1-k^2(t)\sin^2\xi(t)} - k(t)(1-\cos\xi)\right] + \ldots\right\}.$$

The numerical presentation for q(t) should be substituted in the original integral. It is easy to be convinced that the second term of the expansion already yields quantities of a negligible order of smallness. By integrating the remaining expression once by parts we obtain

$$E^0_{\theta,\varphi} = \frac{e^{-i\,k\varepsilon u_+^2}}{\pi(1-\varepsilon\cos\eta)} \int_0^1 e^{-i\,\gamma t^2}\, b^{\text{кр}}_{\theta,\varphi}(t)\,\frac{\partial}{\partial t}\left[\arcsin k(t)\sin\xi(t) - \right. \qquad \text{(A.3)}$$
$$\left. - \arcsin\xi(t)\right] dt + O\left(\frac{1}{\gamma}\right).$$

By differentiation we find:

$$\frac{\partial}{\partial t}\arcsin k(t)\sin\xi(t) = -\varepsilon b\,\frac{\sqrt{a_1 a_2} - t^2\left(\sqrt{a_2+b'}+\sqrt{a_1-b}\,\sqrt{a_1 a_2}\right)}{(a_1-bt^2)(a_2+b't^2)\sqrt{1-t^2}};$$
$$\frac{\partial}{\partial t}\arcsin\xi(t) = -\sin\psi_0\,\frac{\sqrt{aa_1} - t^2\left(\sqrt{a+b}\,\sqrt{a_1-b}+\sqrt{aa_1}\right)}{(a_1-bt^2)(a+bt^2)\sqrt{1-t^2}}.$$

In addition,

$$\sqrt{aa_1} = \frac{t^2\left(\sqrt{a}+\sqrt{b}\right)\left(\sqrt{a_1}-\sqrt{b}\right)\sqrt{aa_1}}{(a_1-bt^2)(a+bt^2)} = \frac{A_1\sqrt{a}}{a+bt^2} - \frac{A_2\sqrt{a}}{a_1-bt^2};$$

$$A_1 = \frac{\sqrt{a}+\sqrt{b}}{\sqrt{a_1(a+b)}-\sqrt{a(a_1-b)}};$$

$$A_2 = \sqrt{\frac{a_1-b}{a+b}}\,A_1;$$

$$\frac{a_1a_2}{(a_1-bt^2)(a_2+b't^2)} = \frac{B_1\sqrt{a_2}}{a_2+b't^2} - \frac{B_2\sqrt{a_1}}{a_1-bt^2};$$

$$B_1 = \frac{\sqrt{a_2+b'}}{\sqrt{a_1(a_2+b')}-\sqrt{a_2(a_1-b)}}; \quad B_2 = \sqrt{\frac{a_2-b}{a_2+b'}}\,B_1.$$

By substituting these correlations into (A.3) we arrive at integrals which coincide in form with those previously computed [see (32) and so forth]. One can therefore immediately write the result of integration. Since $\gamma>>1$ always in the examined case, then, by using the asymptotics of the Lommel function, we find

$$E^0_{\theta,\varphi}(\vartheta, \varphi=(\pi-\psi_0)) = \frac{a_0}{1-\varepsilon\cos\vartheta}\left\{e^{-i\,k\alpha u_-^2+i\frac{\pi}{4}}\left(\frac{\varepsilon\sin\theta}{\sqrt{a_1-b}\sqrt{a_2+b'}}-\right.\right. \tag{A.4}$$

$$\left.-\frac{1}{\sqrt{a_2-b}\sqrt{a+b}}\right)+e^{-i\,k\alpha u_+^2-i\frac{\pi}{4}}\left[B_1F\left(\frac{\gamma a_2}{b'}\right)\varepsilon\sin\vartheta-\frac{B_2\varepsilon\sin\vartheta}{\sqrt{a_1}}-\right.$$

$$\left.\left.-A_1F\left(\frac{\gamma a}{b}\right)+\frac{A_2}{\sqrt{a_1}}\right]\right\}.$$

Passing in this expression from the letter designations to the corresponding functions of the angles, after simple computations we obtain

$$E^0_{\theta,\varphi}(\vartheta, \varphi=(\pi-\varphi_0)) = -a_0\left[P_{(-)}e^{-i\,k\alpha u_-^2+i\frac{\pi}{4}}+P_{(+)}e^{-i\,k\alpha u_+^2-i\frac{\pi}{4}}\right], \tag{A.5}$$

which is identical to (33) with accuracy to the sign.

Consequently, the marginal waves in the region of angles $0<\theta<\pi$ are described by the same analytical relationship. In this case

$$P_{(+)} = \frac{1}{(1-\varepsilon\cos\vartheta)\sin\psi_0}\left[\cos\frac{\vartheta-\psi_0}{2}F\left(\frac{\gamma a}{b}\right)-\left(\varepsilon\sin\frac{\vartheta+\psi_0}{2}-\right.\right.$$

$$\left.\left.+\sin\frac{\vartheta-\psi_0}{2}\right)F\left(\frac{\gamma a_2}{b'}\right)\right].$$

Bibliography

1. Yerukhimovich, Yu. A. "Approximate Computation of Scattered Field Using Phase Structure of the Field," Radiotekhnika i elektronika, No. 1, 1967, pp. 22-27.

2. Ufimtsev, P. Ya. Metod krayevykh voln v fizicheskoy teorii difraktsii ["Method of Marginal Waves in the Physical Theory of Diffraction"], Moscow, Izd-vo Sovetskoye radio, 1962.

3. Yanke, B.; Emde, F.; Lyesh, F. Spetsial'nyye funktsii ["Special Functions"], Moscow, Nauka, 1964.

4. Rush, V. "Scattering ffrom Hyperboloid Reflector in Cassegrain System," IEEE Transaction, AP-11, No. 4, 1963, pp. 414-421.

5. Vatson, G. N. Teoriya Besselevykh funktsiy ["Theory of Besselian Functions"], I. L. 1949.

6. Dekanonsidze, Ye. N. Tablitsy tsilindricheskiky funktsiy ot dvukh peremennykh ["Tables of Cylindrical Functions from Two Variables"] Academy of Sciences, USSR, 1956.

7. Yerukhimovich, Yu. A.; and Pimenov, Yu. V. "Approximate Computation of Cylindrical Functions from Two Actual Variables," Zhurnal vychisl. matem. i matem. fiziki, No. 3, 1969, p. 691.

8. Yerukhimovich, Yu. A. "Scattering of Spherical Wave on Truncated Paraboloid of Rotation," Radiotekhnika, No. [illegible] 1969, pp. 59-71.

BROAD-DIRECTIONAL LENS ANTENNAS MADE OF AN INHOMOGENEOUS DIELECTRIC

Ye. G. Zelkin and R. A. Petrova

Summary

Broad-directional lens antennas are examined with refraction index $n(R,\phi)=\frac{n(\phi)}{R}$ and broad-directional lens antennas that are computed with the help of the conformal transform method.

A calculation is made of the refraction index and the beam trajectory index in these lenses.

Introduction

In many practical cases it is necessary to produce an antenna with a broad beam pattern, for example, in a sector over 180°. Development of antennas with these broad patterns presents great difficulties. It is sufficient to say that the open end of the wave guide radiates only in the 120-130° sector. In order to expand the pattern, we have to resort to special measures, for example, the use of dielectric inserts in the wave guide which is constricted on the end. However, all the known methods of expanding the pattern generally impair the wide-band nature of the antenna.

The use of lens antennas made of an inhomogeneous dielectric is a very promising trend in the development of broad-directional antennas. They have a number of advantages. The chief ones are: operation in a broad band of frequencies and preservation of the polarization properties of the antenna emitter.

It should be noted that a broad-directional pattern can be obtained with the help of lenses made of an inhomogeneous dielectric with the most diverse laws for the change in the refraction index inside of them.

This work examines several lenses made of inhomogeneous dielectric with a broad beam pattern (to 360°). It calculates the refraction indices of these lenses, as well as the trajectories of the beams passing in them.

It is common knowledge that the initial equation to compute the lens by the method of geometric optics is the eikonal equation

$$(\nabla L)^2 = n^2, \qquad (1)$$

where n--the function of three variables in a general case.

It is a very complicated task to find the solution to this equation in a general form which satisfies the condition of obtaining a broad beam pattern.

We will examine below a simplified task when the refraction index in the lens changes according to the law $n(R, \varphi) = \frac{n(\varphi)}{R}$. This law for the change in the refraction index makes it possible to separate the variables in equation (1), and to determine the unknown function $n(\phi)$.

The method of conformal transforms provides broad potentialities

for computing the broad-directional lenses. There are known lenses in the literature that are made of an inhomogeneous dielectric which focus rays into parallel beam (lenses of Mikaelyan, Maxwell, Lyuneberg et al.). The refraction indices, beam trajectories, wave front and other characteristics have been computed for these lenses. All the rays which emerge from the lenses indicated above are perpendicular to the aperture plane. In the case of a broad-directional lens, the aperture must not be flat, but have the shape of a sphere, while the rays must emerge from it not in a parallel but in a spherically diverging bundle which is perpendicular to the aperture surface.[1] Thus, in order to obtain a broad-directional pattern, one can conformally depict a lens with flat aperture which focuses the rays into a parallel beam, into a lens with aperture which has the shape of a sphere. The main properties of the conformal depiction: preservation of the angles and constancy of the strains will guarantee transformation of the flat aperture into a spherical one, and the parallel beam of rays into a spherically diverging beam.

Calculation of Lens Parameters with Refraction Index

$$n(R, \varphi) = \frac{n(\varphi)}{R}$$

Calculation of the refraction index. We will examine a cylindrical lens with refraction index $n(R, \varphi) = \frac{n(\varphi)}{R}$, where R and ϕ--polar coordinates. Since in cylindrical lenses, all the beams lie in the plane z=const, then for simplicity we will examine the course of the beams in the plane z=0.

In our case, the eikonal equation in coordinate writing has the following appearance:

$$\left(\frac{\partial L}{\partial R}\right)^2 + \frac{1}{R^2}\left(\frac{\partial L}{\partial \varphi}\right)^2 = n^2(\varphi)\,\frac{1}{R^2} \qquad (2)$$

or

$$R^2\left(\frac{\partial L}{\partial R}\right)^2 + \left(\frac{\partial L}{\partial \varphi}\right)^2 = n^2(\varphi). \qquad (2a)$$

*In further calculation of the lens we will assume that it has a phase center which coincides with the geometric center of the sphere. This condition for guaranteeing a broad beam pattern is sufficient, but is not necessary in the general case

We will look for the solution in the form

$$L = f(R) + f_1(\varphi), \tag{3}$$

then

$$R^2 f'^2(R) + f_1'^2(\varphi) = n^2(\varphi). \tag{4}$$

Equation (4) is satisfied on the condition

$$\left.\begin{aligned} R^2 f'^2(R) &= a_1^2 \\ f_1'^2(\varphi) &= n^2(\varphi) - a_1^2 \end{aligned}\right\}, \tag{5}$$

where a_1--random constant of separation of the variables. From here

$$f(R) = \int \frac{a_1}{R}\, dR = a_1 \ln R + a, \tag{6}$$

where a--integration constant:

$$f_1(\varphi) = \int \sqrt{n^2(\varphi) - a_1^2}\, d\varphi. \tag{7}$$

By substituting expressions (6) and (7) into (3), we have

$$L = \int \sqrt{n^2(\varphi) - a_1^2}\, d\varphi + a_1 \ln R + a. \tag{8}$$

One can apply to equation (8) the study method presented in book [1]. After differentiating the complete integral for a_1, and after equating the result to the constant β_1, we obtain an equation for the family of rays which depend on the two constants a_1 and β_1:

$$\ln R = \int \frac{a_1}{\sqrt{n^2(\varphi) - a_1^2}}\, d\varphi + \beta_1. \tag{9}$$

We have obtained an integrated equation in relation to the unknown function $n(\phi)$. The constant β_1 is defined from the boundary conditions, while a_1 is the ray parameter: for each ray, the parameter a_1 is a constant quantity, however, its value changes from ray to ray.

We will determine the constant β_1. For this purpose, we will find the quation of rays which emerge from point A (fig. 1), whose

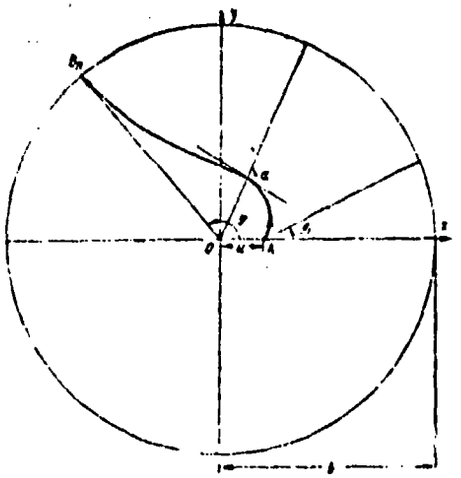

Figure 1.

coordinates:

$$R_A = d, \ \varphi_A = 0. \qquad (10)$$

We will secure the lower limit of the indefinite integral in expression (9) after using the boundary conditions (10):

$$\ln R = \int_{\varphi_A} \frac{a_1 d\varphi}{\sqrt{n^2(\varphi) - a_1^2}} + \ln d, \qquad (11)$$

from which it follows that $\beta_1 = \ln d$.

We will now find the limits for change in a_1. For this purpose, we will differentiate equation (11) for ϕ:

$$\frac{d(\ln R)}{d\varphi} = \frac{a_1}{\sqrt{n^2(\varphi) - a_1^2}}, \qquad (12)$$

from which

$$R\frac{d\varphi}{dR} = \frac{\sqrt{n^2(\varphi) - a_1^2}}{a_1}. \qquad (13)$$

As is known $R\frac{d\varphi}{dR} = \operatorname{tg}\alpha$,

where α--angle between the radius-vector and tangent to the beam (fig.1).

We will examine the rays emerging from point A at angles $0 \leqslant \varphi_1 \leqslant \frac{\pi}{2}$.

$tg\alpha_A=\infty$ corresponds to the extreme ray which emerges vertically upwards $\varphi_1=\frac{\pi}{2}$, while $tg\alpha_A=0$ corresponds to the central ray ($\phi_1=0$). Consequently, the parameter a_1 which changes in limits $n_{(0)}\geq a_1\geq 0$ corresponds to the rays lying in the sector $0\leq\phi_1\leq\frac{\pi}{2}$.

We require that all the rays which emerge from point A and which are defined by the values a_1 in the indicated limits, emerge from the lense at points B_n which lie on the circumference of radius R=b. Then

$$\int_{\varphi_A}^{\varphi_{B_n}}\frac{a_1 d\varphi}{\sqrt{n^2(\varphi)-a_1^2}}=\ln\frac{b}{d}. \qquad (14)$$

Equation (14) can be solved in relation to $n(\phi)$ if the value n is assigned at some point. We will designate:

$$n^2(\varphi)=u,\ \psi=\frac{d\varphi}{du},\ a_1^2=h. \qquad (15)$$

With $\varphi=0$ $u=n^2(0)=u_0$.

Since we require that all the rays emerge at points B_n perpendicularly to circumference R=b, then on this circumference $tg\alpha=0$, and consequently, with

$$\varphi=\varphi_{B_n}\ u_{B_n}=n^2(\varphi_{B_n})=a_1^2=h. \qquad (16)$$

In the new designations, equation (14) looks like

$$\int_{u_0}^{h}\frac{\psi du}{\sqrt{u-h}}=\frac{\ln b_0}{\sqrt{h}}, \qquad (17)$$

where $b_0=\frac{b}{d}$, while h changes in limits of $0\leq h\leq u_0$. We obtained an Abel type equation, which, as is known, has the solution

$$\psi=-\frac{1}{\pi}\frac{d}{du}\int_{u_0}^{u}\ln b_0\frac{dh}{\sqrt{h(h-u)}}, \qquad (18)$$

but since $\psi=\frac{d\varphi}{du}$, , then

$$\varphi=A\int_{u_0}^{u}\frac{dh}{\sqrt{h(h-u)}}. \qquad (19)$$

where $A = \frac{\ln b_0}{\pi}$.

After taking the integral in the right side, we obtain

$$\varphi = A \ln \frac{u}{2\sqrt{u_0^2 - uu_0} + 2u_0 - u}. \qquad (20)$$

By solving (2) in relation to u, after certain transforms we obtain

$$u = \frac{u_0}{\left(\operatorname{ch} \frac{\varphi}{2A}\right)^2}, \qquad (21)$$

but since $u=n^2(\phi)$, while $u_0=n^2(0)$, then the final expression for the refraction index

$$n(\varphi) = \frac{n(0)}{\operatorname{ch} \frac{\varphi}{2A}}. \qquad (22)$$

We see that the refraction index on the lens aperture depends on the selection of n(0), as well as on the arrangement of the focus in the lens. It is assigned by the quantity d. The dependence of the refraction index on the lens boundary, i.e., with R=b, on the selected parameters n(0) and d is presented in the table below. It does not present the absolute values of the refraction indices, but the ratios of the refraction indices with different ϕ to n(0). The calculations were made for d=0.1 and 0.2b.

It is apparent from the table that the greatest value of the refraction index is with ϕ=0. With an increase in ϕ, the refraction index diminishes, as the change is larger the greater the quantity d, i.e., the further the focus is located from the center of the circle which is the lens aperture.

TABLE

d in relative units	Values of relative quantity $\frac{n(\phi)}{n(0)}$ with different ϕ						
	0°	30	60°	90°	120°	150°	180°
0,1b	1	0,94	0,79	0,61	0,45	0,33	0,23
0,2b	1	0,88	0,64	0,41	0,26	0,15	0,1

The complete refraction index in the lens can be expressed by taking into consideration (22):

$$n(\varphi, R) = \frac{n(0)}{R \operatorname{ch} \frac{\pi\varphi}{2\ln \frac{b}{d}}}. \qquad (23)$$

Calculation of the ray trajectories. In order to find the ray trajectories, it is necessary to substitute expression (22) into formula (11) and to compute the obtained integral:

$$\ln \frac{R}{d} = \int_0^{\varphi} \frac{a_1 d\varphi}{\sqrt{\frac{n^2(0)}{\left(\operatorname{ch} \frac{\varphi}{2A}\right)^2} - a_1^2}}. \qquad (24)$$

We will replace the variables: $x=\operatorname{shk}\phi$, $k = \frac{1}{2A}$ and $c^2 = \frac{n^2(0)}{a_1^2}$, then, equation (24) adopts the appearance

$$\ln \frac{R}{d} = \int_0^{\frac{\operatorname{Ar\,sh} x}{k}} \frac{dx}{\sqrt{c^2 - x^2 - 1}}. \qquad (25)$$

The right side of expression (25) is the tabular integral [2]. By solving it, we obtain

$$\ln \frac{R}{d} = \frac{1}{k} \arcsin \frac{\operatorname{Ar\,sh} x}{k\sqrt{c^2 - 1}}, \qquad (26)$$

from here,

$$\varphi = \sqrt{\left[\frac{n(0)}{a_1}\right]^2 - 1} \sin \frac{\ln \frac{R}{d}}{2A}. \qquad (27)$$

Formula (27) determines the link between ϕ and R with the selected values of d and n(0). By assigning the parameter a_1 in limits from n(0) to 0, we will obtain the trajectories of the rays which emerge from the focus at angles ϕ_1 from 0 to 90°.

The trajectories for e rays for the two cases where d=0.1 and 0.3b are presented in fig. 2 which only depicts the upper half of the lens. The entire lens in this case has the appearance of a sphere with removed middle, where the emitter can be placed.

With d=0.1b, we are c limited to constructing the rays that emerge from the focus at angles from ϕ_1=0° to 74° [in this case, the parameter a_1 changed from n(0) to 0.23 n(0)]. The outer ray (ϕ_1=74°) emerges from the lens perpendicularly to the aperture at angle ϕ=180°.

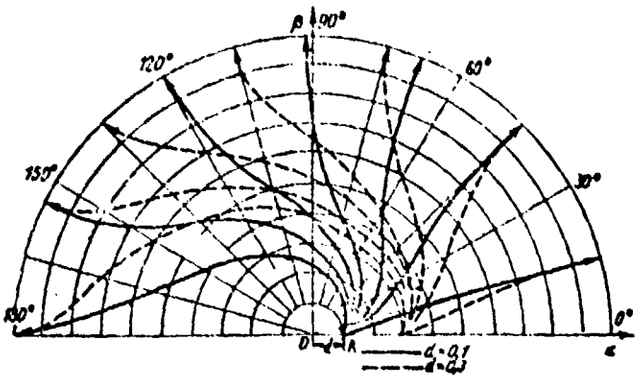

Figure 2.

With d=0.2b, a ray emerges from the lens at angle ϕ=180°. It travels from the focus at angle ϕ_1=71°. This corresponds to the value a_1 which equals 0.1 n(0).

Depending on the selection of values n(0), one can obtain beam patterns of varying width. With d=0.1b, for example, the refraction index on the lens aperture changes from n(0) to 0.23 n(0) with $\phi = \pi$. This means, that with n(0)=4.3, we can create radiation in the 360° sector. With a value of n(0)=1.6, with the same d=0.1b, the emitter ray emerges from the focus at an angle of ϕ_1=52°.

Lens Calculation by the Method of Conformal Transform

Selection of the parameters of the transforming function. We will first examine the known lenses of Maxwell and Mikaelyan [1] as the initial lenses. In the Maxwell lens, the refraction index depends only on the radius of the lens, while in the Mikaelyan lens it depends on one coordinate y. If we examine both lenses in the Cartesian coordinate system, then the aperture of both lenses will be a plane perpendicular to the x-axis and intersecting it at point x=0.

We will examine the pattern of rays in one plane, for example, z=0. All the rays in the indicated lenses intersect the y-axis at a right angle. In order to obtain a broad-directional lens, the rays must intersect the circle at a right angle, consequently, this lens can be produced if the y-axis is conformally transformed into a circle.

We will use the linear-fractional function as the transforming function

$$W = \frac{kZ + l}{mZ + n}, \qquad (28)$$

where $W = \alpha + i\beta$, $Z = x + iy$, while α, β, x and y--respectively the coordinates of the broad-directional and transformable lens. For simplicity,

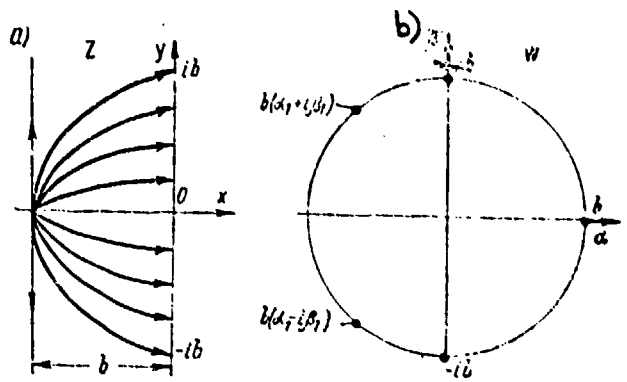

Figure 3.

one of the coefficients, for example, k, can be assumed to be equal to a unit [3]. Thus, the illustration is assigned by three coefficients l, m and n which depend on three complex or six actual parameters.

We will first examine the Mikaelyan lens. Assume that the lens aperture will be 2b (fig. 3a). We will require that the refraction index equal one along the straight lines y=±b. We will transform this aperture into part of a circle which is defined by the coefficients $b(\alpha_1 \pm i\beta_1)$ (fig. 3b). Since it is sufficient to assign three points in order to define the circle, we will take the following as the original three points on the lens aperture: Z=ib, 0, -ib-, and we will transform them into the points $W=b(\alpha_1+i\beta_1)$, b, $b(\alpha_1-i\beta_1)$. We will assume for simplicity that the quantity b=1. In order to find the coefficients l, ma and n, we substitute the values W and the values of Z corresponding to them into formula (28):

$$\left.\begin{aligned} \alpha_1 + i\beta_1 &= \frac{i + l}{mi + n} \\ 1 &= \frac{l}{n} \\ \alpha_1 - i\beta_1 &= \frac{-i + l}{-mi + n} \end{aligned}\right\}, \qquad (29)$$

From which, after certain transforms, we obtain the values for all three coefficients

$$\left.\begin{aligned} n &= l = \frac{\beta_1}{1-\alpha_1} \\ m &= -1 \end{aligned}\right\}. \qquad (30)$$

After substituting the obtained values for the coefficients into formula (28), and after separating the real and imaginary parts, we obtain an expression for x and y through the coordinates α and β:

$$x = \frac{A(\alpha^2+\beta^2-1)}{|(1+\alpha)^2+\beta^2|}, \qquad (31)$$

$$y = \frac{2A\beta}{|(1+\alpha)^2+\beta^2|}, \qquad (32)$$

where $A = \frac{\beta_1}{1-\alpha_1}$.

It is easy to see from formula (31) that the y-axis, which the rays in the Mikaelyan lens are perpendicular to, becomes a circle which is described by the equation $\alpha^2+\beta^2 = 1$. This was also required in the statement of the problem.

Refraction index and trajectories of rays in a broad-directional lens of the Mikaelyan lens type. It is common knowledge [1] that in a Mikaelyan lens of single radius, the refraction coefficient only depends on one coordinate y:

$$n(y) = \frac{n(0)}{\operatorname{ch}\frac{\pi y}{2}}. \qquad (33)$$

In order to guarantee invariance in the optical path, the refraction index in the new lens must be transformed according to the formula:

$$N(\alpha, \beta) = \frac{n(\alpha, \beta)}{|W'|}, \qquad (34)$$

where $n(\alpha,\beta)$ can be obtained from formula (33) after replacement of y through the new coordinates according to (32), and $|W'| = |\frac{dW}{dz}|$ -- modulus of derivative from analytical function W(z). By using expressions (28), (30), (31) and (32), we find

$$|W'| = \frac{(1+\alpha)^2+\beta^2}{2|A|}. \qquad (35)$$

Consequently, the final expression for the refraction index in the broad-directional lens for a Mikaelyan type lens:

$$N(\alpha, \beta) = \frac{2|A|n(0)}{[(1+\alpha)^2+\beta^2]\operatorname{ch}\frac{\pi A\beta}{(1+\alpha)^2+\beta^2}}. \qquad (34a)$$

Formula (34a) makes it possible to compute the refraction indices in a broad-directional lens.

The ray trajectories in the Mikaelyan lens of a single radius are described by the equation

$$\cos\frac{\pi x}{2} = \frac{a_1}{\sqrt{n^2(0)-a_1^2}}\operatorname{sh}\frac{\pi y}{2}, \qquad (36)$$

where a_1--parameter which is constant for each ray and changes from ray to ray. For any ray in a bundle $0 \leq \phi_1 \leq \frac{\pi}{2}$, the parameter a_1 satisfies the condition $0 \leq a_1 \leq n(0)$.

After substituting, instead of x and y, expressions (31) and (32), we obtain an expression which determines the ray trajectories in a broad-directional lens:

$$\cos\frac{\pi A}{2}\frac{\alpha^2+\beta^2-1}{[(1+\alpha)^2+\beta^2]} = \frac{a_1}{\sqrt{n^2(0)-a_1^2}}\operatorname{sh}\frac{\pi A\beta}{[(1+\alpha)^2+\beta^2]}. \qquad (37)$$

The focus of the Mikaelyan lens z_ϕ which has coordinates $x_\phi = -1$, $y_\phi = 0$, according to the formulas for transformation of the coordinates, becomes point w_ϕ with coordinates:

$$\alpha_\phi = \frac{\beta_1+\alpha_1-1}{1-\alpha_1+\beta_1}, \quad \beta_\phi = 0. \qquad (38)$$

Formula (38) shows that the position of the focus in the transformed lens is only determined by the position of the extreme rays in the lens. In a particular case, where the sector of the rays equals ±90°, the lens focus coincides with the geometric center of the circle.

A lens with sector ±120° was examined as an example. For it, $\alpha_1 = -0.5$, $\beta_1 = 0.866$, $A = -0.577$. In this lens, the focus is located at the point with coordinates $\beta_\phi = 0$, $\alpha_\phi = -0.27$. The lines of equal refraction indices (dotted line) and ray trajectories in the lens (solid) are depicted in fig. 4.

We examined above the transform of a Mikaelyan lens of single radius in a broad-directional lens, also of single radius, and it was hypothesized that the refraction coefficient equalled 1 with y=±1. One can examine a more general case where the lens size equals b, while n(y)=1 with a certain y=a. The aperture of this lens equals 2a, and the quantity a is associated with the refraction coefficient n(0) by the correlation

$$a = \frac{2b}{\pi} \operatorname{arch} n(0). \qquad (39)$$

The coordinate transform formulas in this case look like

$$x = \frac{aA}{b} \frac{(\alpha^2 + \beta^2 - b^2)}{[(\alpha + b)^2 + \beta^2]}, \quad y = \frac{2\alpha\beta A}{[(\alpha + b)^2 + \beta^2]}. \qquad (40)$$

The refraction coefficients

$$N_1(\alpha, \beta) = \frac{n(0)}{|W_1'| \operatorname{ch} \frac{a\beta A}{[(\alpha + b)^2 + \beta^2]}}. \qquad (41)$$

The trajectories of the rays are described by the equation

$$\cos \frac{\pi}{2} \frac{aA}{b} \frac{\alpha^2 + \beta^2 - b^2}{(\alpha + b)^2 + \beta^2} = \frac{a_1}{\sqrt{n^2(0) - a_1^2}} \operatorname{sh} \frac{\pi a A \beta}{(\alpha + b)^2 + \beta^2}. \qquad (42)$$

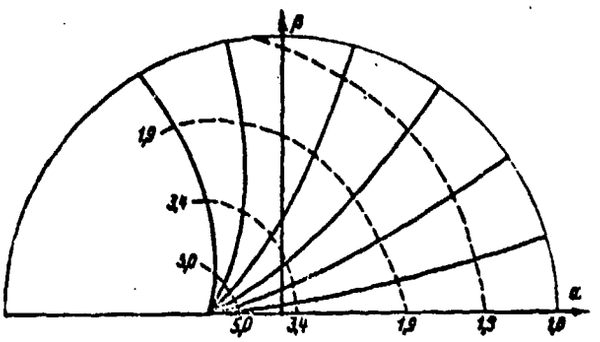

Figure 4.

Refraction Coefficient and Trajectories of Rays in Broad-Directional Lens of the Maxwell Lens Type. We will now examine the Maxwell lens, for example, of single radius and will transform it

into a broad-directional lens also of a single radius. This transform is reduced to the previously examined transform of the Mikaelyan lens with aperture equal to 2, and the refraction coefficient equal to 1 with y=±1, and consequently, the transform coefficients, coordinates x and y, and the modulus of the derivative W(z) are reflected correspondingly by formulas (30), (31), (32) and (35).

In a Maxwell lens of single radius, the refraction coefficient

$$n(x, y) = \frac{n(0)}{1 + x^2 + y^2}, \qquad (43)$$

while in the broad-directional, obtained on the basis of this lens, correspondingly

$$N(\alpha, \beta) = \frac{2|A|\, n(0)}{[(1+\alpha)^2 + \beta^2](1+A^2) - 4\alpha A^2}. \qquad (44)$$

It is easy to show that the lines of equal values for the refraction coefficients $N(\alpha, \beta)$=const are circles with center that is shifted in relation to the beginning of the coordinates. These circles are determined by the expression

$$\delta^2 + \beta^2 - 2\delta \frac{2A^2}{A^2+1} + \frac{2(2A^2C - |A|)}{C(A^2+1)} = 0, \qquad (45)$$

where $\delta = 1+\alpha$, a $C = \frac{N(\alpha, \beta)}{n(0)}$.

The center of these circles is located at the point with coordinates:

$$\alpha_0 = \frac{A^2-1}{A^2+1}, \quad \beta_0 = 0. \qquad (46)$$

while the radii of the circles

$$R_0 = \frac{1}{A^2+1}\sqrt{\frac{A^2+1}{C} - 2|A|}. \qquad (47)$$

The lens focus is located, as before, at the point with coordinates:

$$\alpha_\phi = \frac{\beta_1 + \alpha_1 - 1}{\beta_1 - \alpha_1 + 1}, \quad \beta_\phi = 0.$$

The trajectories of the rays in the Maxwell lens of single radius are described by the equation

$$x^2 + y^2 + 2y \operatorname{ctg} \gamma = 1, \qquad (48)$$

where γ--angle of emergence of the ray from the lens focus.

After substituting expressions (31) and (32) into formula (48), we obtain a formula to compute the trajectories of the rays in a broad-directional lens:

$$\frac{A^2(\alpha^2+\beta^2-1)^2+4\beta^2A^2}{[(1+\alpha)^2+\beta^2]^2}+\frac{4A\beta\operatorname{ctg}\gamma}{[(1+\alpha)^2+\beta^2]}-1=0. \qquad (49)$$

After transforming this formula, it is easy to be convinced that the trajectories of the rays have the shape of circles which depend on the γ parameter:

$$\alpha^2+\beta^2-2\alpha\left(\frac{A^2+1}{A^2-1}\right)+2\beta\frac{2A\operatorname{ctg}\gamma}{A^2-1}+1=0, \qquad (49a)$$

with centers at the points with coordinates:

$$\alpha_0=\frac{A^2+1}{A^2-1},\ \beta_0=-\frac{2A\operatorname{ctg}\gamma}{A^2-1} \qquad (50)$$

and radii

$$R_0=\frac{2A}{(A^2-1)\sin\gamma}. \qquad (51)$$

As an example, the lens with radiation sector ±120° was computed. The lines of equal refraction coefficients (dotted lines) and the trajectories of the rays in this lens (solid line) are presented in fig. 5.

Calculation of a broad-directional lens according to the type of isotropic emitter. The method of conformal transformation makes it possible to obtain broad-directional lenses not only based on the known lenses, but also quite new ones.

As an example, we will examine a broad-directional lens which was obtained based on an isotropic emitter illustrated in fig. 6. It is assumed here that the hypothetical isotropic emitter (fig. 6a) is located in the center of a spherical lens made of a uniform

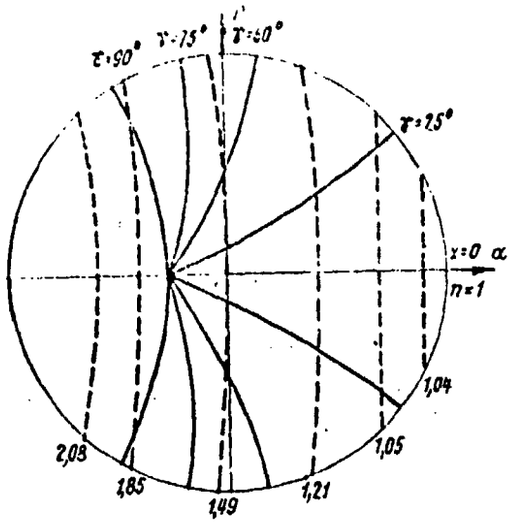

Figure 5.

dielectric or nonuniform dielectric, but with refraction index that changes only for the radius.

As before, we will examine the pattern of distribution for the refraction coefficients and the ray trajectories in the Z=0 plane. We will conformally depict the right semicircle with outer rays at points with coordinates x=0 and y=±1 into a broader spectrum with outer rays at the points with coordinates $\alpha_1+i\beta_1$ (fig. 6b). The unknown piecewise-linear function for this transform has the coefficients:

$$n=1,\ l=m=\frac{\alpha_1}{1+\beta_1} \qquad (52)$$

and is written as follows:

$$W=\frac{B+z}{Bz+1}, \qquad (53)$$

where $B=\frac{\alpha_1}{1+\beta_1}$.

By separating the actual and the imaginary parts, we obtain expressions for x and y through the new coordinates α and β:

$$x=\frac{\alpha(1+B^2)-B(\alpha^2+\beta^2+1)}{(1-\alpha B)^2+\beta^2B^2}, \qquad (54)$$

$$y=\frac{\beta(1-B)}{(1-\alpha B)^2+\beta^2B^2}. \qquad (55)$$

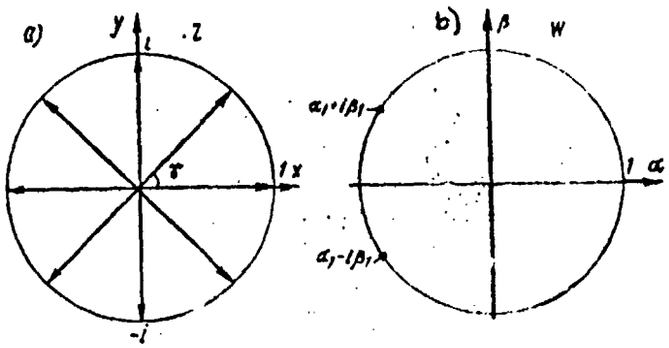

Figure 6.

If we assume that the refraction coefficient in the original lens has a constant value n(0), then we can find the refraction coefficient in a broad directional lens, after preliminarily determining the modulus of the derivative W(z). For this transform

$$|W'| = \frac{|1-B^2|}{(Bx+1)^2+B^2y^2}, \qquad (56)$$

where x and y are determined by formulas (54) and (55). The final expression for the refraction coefficient

$$N(\alpha, \beta) = \frac{n(0)(1-B)[(1+B)^2(1-\alpha B)^2+\beta^2B^2]}{(1+B)[(1-\alpha B)^2+\beta^2B^2]^2}. \qquad (57)$$

The point of location of the emitter whose coordinates are x=0, y=0 in the transformed lens becomes the point with coordinates $\alpha_\phi = B$, $\beta_\phi = 0$.

In the original lens, the ray trajectories are segments of straight lines:

$$y = x \operatorname{tg} \gamma, \qquad (58)$$

where γ is the angle of the ray emergence.

In the new lens, the ray trajectories are circles described by the equation

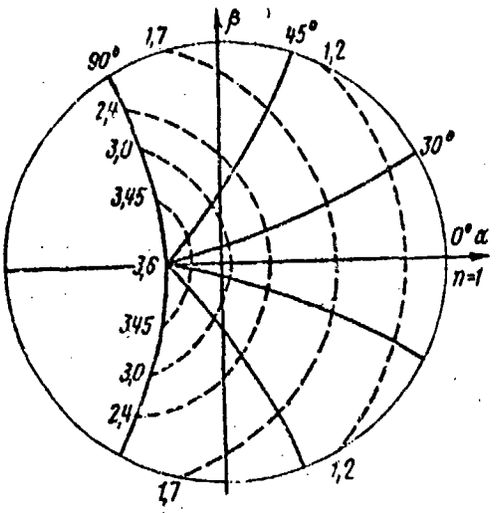

Figure 7.

$$\alpha^2+\beta^2-\alpha\left(\frac{1+B^2}{B}\right)+\frac{\beta(1-B)\operatorname{ctg}\gamma}{B}+1=0, \qquad (59)$$

with centers at the points

$$\alpha_0=\frac{1+B^2}{2B},\ \beta_0=-\frac{(1-B)\operatorname{ctg}\gamma}{2B} \qquad (60)$$

and radii

$$R_0=\sqrt{\alpha_0^2+\beta_0^2-1}. \qquad (61)$$

The ray trajectories (solid line) and the refraction coefficients (dotted line) that were obtained for a lens with outer rays at points $\alpha_1=-0.5$ and $\beta_1=0.866$ (sector ±120°) and with coefficient $n(0)=1.73$, are presented in fig. 7.

This calculation was made for an isotropic emitter located in a uniform medium, however similar calculations can be made for the original lens with refraction coefficient that changes with the radius according to any law.

Bibliography

1. Fel'd, Ya. N.; and Benenson, L. S. Antenno-fidernyye ustroystva ["Antenna-Feeder Devices"], Pt. 2, 1959.

2. Ryzhik, I. M.; and Gradshteyn, N. S. Tablitsy integralov, ryadov, summ i proizvedeniy ["Tables of Integrals, Series, Sums and Products"], Fizmatgiz, 1963.

3. Lavrent'yev, M. A.; and Shabat, B. V. Metody teorii funktsiy kompleksnogo peremennogo ["Methods of the Theory of Functions of the Integrated Variable"], Fizmatgiz, 1958.

MODELING BEAM PATTERNS OF LINEAR ANTENNAS

K. S. Shcheglov

Summary

A method is examined for mathematical modeling on a computer of the beam patterns of antennas based on the use of Kotel'nikov's theorem. The values of the patterns for a number of reference directions are used for complete analysis of the properties of the pattern, including directive gain and scattering coefficient.

The examined algorithm is applied to computing antennas by the method of statistical tests (Monte Carlo method) which consists of modeling random patterns.

Introduction

Difficulties in analytical examination of beam patterns of antennas with complicated amplitude-phase distributions in the aperture have led to the need for development of special methods of study. They include, on the one hand, the methods of graphic modeling of the patterns using different types of analog devices and plans equivalent to the antenna [1]. On the other hand, the development of computer equipment has afforded broad possibilities of using the methods of mathematical modeling of antenna patterns [2,3]. As compared to the methods of the first group, these methods reduce to a minimum the loss of time and resources with considerably greater accuracy of the results.

Pattern modeling is especially important in studying antennas with random distributions in the aperture caused by errors in fabrication or which are especially assigned. The statistical theory of these antennnas [4] makes it possible to define the characteristics for the main pattern parameters only in a statistical sense. Only the class of normal errors is subject to detailed analysis. These characteristics determine the properties of the pattern in a group of single-type antennas.

It is important to directly calculate the individual realizations of random patterns and to make a subsequent statistical study of the parameters of the pattern group. These tasks are solved in the framework of the method of statistical tests, the Monte Carlo method [5] which has become popular with the development of computer equipment. In the most general form, the Monte Carlo method consists of solving different problems of computer mathematics by constructing a random process for each case with parameters which are equal to the unknown quantities of this problem. As applied to computing antennas, this means that a number of random realizations are obtained on the computer for distribution in the aperture with required statistical properties and the patterns corresponding to them are defined.

Based on a number of realizations of random patterns, the probability estimates of their parameters are determined, including those such as coefficients of scattering which are difficult to obtain by

other methods. In this case the law of distribution of errors can be arbitrary.

The method examined below can be applied to problems of heuristic calculation of antennas. In this case, the modeling method is used to select the most successful random distributions of discrete emitters (or their amplitudes) which yield satisfactory patterns. A further task in this case is accurate fulfillment of the found random function for the arrangement of the elements (distribution of amplitudes).

We note in conclusion that in addition to the tasks of computing antennas, modeling the patterns is also used to model systems in which these antennas are used.

Discrete Presentation of the Beam Patterns

Assume that in the aperture of a linear antenna of length L, the distribution a(s) is assigned and is equal in a general case to:

$$a(s) = a_0(s) + \gamma_1(s) + i\varkappa(s). \qquad (1)$$

The beam pattern of this antenna

$$F(u) = \int_{-1}^{1} a(\xi)\, e^{iu\xi}\, d\xi, \qquad (2)$$

where $u = \frac{kL}{2}\cos\vartheta$, ϑ --angle which is read off from the antennna axis, ξ--normed coordinate of the aperture point, k--wave number in a free space (fig. 1).

If the antenna aperture is stimulated by a wave with wave number γ, one should place $u-\beta$ in expression (2) instead of the quantity u in the exponent, where $\beta = \gamma \frac{L}{2}$. This replacement does not affect the nature of the F(u) relationship and must only be taken into consideration in the transition to the angular coordinate ϑ, in particular, in computing the directive gain and the scattering coefficient of the antenna.

In accordance with (1), we present the pattern (2) in the form

$$F(u) = F_a(u) + F_\gamma(u) + iF_\varkappa(u). \qquad (3)$$

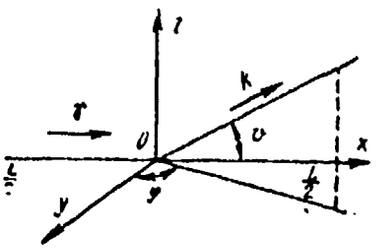

Figure 1.

If in the distribution of a(s) we can isolate a component which is convenient for analytical integration, it should be included in a_0, otherwise, we consider $a_0=0$ and correspondingly, $F_a=0$.

For convenience we will introduce the following designations:

$$g=\int_{-1}^{1}\tau_1(\xi)\cos u\xi\,d\xi;\quad b=\int_{-1}^{1}\varkappa(\xi)\cos u\xi\,d\xi;$$

$$h=\int_{-1}^{1}\tau_1(\xi)\sin u\xi\,d\xi;\quad d=\int_{-1}^{1}\varkappa(\xi)\sin u\xi\,d\xi. \qquad (4)$$

Thus, the pattern (3) can be presented in the form

$$F=F_0+(g-d)+i(b+h). \qquad (5)$$

Direct numerical computation of the pattern with the help of formula (2) is inconvenient with a large number of points for u. In addition, determination of a number of important characteristics of the antenna (amplification, scattering coefficient, position of the main maximum, etc.) by direct methods is associated with cumbersome calculations.

In this respect, we will use presentation of the pattern in the form of a series for reference functions that, for example, are very popular in the tasks of antenna synthesis [6,7]. According to Kotel'nikov's theorem [7,8] or the theorem of readings, the beam pattern examined as a function with limited spectrum (distribution) can be presented in the form (fig. 2) of a series for the functions $\frac{\sin x}{x}$:

$$F(u)=\sum_{m=-\infty}^{\infty}F(m\pi)\frac{\sin(u-m\pi)}{(u-m\pi)}. \qquad (6)$$

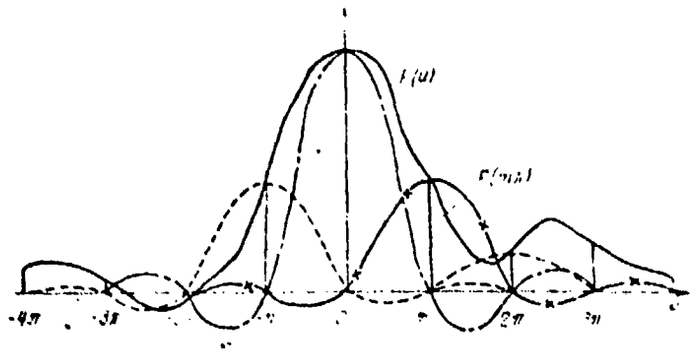

Figure 2.

The reference functions $\frac{\sin(u-m\ \pi)}{(u-m\ \pi)}$ are arranged uniformly with interval $\Delta u=\pi$ on the u axis. The coefficients in (6) with them are equal to the values of the pattern F(u) in the reference points $u=m\Delta u$, $m=0, \pm 1, \pm 2\ldots$

We will isolate the real and imaginary parts in pattern (5):

$$F = X + iY,$$

where $X = A_0(u) + A_1(u);\ Y = C_0(u) + C_1(u),$

and $A_1(u)$ and $C_1(u)$ according to (6) equal:

$$A_1(u) = \sum_{m=-\infty}^{\infty} (g_m - d_m) \frac{\sin(u - m\pi)}{(u - m\pi)},$$

$$C_1(u) = \sum_{m=-\infty}^{\infty} (b_m + h_m) \frac{\sin(u - m\pi)}{(u - m\pi)}. \qquad (8)$$

If we can isolate the component a_0 in distribution (1), the function

$$A_0(u) = \int_{-1}^{1} a_0(\xi) \cos u\xi\, d\xi \qquad (9)$$

will correspond to the "summary" pattern, while

$$C_0(u) = \int_{-1}^{1} a_0(\xi) \sin u\xi\, d\xi \qquad (10)$$

--the "differential."

The index m in the functions g_m-d_m in (8) means that they were computed for the value of the argument $u=m\pi$. The functions g and b are even for u; h and d are odd. Expressions (8) can therefore be presented in the form:

$$A_1(\pm u) = \sum_{m=0}^{\infty} \varepsilon_m \{g_m(s_m + s_{-m}) \pm d_m(s_m - s_{-m})\}, \qquad (11)$$

$$C_1(\pm u) = \sum_{m=0}^{\infty} \varepsilon_m \{b_m(s_m + s_{-m}) \pm h_m(s_m - s_{-m})\}, \qquad (12)$$

$$\varepsilon_m = \begin{cases} \frac{1}{2} \text{ with } m = 0, \\ 1 \text{ with } m = 1, 2, \ldots \end{cases}$$

The following designation is adopted in formulas (11)-(12) for convenience

$$s_m = \frac{\sin(u - m\pi)}{(u - m\pi)}. \qquad (13)$$

In the reference directions $u=m\pi$, the function $s_m=1$, the remaining $s_n=0$ $(n\neq m)$ and the function F(u) in (6) equals its reference value.

Directive Gain and Scattering Coefficient

By using the discrete concept (6) of the beam pattern, we can find expressions for the directive gain which are convenient for calculation on a computer

$$G = \frac{4\pi p_{\text{макс}}}{P_\Sigma} \qquad (14)$$

and scattering coefficient

$$\zeta = \frac{P_{6л}}{P_\Sigma} = 1 - \frac{P_{гл}}{P_\Sigma} \qquad (15)$$

of a linear antenna.

In expressions (14) and (15), $P_{макс}$ is the level of power in the main direction, P_Σ--complete emitted power, $P_{6л}$ and $P_{гл}$ --powers emitted in the region of lateral lobes and in the main lobe respectively.

For a linear antenna, the complete emitted power

$$P_\Sigma = \int_0^{2\pi}\int_0^{\pi} p(u)\sin\vartheta\, d\vartheta\, d\varphi = \frac{4\pi}{\lambda l}\int_{-u_0}^{u_0} p(u)\, du, \qquad (16)$$

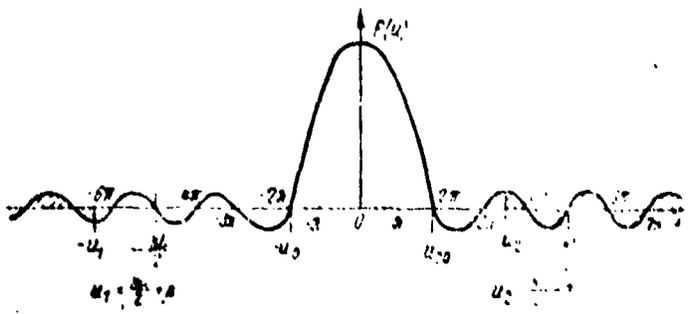

Figure 3.

where $u_1 = \frac{kL}{2}(1 + \Delta)$ and $u_2 = \frac{kL}{2}(1-\Delta)$--boundaries of change in the generalized variable u which correspond to the boundaries of the real pattern $\vartheta=0$ and π, while $\Delta = \gamma/k$.

The power $P_{\text{гл}}$ which is contained in the main lobe, is determined by the same correlation (16) with replacement of u_1 and u_2 by the coordinates u_{10} and u_{20} (fig. 3) of the boundaries of the main lobe.

If $\Delta > 0$, the main lobe is inclined towards the axis, therefore its right boundary $\vartheta < \vartheta_{\text{макс}}$ is determined from the condition

$$u_{20} = \begin{cases} u_{10} & u_{10} < u_2, \\ u_2 & u_{10} > u_2. \end{cases} \qquad (17)$$

Since the expression for the pattern p(u) consists of three terms

$$p(u) = (A_0^2 + C_0^2) + 2(A_0A_1 + C_0C_1) + (A_1^2 + C_1^2), \qquad (18)$$

one can correspondingly divide the integral (16) into parts

$$\Pi_\Sigma = \int_{-u_1}^{u_2} p(u)\,du = \Pi_1 + \Pi_2 + \Pi_3. \qquad (19)$$

We will first compute the last term in the right side of (19):

$$\Pi_3 = \int_{-u_1}^{u_2} (A_1^2 + C_1^2)\,du =$$

$$= \sum_{m=-\infty}^{\infty} \sum_{n=-\infty}^{\infty} [(g_m - d_m)(g_n - d_n) + (b_m + h_m)(b_n + h_n)]\, T_{m,n}. \qquad (20)$$

The coefficients in series (20)

$$T_{m,n}(-u_1, u_2) = \int_{-u_1}^{u_2} \frac{\sin(u - m\pi)}{(u - m\pi)} \frac{\sin(u - n\pi)}{(u - n\pi)}\,du. \qquad (21)$$

In the infinite interval $-\infty < u < \infty$, the functions s_m [see (11)] are orthogonal with m whole

$$T_{m,n}(-\infty, \infty) = \pi\delta_{m,n}, \text{ where } \delta_{m,n} = \begin{cases} 1 & m = n \\ 0 & m \neq n. \end{cases}$$

For finite values u_1 and u_2, the functions $T_{m,n}$ equal

$$T_{\substack{m,n \\ m \neq n}}(-u_1, u_2) = \frac{(-1)^{m+n}}{2\pi(m-n)} \left\{ L(v) \Big|_{-u_1-m\pi}^{u_2-m\pi} - L(v) \Big|_{-u_1-n\pi}^{u_2-n\pi} \right\}. \quad (22)$$

The functions

$$L(v) = \ln v - \mathrm{Ci}(2v)$$

are even. This follows from presentation of the integral cosine Ci(x) in the form of a series, therefore the limits of integration in (22) are taken according to the modulus

$$T_{m,m}(-u_1, u_2) = Q(v) \Big|_{-u_1-m\pi}^{u_2-m\pi}, \quad (23)$$

where

$$Q(v) = \mathrm{Si}(2v) - \frac{1-\cos 2v}{2v}.$$

The function Q(ν) is odd.

For the functions L(ν) and Q(ν), one can obtain expressions in the form of the series:

$$L(v) = \sum_{k=1}^{\infty} (-1)^{k-1} \frac{2^{2k} v^{2k}}{(2k)(2k)!}; \quad Q(v) = \sum_{k=1}^{\infty} (-1)^{k-1} \frac{2^{2k-1} v^{2k-1}}{(2k-1)(2k)!} \quad (24)$$

(in the function L(ν), the constant c-ln2 which is not important for computation of $T_{m,n}$ is omitted, where c--Euler's constant). With $\nu \gg 1$, one should substitute in L(ν) and Q(ν) the asymptotic expressions for the functions Si(x) and Ci(x).

After using the properties of symmetry of the functions (4) for u and the properties of the functions $T_{m,n} = T_{n,m}$, one can significantly reduce the double sum (20) which is cumbersome to compute, by passing to summation in the sector $0 \leq m \leq \infty$, $m \leq n < \infty$.

The final expression for Π_3:

$$\left.\begin{aligned} \Pi_3 = \sum_{m=0}^{\infty} \sum_{n=-m}^{\infty} F_{m,n} \varepsilon_m \varepsilon_n [(b_m b_n + g_m g_n)\tau_1 + \\ + (b_m h_n - g_m d_n)\tau_2 + (b_n h_m - g_n d_m)\tau_3 + (h_m h_n + d_m d_n)\tau_4 \end{aligned}\right\}, \quad (25)$$

where

$$E_{m,n} = \begin{cases} 1 \text{ with } m = n, \\ 2 \text{ with } m \neq n; \end{cases} \quad \varepsilon_m = \begin{cases} 1/2 \text{ with } m = 0, \\ 1 \text{ with } n = 1, 2, 3 \ldots \end{cases}$$

The functions τ equal:

$$\begin{aligned} \tau_1 = T_{m,n} + T_{m,-n} + T_{-m,n} + T_{-m,n}; \ \tau_3 = T_{m,n} + \\ + T_{m,-n} - T_{-m,n} - T_{-m,-n}, \\ \tau_2 = T_{m,n} - T_{m,-n} + T_{-m,n} - T_{-m,-n}; \ \tau_4 = T_{m,n} - T_{m,-n} - \\ - T_{-m,n} + T_{-m,-n}. \end{aligned} \quad (26)$$

With discrete presentation of the patterns (6), there is no difficulty in computing the first two terms in (19). For this purpose we can use direct integration for u. If the pattern $F_0 = A_0 + iC_0$ can be represented as a finite number of terms of the type of functions $\frac{\sin x}{x}$, the integral $\Pi_2 = 2 \int_{-u_1}^{u_2} (A_0 A_1 + C_0 C_1)\, du$ is expressed by a simple series.

Thus, if in the distribution we isolate the component of "summary" distribution of the type $a_{0\Sigma} = 1 + q\eta_\xi$, the pattern looks like:

$$A_{0\Sigma} = s_0 + \frac{1}{2} q (s_1 + s_{-1}); \ C_{0\Sigma} = 0.$$

In this case

$$\left.\begin{aligned} \Pi_1 = T_{0,0} + q(T_{0,1} + T_{0,-1}) + \frac{1}{4} q^2 (T_{1,1} + 2T_{1,-1} + T_{-1,-1}) \\ \Pi_2 = 2 \sum_{m=0}^{\infty} \varepsilon_m \{g_m (v_m + v_{-m}) - d_m (v_m - v_m)\} \end{aligned}\right\}, \quad (27)$$

where

$$v_m = \int_{-u_1}^{u_2} A_{0\Sigma} s_m du = T_{0,m} + \frac{1}{2} q (T_{1,m} + T_{-1,m}).$$

For the "differential" distribution $a_{0\lambda}(\xi) = c\left(\sin\pi\xi + \rho\sin\frac{\pi}{2}\xi\right)$ the pattern

$$A_{0\lambda} = 0;\ C_{0\lambda} = c\left\{(s_1 - s_{-1}) + \rho\left(s_{\frac{1}{2}} - s_{-\frac{1}{2}}\right)\right\}$$

and

$$\left.\begin{aligned} \Pi_1 &= 2c^2\left\{(T_{1,1} - T_{1,-1}) + 2\rho\left(T_{1,\frac{1}{2}} - T_{1,-\frac{1}{2}}\right) + \right.\right. \\ &\qquad \left.\left. + \rho^2\left(T_{\frac{1}{2},\frac{1}{2}} - T_{\frac{1}{2},-\frac{1}{2}}\right)\right\} \\ \Pi_2 &= 2c\sum_{m=0}^{\infty}\varepsilon_m\left\{b_m(\nu_m + \nu_{-m}) + h_m(\nu_m - \nu_{-m})\right\} \end{aligned}\right\}, \qquad (28)$$

$$\nu_m = \int_{-a_1}^{u_2} C_{0\lambda}\, s_m\, du = (T_{1,m} - T_{-1,m}) + \rho\left(T_{\frac{1}{2},m} - T_{-\frac{1}{2},m}\right).$$

The functions $T_{m,n}$ with semiwhole indices equal:

$$T_{m,\pm\frac{1}{2}} = \mp\frac{(-1)^m}{\left(m \mp \frac{1}{2}\right)2\pi}\left\{\mathrm{Si}(2v)\Big|_{-u_1-m\pi}^{u_2-m\pi} + \mathrm{Si}(2v)\Big|_{-u_1-\pi/2}^{u_2-\pi/2}\right\},$$

$$T_{\frac{1}{2},-\frac{1}{2}} = \frac{1}{\pi}\left[L(2v)\Big|_{-u_1+\frac{\pi}{2}}^{u_2+\frac{\pi}{2}} - L(2v)\Big|_{-u_1-\frac{\pi}{2}}^{u_2-\frac{\pi}{2}}\right].$$

It is easy to find similar expressions in other cases, if the amplitude distribution of a_0 can be expanded into sinusoidal components. If this is difficult to do, a_0 may not be isolated in distribution (1). Then Π_1 and Π_2 automatically equal zero, since the pattern

$$F_0 = A_0 + iC_0$$

equals zero.

Thus, we finally obtain expressions for the directive gain[1]

$$G = kL\frac{p_{\text{макс}}(u)}{\Pi_\Sigma} \qquad (29)$$

[1]For calculation of G we can use a very convenient method which is presented in [8], however it is not suitable for computation of ζ.

and the scattering coefficient

$$\zeta = 1 - \frac{\eta_{\Sigma 0}}{\eta_{\Sigma}}. \qquad (30)$$

The power which is contained in the main lobe $\eta_{\Sigma 0}$ is determined by the same ratios as η_{Σ}, with replacement of u_1 and u_2 by the coordinates of the first minimums of the pattern u_{10} and u_{20} [see (17)].

Modeling the Patterns

The effectiveness of mathematical modeling significantly depends on how economically the caclulation program is compiled. In the examined case of the discrete presentation of the pattern, it is important to select M, the number of terms in Kotel'nikov's series (11)-(12) which yields a sufficient degree of approximation. As shown in [7], the standard error of approximating the function $F(u) = \sum_{-\infty}^{\infty} F(k\pi)\, s_k$ by the finite series $F_M(u) = \sum_{-M}^{M} F(k\pi)\, s_k$ equals the energy of the rejected "tails" in the series $\pi\left(\sum_{-\infty}^{-M-1} |F(k\pi)|^2 + \sum_{M+1}^{\infty} |F(k\pi)|^2\right)$.

If the F(u) functions diminishes as $\frac{c}{\nu_k}$, then one can find an estimate for the approximation error:

$$\delta_M |F(u) - F_M(u)| \leqslant \frac{0{,}52 \cdot 2^k c}{\sqrt{2k-1}\,(M\pi)^{\frac{2k-1}{2}}}. \qquad (31)$$

At the points $u = m\pi$, the error δ_m equals zero. From condition (31), we compute the number M which yields permissible error at points $u = m\pi + \frac{1}{2}$ which also replaces the infinite limit of summation in the formulas of the preceding sections.

Modeling of the pattern begins with computations for the selected amplitude distribution (1) of the reference ($u = m\pi$) values of the functions $g_m - d_m$ for formulas (4) for $0 \leq m \leq M$. The calculation $4(M+1)$ of the values for these functions should be made by the Philon method [9]. Numerical integration of expressions of type $\int a(\xi)\cos u\xi\, d\xi$ by this method is done for the number of points needed to integrate only one function $a(\xi)$ by Simpson's method.

The found sequences of the functions $g_m - d_m$ are recorded in the working memory of the machine and are further used for detailed study of the antenna characteristics. These characteristics include the

amplitude and phase patterns (in any sector and with random spacing), the position of the main maximum, width of the pattern, etc. [formulas (7)-(13)], as well as the directive gain and scattering coefficient [formulas (29) and (30)]. Direct integration of the pattern significantly increases the time for determining all of these characteristics.

If we examine discrete antennas, the functions g-d are expressed in the form of sums for the number of elements. However, with a large number of elements, it is more convenient to replace the discrete distribution by a continuous [3].

Random Amplitude Distributions

The technique stated above is convenient for computing antennas by the method of statistical tests (Monte Carlo method). This calculation is reduced to obtaining a series of random patterns with statistical characteristics which are equal to the characteristics of the original, and subsequent statistical processing of these patterns. In the field distribution in the apterture, we isolate the regular component $a_0(\xi)$ [see (1)], and we will consider it to be actual (linear phase shift in the aperture is not significant). The random distortions of complex amplitude in the aperture will be described by the functions η ,χ. By assigning the random statistical nature of η and χ, we model a number of their random realizations (samplings) on a computer and find the random beam patterns which correspond to them.

The functions η and χ are obtained in the form of a discrete sequence of random numbers. The sampling spacing is determined by the assigned accuracy of integrating the function $a(\xi)$.

With amplitude-phase distortions, the vector $a(\xi)$ is subordinate to the generalized Rayleigh distribution--η and χ are independent normal quantities with their own averages, dispersions and correlation coefficients. In the case of phase errors alone, the functions η and χ are interlinked. We will examine the latter case as an example, and present η and χ in the form:

$$\eta = a_0(\xi)\Delta(\xi);\ \chi = a_0(\xi)\delta(\xi). \qquad (32)$$

where $\Delta(\xi) = \cos\psi - 1$ and $\delta(\xi) = \sin\psi$.

We will consider the phase ψ normal, having a zero average, dispersion σ_0^2 and correlation coefficient

$$R = e^{-\frac{1}{\rho^2}(\xi_1-\xi_2)^2} \qquad (33)$$

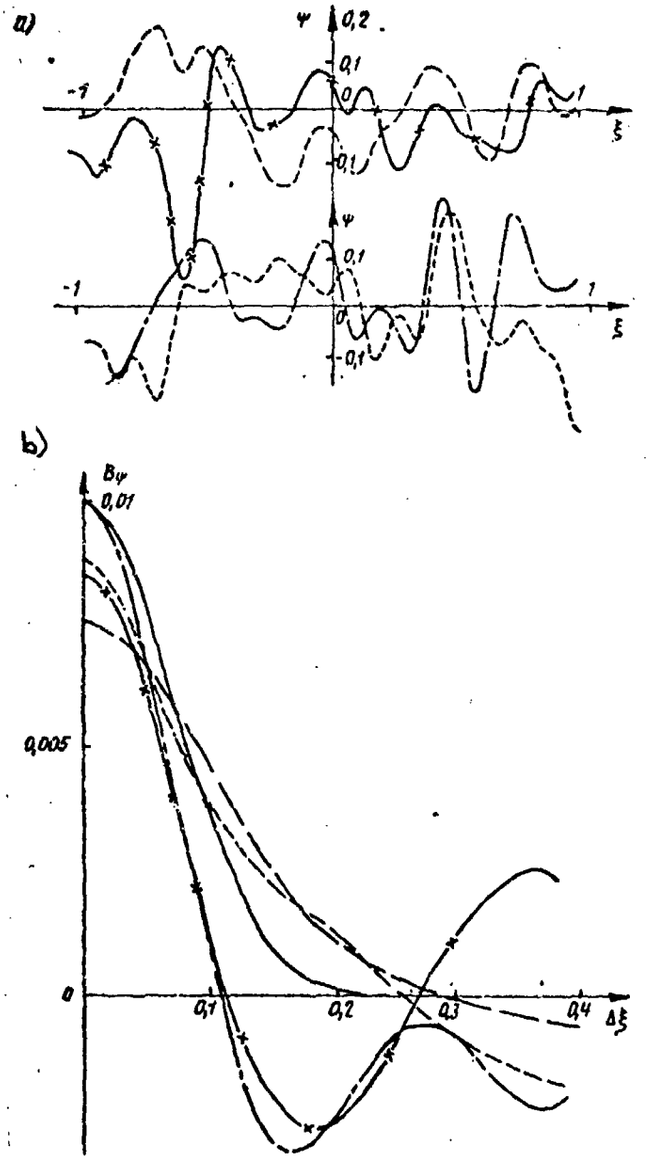

Figure 4.

Figure 4a illustrates the series of random realizations of the function ψ found on the computer for the parameters $\bar{\psi}=0$; $\sigma=0.1$; $\rho=0.1$.

Direct study of the properties of these realizations shows a certain reduction in their percentage of randomness (the average from several samplings $\sigma_0 \approx 0.08$). This is associated with the filtering properties of the machine by means of limitations in the selected program.

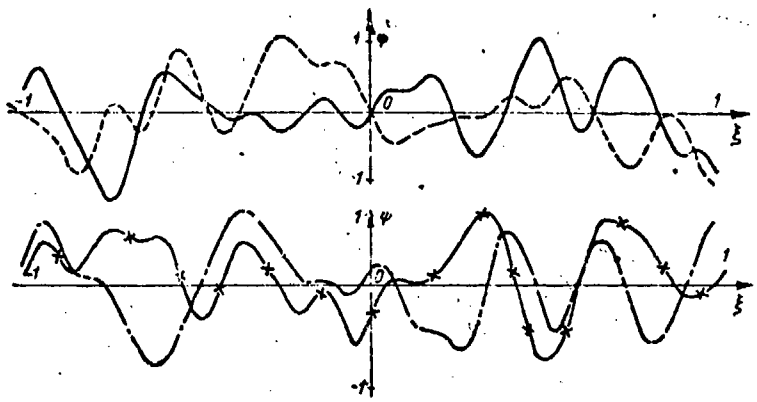

Figure 5.

The correlation coefficient of these realizations is depicted in fig. 4b. Here the original curve (33) (solid line) is plotted for comparison. Figure 5 presents the random samplings of the ψ function with assigned parameters $\bar{\psi} = 0$; $\sigma_0=0.6$; $\rho=0.1$.

Modeling Random Patterns

In order to model the random patterns, each time we make a preliminary computation of the random realizations of the functions η and $\times$ (in the examined case, only the functions ψ). Then the obtained discrete sampling of random numbers is used to compute the functions g_m-d_m. They, in turn, are stored and are the originals for analysis of the beam pattern.

As an example, figure 6 presents a series of random patterns which were computed for realizations of ψ illustrated in fig. 5. The dotted line in this figure illustrates the average pattern of the linear antenna with corresponding parameters.

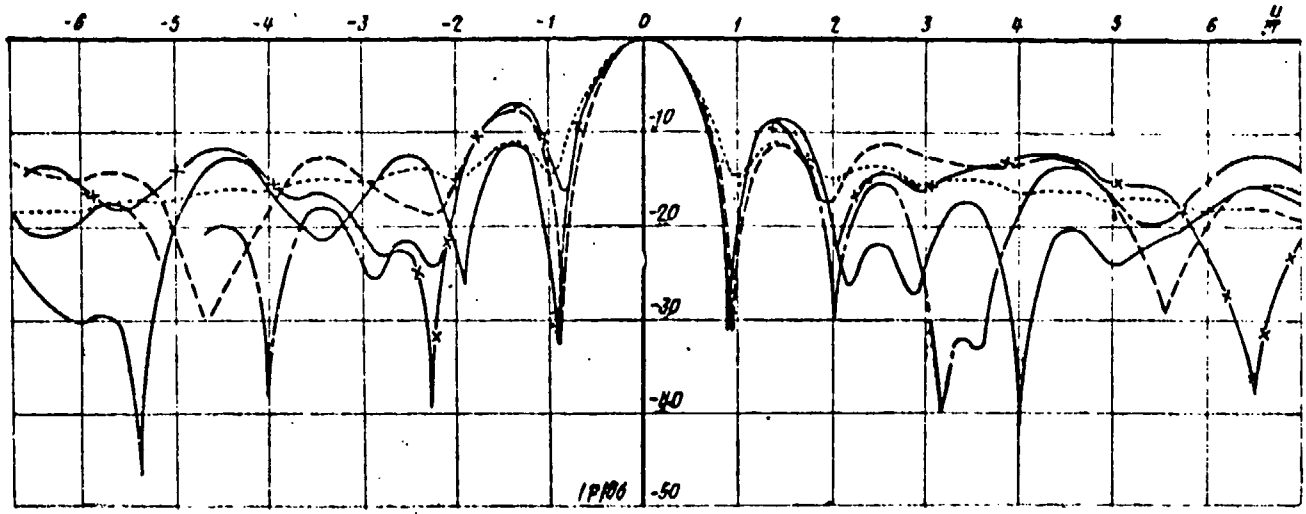

Figure 6.

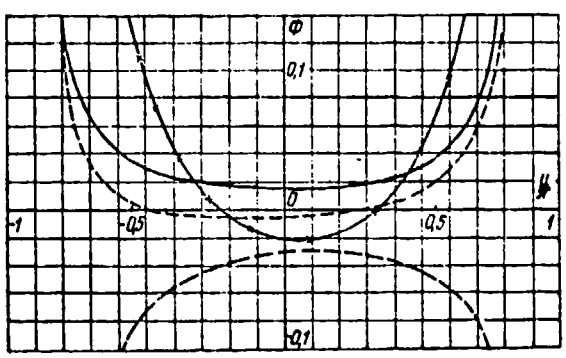

Figure 7.

Figure 7 illustrates the phases of the random patterns for realization of ψ in fig. 5.

When there is a fairly large number of random realizations, we can construct histograms for the main parameters of the patterns. By using the methods of statistical processing of the observation results, the statistical characteristics of the pattern are determined. It is a priori difficult to find the probability properties of the patterns in a whole series of cases, or completely impossible. It is precisely in these cases that the method of statistical tests is called upon to play a larger role.

In conclusion, the author expresses his gratitude to engineer L. D. Klimenko who did a lot of work to program the problem and the corresponding calculations.

Bibliography

1. Zimin, D. B.; and Dolzhenkov, A. A. Radiotekhnika, Vol. 20, No. 2, 1965.

2. Hewson, J.; and Pocello, E. A. The Marconi Rev., Vol. 23, No. 138, 1960, pp. 104-109.

3. Palmer, D. S. The Marconi Rev., Vol. 23, No. 138, 1960, pp. 110-114.

4. Shifrin, Ya. S. Statistika polya lineynoy antenny ["Statistics of the Linear Antenna Field"], Izd. ARTA, Khar'kov, 1962.

5. Bushenko, N. P.; et al., Metod statisticheskikh ispytaniy (metod Monte-Karlo), ["Method of Statistical Tests (Monte Carlo Method)"], SMB, Moscow, GIFML, 1962.

6. Zelkin, Ye. G. Postroyeniye izluchayushchey sistemy po zadannoy diagramme napravlennosti ["Construction of an Emittint System from an Assigned Beam Pattern"], Moscow-Leningrad, Gosenergoizdat, 1963.

7. Khurgin, Ya. I.; and Yakovlev, V. P. Metody teorii tselykh funktsiy v radiofizike, teorii svyzi i optike ["Methods of the Theory of Whole Functions in Radio Physics, Theory of Communications and Optics"], Moscow, GIFML, 1962.

8. Peresada, V. P. Radiotekhnika, Vol. 14, No. 8, 1959, pp. 71-74.

9. Tranter, K. D. Integral'nyye preobrazovaniya v matematicheskoy fizike ["Integral Transforms in Mathematical Physics"], Moscow, GITTL, 1956.

COMPENSATION FOR SYSTEMATIC WEIGHT DEFORMATIONS OF MIRROR SYSTEM OF PARABOLIC RADIO TELESCOPES

B. A. Poperechenko and N. M. Feyzulla

Summary

An examination is made of the nature of the phase errors in field distribution in the aperture of a radio telescope which develop under the influence of weight deformations of the main mirror and the support structures of the irradiating system.

Based on an analysis of the normed functions of individual components in the errors, a technique for their mutual compensation is suggested.

Introduction

The trend of developing full-rotating mirror-parabolic radio telescopes is characterized by a constant rise in the dimensions of the mirrors. This raises the primary problem of maintaining the shape of their working surface.

At the early stages of development of the technology of mirror antennas, the striving to guarantee accuracy was expressed as a requirement that the deviation from the ideal profile would not exceed the assigned limit (usually 1/16 of the working wavelength) over the entire or part of the mirror surface.

Of course, this places excessively strict requirements on both the technology and the design.

The statistical approach [1,2,3] makes it possible to consider more completely the factors which influence the quality indicators of the mirror radio telescopes.

The influence of the statistical factors is considerably reduced in the radio telescopes whose reflecting surface is designed in the form of precisely formed panels which are set during the initial adjustment. Consequently, the main factor which determines the limiting working wavelength is the deformation of the design under the influence of wind (to a considerable measure accidental) and weight (systematic) loads.

The attempt to reduce these deformations to a given limit results in the unjustified increase in the weight of the metal structures. Therefore, in the practice of designing large radio telescopes, different methods are encountered more often for compensating for the deformations. These methods reduce the requirements for rigidity of the designs.

There are known methods, for example, of compensating with the help of automatic correction for the position of individual elements in the working surface of the main mirror, or counterreflector of the radio telescope [4,5]. In this case, a considerable number of tracking devices are used with fairly cumbersome power actuating mechanisms. The placement of these mechanisms on the designs of the radio telescope significantly increases the weight of its mirror.

It is therefore more promising to use the method based on the mutual compensation for deformations of different elements in the mirror system: metal structures of the main mirror and support structures of the irradiating system. In this case, the main mirror is designed not for the minimum of deformations, but for the minimum deviation of its surface from the profile which is the most convenient for mutual compensation [6].

This method makes it possible to compensate only for systematic deformations which develop under the influence of the weight loads. But, if one considers that this percentage of deformation for large radio telescopes is no less than 85%, and with an increase in the dimensions of the radio telescope, it increases even more, then it becomes understandable why this method of compensation is promising precisely for large instruments.

This work examines the mutual weight compensation for deformations in metal structures of the mirror system of radio telescopes. It is done by selecting the rigidity of the support structures of the irradiating system and the loads on these structures, and in certain limits, by selecting the distribution of rigidity between the design elements of the main mirror.

In this case, the supports of the irradiating system must be designed so that the required laws for movement of the primary irradiator and counterreflector are guaranteed in a vertical plane in the function of the elevation position of the radio telescope. Further, the indicated longitudinal and transverse shifts in the primary irradiator and the counterreflector, and the rotation angle of the latter will be called the compensation parameters. In addition, it is suggested that the elevation correction which is made in the guidance system of the radio telescope be used as the compensation parameter. All the indicated weight compensation parameters must be programmed.

It should be noted that selection of the distribution of rigidity between the design elements of the main mirror makes it possible to obtain that law of large-scale deformations of its surface which promotes the most complete weight compensation.

General Correlations

In order to compute the compensation parameters, we will write the equation of the phase front [7] in the aperture of the radio telescope with regard for all the indicated distortions in the mirror system as applied to a two-mirror system of irradiation. This plan is used most often in the short wavelength region of the working range of the radio telescope, where compensation for deformations is primarily needed. We note that the weight deformations of the reflecting surface of the counterreflector proper are not used in the calculation. They are usually insignificant.

We will use the Cartesian coordinate system with beginning at the focus of an undistorted main mirror with axis z which coincides with its focal axis (fig. 1). We will designate the position of the phase center of the irradiator with regard for the weight displacements

$$\bar{X}_1 = \bar{j}\Delta\Phi_y + \bar{k}(-\Phi + \Delta\Phi_z) = \Delta\bar{\Phi} - \bar{k}\Phi.$$

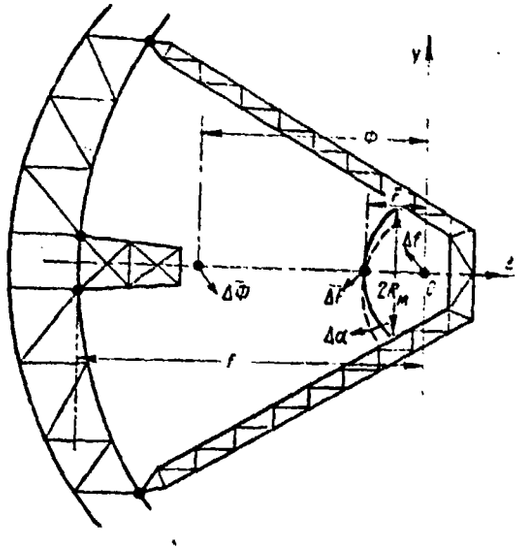

Figure 1.

The weight displacements of the apex of a small mirror will be characterized by the vector

$$\Delta\bar{X}_2 = \bar{j}\Delta F_y + \bar{k}\Delta F_z = \Delta\bar{F},$$

while its angular deviation from the calculated position under the influence of the weight loads, by the angle $\Delta\alpha$.

It is assumed everywhere that the weight loads cause shifts in the elements of the irradiating system only in a vertical plane.

The profile of the main mirror with regard for its weight deformations

$$\bar{R} = \bar{i}(x + \delta x(x, y)) + \bar{j}(y + \delta_y(x, y)) + \bar{\kappa}\left(\frac{x^2+y^2}{4f^2} - f + \delta_z(x, y)\right),$$

where f--focal distance of the main mirror,
$\delta_x, \delta_y, \delta_z$--components of the deviation of the surface from parabolic shape under the influence of weight loads.

The hyperbolic profile of the displaced small mirror

$$\bar{\rho} = \bar{i}x_M + \bar{j}[y_M + \Delta F_y - \Delta\alpha(F + z_M)] + \bar{\kappa}[z_M + \Delta F_z + \Delta\alpha y_M],$$

where

$$z_M = \left(\frac{\Phi}{2} - F\right)\sqrt{1 + \frac{x_M^2 + y_M^2}{F(\Phi - F)}} - \frac{\Phi}{2},$$

Φ--calculated distance between the foci of the main and small mirror,
F--calculated distance of the apex of the small mirror from the focus of the main mirror.

We will write the ratios that interlink the incident and reflected wave fronts for both mirrors. We will express the single perpendicular to the front of the incident wave as

$$\bar{r}_M = \frac{\bar{\rho} - \bar{X}_1}{|\bar{\rho} - \bar{X}_1|} \quad \text{and} \quad \bar{r} = \frac{\bar{R}}{|\bar{R}|}.$$

The perpendicular for the front of the reflected wave is written as

$$\bar{\xi}_M = \frac{\bar{Y}_M - \bar{\rho}}{|\bar{Y}_M - \bar{\rho}|} \quad \text{and} \quad \bar{\xi} = \frac{\bar{Y} - \bar{R}}{|\bar{Y} - \bar{R}|},$$

where $\bar{Y}_M$ and $\bar{Y}$--vectors of the surface of the front of the reflected wave for the small and main mirrors respectively.

The single perpendiculars to the surface of the mirrors are correspondingly equal to:

$$\bar{\eta}_M = \frac{\frac{\partial \bar{\rho}}{\partial x} \times \frac{\partial \bar{\rho}}{\partial y}}{\left| \frac{\partial \bar{\rho}}{\partial x} \times \frac{\partial \bar{\rho}}{\partial y} \right|} \quad \text{and} \quad \bar{\eta}_1 = \frac{\frac{\partial \bar{R}}{\partial x} \times \frac{\partial \bar{R}}{\partial y}}{\left| \frac{\partial \bar{R}}{\partial x} \times \frac{\partial \bar{R}}{\partial y} \right|}.$$

The condition for equality of the angles of incidence and reflection looks like

$$\bar{\xi}_M - \bar{r}_M = -2\bar{\eta}_M (\bar{\eta}_M \bar{r}_M) \quad \text{and} \quad \bar{\xi} - \bar{r} = -2\bar{\eta}_1 (\bar{\eta}_1 \bar{r}).$$

Then the equations of the fronts

$$Y_M = \bar{X}_1 + 2\bar{\eta}_M (\bar{\eta}_M (\bar{\rho} - \bar{X}_1)), \quad \bar{Y} = 2\bar{\eta}_1 (\bar{\eta}_1 \bar{R}).$$

The equations of errors d in the form of wave fronts are expressed as a scalar product of the vectors for the deformed and non-deformed wave fronts:

$$d_M = \bar{n}_M Y_M, \quad d = \bar{n}\bar{Y}.$$

Here $\bar{n}$--perpendicular to the planar surface, perpendicular to the direction of the maximum radiation of the antenna. Bearing in mind the already mentioned small elevation correction for the position of the radio axis of the antenna $\Delta\beta$, we write $\bar{n} \approx \bar{j}\Delta\beta + \bar{k}$.

The perpendicular to the undistorted spherical front which is reflected from the small mirror, is expressed through the current coordinates of the point on the surface of this mirror:

$$n_M = \frac{\bar{i}x_M + \bar{j}y_M + \bar{\kappa}\left[\left(\frac{\Phi}{2} - F\right)\sqrt{1 + \frac{x_M + y_M}{F(\Phi - F)}} - \frac{\Phi}{2}\right]}{\sqrt{x_M^2 + y_M^2 + \left[\left(\frac{\Phi}{2} - F\right)\sqrt{1 + \frac{x_M^2 + y_M^2}{F(\Phi - F)}} - \frac{\Phi}{2}\right]^2}}.$$

The positive values d_M and d correspond to the shortened rays, and consequently, the leading phase.

The resulting errors in the phase front which take into consideration both the deformation of the main mirror, and the mutual movements of all irradiation elements, will be presented approximately as the sum $\Delta \approx d + d_M$.

This summation suggests the insignificance of the error in determining d_M near the surface of the main mirror as a consequence of ignoring the difference in the directions of the radius from the begining of the coordinates and the true beam that is reflected from the small mirror. We will estimate the limits of correctness of this hypothesis.

It follows from the equation of the eikonal for a uniform medium that

$$|\operatorname{grad}_s L|^2 = 1 - |\operatorname{grad}_q L|^2,$$

where

$$L = q(x, y) - d_{M_{\text{ист}}}(x, y),$$

$\operatorname{grad}_s L$--gradient of eikonal in plane tangential to the sphere,
$\operatorname{grad}_q L$--the same, in a radial direction,
$q(x,y)$--equation of spherical surface.

By transforming the right side of the equality, we obtain

$$|\operatorname{grad}_s L|^2 = |\operatorname{grad}_s d_{M_{\text{ист}}}(x, y)|^2 = (1 + |\operatorname{grad}_q L|)(1 - |\operatorname{grad}_q L|) =$$
$$= \left(2 + \frac{\partial d_{M_{\text{ист}}}}{\partial q}\right)\frac{\partial d_{M_{\text{ист}}}}{\partial q} \approx 2\frac{\partial d_{M_{\text{ист}}}}{\partial q},$$

where we assume $\frac{\partial d_{M_{\text{ист}}}}{dq} \ll 1$.

Then the error in determining the distortion of the phase front at the surface of the main mirror that we are interested in

$$|\delta d| = (|Y_M|(x_M, y_M) - q)\frac{\partial d_{M_{\text{ист}}}}{\partial q} =$$
$$= \frac{(|Y_M|(x_M, y_M) - q)\,|\operatorname{grad}_s d_{M_{\text{ист}}}(x, y)|}{2}.$$

Taking into consideration that $d_M(x,y)$ basically has a large-scale nature, in our estimates one can consider with sufficient accuracy that

$$\operatorname{grad}_s d_{M_{\text{ист}}}(x, y) \approx \operatorname{grad} d_M(x, y).$$

For quantitative estimate, we will adopt the quantity of permissible error in computing the weight compensation 1/20 -1/30 from the shortest working wave of the TNA-1500 radio telescope with a main mirror 64 m in diameter with focal distance of 23.6 and counter-reflector 5 m in diameter. This quantity is about 1 mm.

Then the maximum permissible value

$$|\operatorname{grad} d_M(x, y)|_{\text{доп}} = \sqrt{\frac{2|\delta d|}{|R|-q}} \approx 10^{-2}.$$

This corresponds, for example, to 10 mm deviation in the phase front from the sphere for 1 m of the displacement on the sphere surface near the small mirror.

A fairly smooth nature of deformations in the main mirror is also hypothesized in the further calculations. This is always guaranteed in real designs.

Taking into consideration the adopted limitations, and omitting in the expressions d_M and d the quantities of the second order of smallness and the constant components, after all the necessary calculations, we obtain the unknown distortions in the expressions of the wave fronts:

$$d_M = \frac{-2\Delta F_z \sqrt{1+\frac{x_M^2+y_M^2}{F(\Phi-F)}} - \frac{y}{F}\left\{2\Delta F_y \frac{\frac{\Phi}{2}-F}{\Phi-F} - 2\Delta\alpha \frac{\frac{\Phi^2}{4}}{\Phi-F}\right\} \times \rightarrow}{1+\frac{x_M^2+y_M^2}{F(\Phi-F)}\frac{\Phi^2}{4F(\Phi-F)}}$$

$$\rightarrow \times \left[\sqrt{1+\frac{x_M^2+y_M^2}{F(\Phi-F)}} - \left(\frac{\frac{\Phi}{2}-F}{\frac{\Phi}{2}}\right)^2\right] + \Delta\Phi_y \frac{\frac{\Phi}{2}}{\Phi-F} \times \rightarrow$$

$$\rightarrow \times \left[\sqrt{1+\frac{x_M^2+y_M^2}{F(\Phi-F)}} - \frac{\frac{\Phi}{2}-F}{\frac{\Phi}{2}}\right] \Delta\Phi_z 2\sqrt{1+\frac{x_M^2+y_M^2}{F(\Phi-F)}} +$$

$$+ \Delta\Phi_z \frac{\left(\frac{\Phi}{2}-F\right)\sqrt{1+\frac{x_M^2+y_M^2}{F(\Phi-F)}} - \frac{\Phi}{2}}{\frac{\Phi}{2}\sqrt{1+\frac{x_M^2+y_M^2}{F(\Phi-F)}} - \left(\frac{\Phi}{2}-F\right)},$$

$$d = \Delta\beta\, y + \frac{-\frac{x}{f}\,\delta_x(x,\ y) - \frac{y}{f}\,\delta_y(x,\ y) + 2\delta_z(x,\ y)}{1 + \frac{x^2 + y^2}{4f^2}}.$$

In order to add these two expressions with regard for the approximation that has been made, we will express it through the same argument x,y. For this purpose we use the link between x,y and x_M, y_M which follows from the geometric considerations:

$$\frac{x_M}{x} = \frac{y_M}{y} = \frac{\left(\frac{\Phi}{2} - F\right)\sqrt{1 + \frac{x_M^2 + y_M^2}{F(\Phi - F)}} - \frac{\Phi}{2}}{\frac{x^2 + y^2}{4f} - f} = \frac{z_M}{z}.$$

We obtain a solution for the given system of equations:

$$y_M = y\,\frac{Ff - (\Phi - F)\frac{x^2 + y^2}{4f}}{\left(\frac{x^2 + y^2}{4f} - f\right)^2 - \left(\frac{\Phi}{2} - F\right)^2 \frac{x^2 + y^2}{F(\Phi - F)}},$$

$$x_M = x\,\frac{Ff - (\Phi - F)\frac{x^2 + y^2}{4f}}{\left(\frac{x^2 + y^2}{4f} - f\right)^2 - \left(\frac{\Phi}{2} - F\right)^2 \frac{x^2 + y^2}{F(\Phi - F)}}.$$

With regard for the obtained correlations in the coordinates of the main mirror surface

$$d_M = \frac{2\Delta F_z AB + \Delta\Phi_z\,(-AB + E^2)\frac{x^2 + y^2}{4f^2} \cdot 4\,\frac{\left(\frac{\Phi}{2} - F\right)\frac{\Phi}{2}}{F^2} + \rightarrow}{G}$$

$$\rightarrow + y\left\{2\Delta F_y \frac{\frac{\Phi}{2} - F}{F(\Phi - F)} A^2 + 2\Delta\alpha \frac{\left(\frac{\Phi}{2}\right)^2}{F(\Phi - F)} AD - \Delta\Phi_y \frac{\frac{\Phi}{2}}{F(\Phi - F)} AC\right\}$$

$$G$$

where

$$A = \left(\frac{x^2 + y^2}{4f^2} - 1\right)^2 - \frac{4\left(\frac{\Phi}{2} - F\right)^2}{F(\Phi - F)} \frac{x^2 + y^2}{4f^2};\quad B = \left(\frac{x^2 + y^2}{4f^2}\right) -$$

$$-1+\frac{4\frac{\Phi}{2}\left(\frac{\Phi}{2}-F\right)}{F(\Phi-F)}\frac{x^2+y^2}{4f^2};$$

$$C=\frac{x^2+y^2}{4f^2}-1+\frac{\frac{\Phi}{2}-F}{\frac{\Phi}{2}}\left(\frac{x^2+y^2}{4f^2}+1\right)^2;\ D=\left(\frac{x^2+y^2}{4f^2}\right)^2-1+$$

$$+\left(\frac{\frac{\Phi}{2}-F}{\frac{\Phi}{2}}\right)^2\left(\frac{x^2+y^2}{4f^2}-1\right)^2+\frac{4\left(\frac{\Phi}{2}-F\right)^2}{F(\Phi-F)}\left[\frac{\frac{\Phi}{2}}{\frac{\Phi}{2}-F}-\right.$$

$$\left.-\frac{\left(\frac{\Phi}{2}-F\right)^2}{\left(\frac{\Phi}{2}\right)^2}\right]\frac{x^2+y^2}{4f^2};$$

$$E=\frac{x^2+y^2}{4f^2}-\frac{F}{\Phi-F};\ G=B^2+E^2\frac{x^2+y^2}{4f^2}\frac{4\left(\frac{\Phi}{2}-F\right)^2}{F^2}.$$

The obtained expressions d and d_M may be used to compute the mutual compensation of the axial and transverse deformations of the main mirror and the designs for attaching the irradiating system.

The design calculation of the mirror does not reveal the three components of deformations $\delta_x(x,y)$, $\delta_y(x,y)$ and $\delta_z(x,y)$ indicated in the formulas above, but the two functions equivalent to them $\delta_r(r,\phi)$ and $\delta_z(r,\phi)$ expressed in a cylindrical system of coordinates, where

$$\delta_x(x,\ y)=\delta_r(r,\ \varphi)\cos\varphi;\ \delta_y(x,\ y)=\delta_r(r,\ \varphi)\sin\varphi;$$
$$\delta_z(x,\ y)=\delta_z(r,\ \varphi);\ r=\sqrt{x^2+y^2};\ \operatorname{tg}\varphi=\frac{y}{x}.$$

Then in the cylindrical system of coordinates

$$d=\Delta\beta r\sin\varphi+\frac{-\frac{r}{f}\delta_r(r,\ \varphi)\cos^2\varphi-\frac{r}{f}\delta_r(r,\ \varphi)\sin^2\varphi+2\delta_z(r,\ \varphi)}{1+\frac{r^2}{4f^2}}.$$

We transform the obtained expression:

$$d=\frac{1}{1+\frac{r^2}{4f^2}}\left\{2\delta_z-\frac{r}{f}\delta_r+r\sin\varphi\left[\Delta\beta\left(1+\frac{r^2}{4f^2}\right)\right]\right\}.$$

By isolating in the expression for d, the axisymmetrical component and the first angular harmonics, we will obtain the final expressions which are convenient for the compensation calculations:

$$d_0 = -\frac{1}{1+\frac{r^2}{4f^2}}\left(2\delta_{z_0} - \frac{r}{f}\delta_{r_0}\right), \tag{1}$$

$$d_1 = \left[\frac{2\delta_{z_1} - \frac{r}{f}\delta_{r_1}}{1+\frac{r^2}{4f^2}} + r\Delta\beta\right]\sin\varphi, \tag{2}$$

$$d_{выем} = d - d_0 - d_1. \tag{3}$$

Thus, the resulting error

$$Д = \frac{2\Delta F_z AB + \Delta\Phi_z\left[-AB + E^2\frac{r^2}{4f^2} - \frac{4\frac{\Phi}{2}\left(\frac{\Phi}{2}-F\right)}{F^2}\right]}{G} +$$

$$+ \frac{r\sin\varphi\left\{2\Delta F_y A^2\frac{\frac{\Phi}{2}-F}{F(\Phi-F)} + 2\Delta\alpha\, AD\frac{\left(\frac{\Phi}{2}\right)^2}{F(\Phi-F)} - \Delta\Phi_y\, AC\frac{\frac{\Phi}{2}}{F(\Phi-F)}\right\}}{G} +$$

$$+ \frac{2\delta_z - \frac{r}{f}\delta_r}{1+\frac{r^2}{4f^2}} + r\Delta\beta\sin\varphi - \Delta F_z(\beta)\Delta_1\left(\frac{r}{f}\right) +$$

$$+ \Delta\Phi_z(\beta)\Delta_2\left(\frac{r}{f}\right) + r\sin\varphi\left\{\frac{\Delta F_y(\beta)}{F}\Delta_3\left(\frac{r}{f}\right) + \Delta\alpha(\beta)\Delta_4\left(\frac{r}{f}\right) +\right.$$

$$\left. + \frac{\Delta\Phi_y(\beta)}{\Phi-F}\Delta_5\left(\frac{r}{f}\right)\right\} + \frac{2\delta_z(\beta, r, \varphi) - \frac{r}{f}\delta_r(\beta, r, \varphi)}{1+\frac{r^2}{4f^2}} + r\sin\varphi\Delta\beta(\beta),$$

where $\Delta F_z(\beta)$, $\Delta\Phi_z(\beta)$, $\Delta F_y(\beta)$, $\Delta\alpha(\beta)$, $\Delta\Phi_y(\beta)$, $\Delta\beta(\beta)$ --parameters of compensation and $\Delta_i\left(\frac{r}{f}\right)$--normed functions of partial distortions of the wave front for the corresponding parameters of compensation.

The condition for complete compensation is presented in the form of the equality $Д$ to the constant for each of the angles β. Since this condition is not feasible in accuracy, then from $Д$ we should isolate the part which completely satisfies this condition with the minimum residual part. This residual in the final analysis also limits the maximum wave of the radio telescope.

Since in real designs, the calculation is not successful in determining and realizing the compensation parameters with the necessary precision, then one should stipulate the possibility of regulating their dependences on β.

The compensation parameters $\Delta F_x(\beta)$, $\Delta F_y(\beta)$, $\Delta\Phi_x(\beta)$, $\Delta\Phi_y(\beta)$ contain nonregulated and regulated parts. The first of them inevitably arise as a consequence of the nonabsolute rigidity of the design of the irradiating system. The second are created by force and are roughly regulated through selecting the rigidity of the designs in planning, as well as more accurately by selecting the weight and arrangement of the adjustment loads when the compensation system is tuned. The compensation system tuning is controlled with the use of special control and measuring equipment accordng to the technique examined below.

Calculation of the Compensation Parameters

In addition to the analytical solution to the problem of minimizing the errors in the wave front that requires the use of a computer, a graph-analytical method of compensation computation is also possible. We will examine it in the example of the TNA-1500 radio telescope with diameter 64 m with focal distance 23.6 m ($2\psi_0=136°$). We will take two variants of the two-mirror plan: with fairly large focal distance of the small hyperbolic mirror $\Phi=f=23.6$ m (distance between the focuses and with fairly small focal distance 5 m). The latter variant corresponds to the distance of the irradiator from the apex of the small mirror 3.5 m. With $2\psi_0=136°$, the parameters of the mirror system which are used in the calculation are given in the following table for both versions.

TABLE

Versions	Geometric parameters of mirror system						
	Φ, м	$F(\Phi-F)$, м²	$\frac{\Phi}{2}-F$, м	F, м	$\frac{\Phi}{2}\left(\frac{\Phi}{2}-F\right)$, м²	$\Phi-F$, м	$\frac{\Phi}{2}$, м
Version I	23,6	39	10	1,8	118	21,8	11,8
Version II	5	5,25	1,0	1,5	2,5	3,5	2,5

In calculating the parameters presented in the table, the following correlation was used

$$F(\Phi - F) = -\frac{1}{2}\frac{R_M}{\sin^2\psi_0}\left\{\frac{R_M}{\sin^2\psi_0} - \Phi\cos\psi_0 - \sqrt{\left(\frac{R_M}{\sin^2\psi_0} - \Phi\cos\psi_0\right)^2 + 4\left(\frac{\Phi}{2}\right)^2\sin^2\psi_0}\right\} = Q.$$

From here, with assigned Φ

$$F = \frac{\Phi}{2} - \sqrt{\left(\frac{\Phi}{2}\right)^2 - Q}.$$

For both versions, we will construct graphs for normed functions for each of the compensation parameters (fig. 2):

for $\Delta F_z(\beta)$:

$$\Delta_1\left(\frac{r}{f}\right) = \frac{2B}{G}; \qquad (4)$$

for $\Delta\Phi_z(\beta)$

$$\Delta_2\left(\frac{r}{f}\right) = \frac{-B + \frac{E^2}{A}\frac{r^2}{4f^2}4\frac{\frac{\Phi}{2}\left(\frac{\Phi}{2} - F\right)}{F^2}}{\frac{G}{A}}; \qquad (5)$$

for $\frac{\Delta F_y}{F}$

$$\Delta_3\left(\frac{r}{f}\right) = \frac{2A\frac{\frac{\Phi}{2} - F}{\Phi - F}}{\frac{G}{A}}; \qquad (6)$$

for $\Delta_z(\beta)$

$$\Delta_4\left(\frac{r}{f}\right) = -\frac{2D\frac{\frac{\Phi}{2}}{F(\Phi - F)}}{\frac{G}{A}}; \qquad (7)$$

for $\frac{\Delta\Phi_y(\beta)}{\Phi - F}$

$$\Delta_5\left(\frac{r}{f}\right) = -\frac{C\frac{\frac{\Phi}{2}}{p}}{\frac{G}{A}}. \qquad (8)$$

Compensation for the weight deformations in the main mirror is

achieved by selecting the scale of the functions $\Delta_i(\frac{r}{f})$ separately for symmetrical (Δ_1, Δ_2) and skew-symmetric (first version) (Δ_3, Δ_4, Δ_5) components as applied to the law of its deformations $d(\frac{r}{f})$. As the elements which realize the weight compensation in the design of the radio telescope, the central arrow of the irradiator and its fastening elements on the main mirror, the support shape of the small mirror and the elements of fastening it to the beam, and the device of elevation compensation in the guidance system are used. In addition, it stands

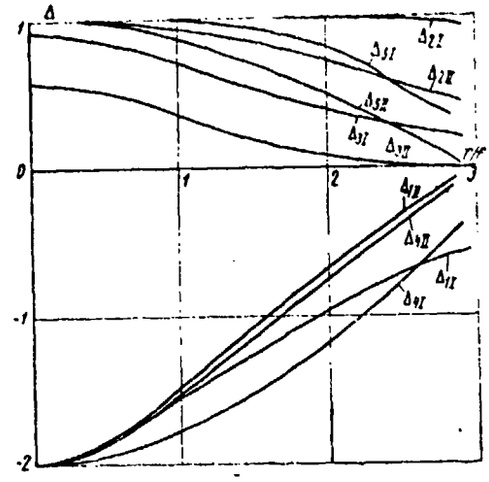

Figure 2.

to reason that measures are taken in designing the main mirror so that the functions d_0 and d_1 are obtained which are the most convenient for compensation. It is apparent from the graphs in fig. 2 that depending on the geometric parameters of the irradiating system, the nature of the function Δ_i changes. This can also be used for weight compensation.

The criterion for optimal compensation is the minimum value of the standard error of the phase front $\sigma(\beta)$ which is average in the entire working interval of the antenna positions in the half-space:

$$\sigma_{cp} = \frac{1}{\frac{\pi}{2}} \int_0^{\frac{\pi}{2}} \sigma(\beta) \cos\beta \, d\beta.$$

where $$\sigma(\beta) = \sqrt{\frac{1}{S_0}\int_{S_0}\frac{I_0(s)}{I_{0m}}[d_{\text{выбеш}}(s,\beta)+d_{\text{остат}}(s,\beta)]^2\,ds}$$

--effective (with regard for the distribution of amplitudes in the aperture) standard error in the phase front.

The formula for $\sigma(\beta)$ designates:

$\frac{I_0(s)}{I_{0m}}$ — aperture distribution of field,

$d(s,\beta)$ — determined by expression (3),

$d_{\text{остат}}$ — error in phase front as a consequence of incomplete weight compensation of the symmetrical and skew-symmetrical deformation components.

The adjustment and verification of the system of weight compensation of the radio telescope uses a range finder device which controls the displacement of the datum marks attached to the working surface of the main mirror. The two-way device of the range finder is installed near the focus or directly in the focus of the corresponding irradiation circuit. The initial attachment of the long-range device is made with the zenith position of the radio telescope from the results of high-precision geodetic control of the condition of its working surface and the position of the elements in the irradiating system.

The functioning of the compensation system is checked from the change in distances to the datum points with a change in the angle of the radio telescope site. In this case, in order to eliminate the effect of the variable weight components of deformations that develop under the influence of the wind loads, one-sided solar heating, etc. it is expedient to control the distances to the datum points in the range of azimuth positions in limits of 360° for each fixed angle of the site.

For a one-mirror system, if it is necessary, compensation of the weight deformations can also be done. In this case, the functions for compensation for the axisymmetrical deformations Δ_6 and for the skew-symmetrical deformations Δ_7 are expressed through displacement

in the phase center of the irradiator Δf_z and Δf_y by the formulas:

for $\Delta f_z(\beta)$ $$\Delta_6\left(\frac{r}{f}\right) = -\frac{2}{1+\frac{r^2}{4f^2}};$$

for $\Delta f_y(\beta)$ $$\Delta_7\left(\frac{r}{f}\right) = -\frac{\frac{1}{f}}{1+\frac{r^2}{4f^2}}.$$

Distortions in the phase front under the influence of Δf_z and Δf_y and deformation of the mirror

$$\Delta = \Delta f_z(\beta)\Delta_6\left(\frac{r}{f}\right) + r\sin\varphi\,\Delta f_y(\beta)\Delta_7\left(\frac{r}{f}\right) + d.$$

The compensation technique is the same as for the two-mirror system.

The suggested method of mutual weight compensation of the main mirror and the support of the irradiator system is done by selecting the laws of weight deformations without making excessively high requirements for the absolute rigid metal structures of the mirror system. The calculations confirm the feasibility of the indicated requirements and the obtaining of a significant weight compensation. This method should be acknowledged as one of the main means of guaranteeing the possible operation of especially large radio telescopes in the centimeter wave range. Since the percentage of weight deformations as compared to the wind deformations rises for larger radio telescopes with an increase in their diameter, then the effectiveness of this method for these radio telescopes must rise. In this case, the optimal movement of the support structures of the irradiating system can be guaranteed not only by selecting their rigidity and loads, but also by forced movement of the elements in the irradiating system.

In conclusion, the authors express their gratitude to I. V. Vavilova for detailed and useful discussion of the article manuscript.

Bibliography

1. Ruse, J. M. "Antenna Tolerance Theogr. Review," Proc. IEEE, 54, No. 4, 1966, pp. 633-640.

2. Salomonovich, L. Ye. "Statistical Evaluation of the Effect of Accuracy and Rigidity of Antenna of Radio Telescope on Its Parameters," Tr. FIAN, 28, 1965, 100-103.

3. Bracewell, R. N. "Tolerance Theory of Large Antennas," IRE Trans. AR-9, No 1, 1961, p. 49-58.

4. Tyrrell, F. C.; and Asce, F. "The Big Dish," Civil Eng., USA, November, 1959.

5. Ayzenberg, A. L. "Possibilities of Phase Correction on Small Mirror in Two-Mirror Antenna," Antenny ["Antennas"], collection edited by A. A. Pistol'kors, No. 2, 1967.

6. Kristen Rolifs, "Das Bonner 90 m Radioteleskop," Sterne und Weltrum, Vol. 5, No. 5, 1966, pp. 104-107.

7. Kellecher, K. S. "Relation Concerning Wave Fronts and Reflectors," J.A.P., Vol. 20, No. 6, 1950. p. 573.

INPUT IMPEDANCE OF SYSTEM MADE OF INTERSECTING LOW-SET VIBRATORS

V. P. Kul'tsep

Summary

The Hansen-Bekerly method is used to determine the input impedance of a system made of symetrical vibrators with sinusoidal current distribution which intersect at the power point and are suspended at a low altitude above the earth.

A single low-set vibrator is examined as a particular case. Results are presented from measurements of the input impedance of the system of intersecting vibrators in the short-wave and medium-wave ranges.

Introduction

In determining the complete input impedance of a low-set symmetrical vibrator, the latter is generally represented by equivalent segments of a long line. The linear parameters of the line are found by analyzing a line of infinite length with the same geometry of the cross section. This calculation provides values of the reactive part of the complete input impedance which are satisfactory for practice. The results of this calculation show that the input impedance of a low-set vibrator is mainly determined by the linear successive impedance R_1 which lies in limits from $30\pi^2/\lambda$ Ohm/m for ground with infinite conductance to $60\pi^2/\lambda$ Ohm/m for purely dielectric ground[1,2].

The generalized method of How makes it possible to obtain a constant component of the input impedance which does not depend on the frequency [1]. Dipole [3] and multipole components are also known which are proportional to the square and higher degrees of frequency.

All the components can be taken into account by introducing a certain equivalent linear impedance $R_{1э}$ which for short conductors may significantly exceed R_1 [4], or by computing the input impedance by one of the strict methods. Two methods are quite strict on the condition that the current distribution is assigned: the directed emf and the Hansen-Bekerly. These methods are equivalent in the strictness of general expressions. However, in computing the near-earth antennas by the first method, the emf which is directed by a field reflected from the earth, is only taken into account approximately, especially for the induction components of the field. In particular, the constant component of losses in computing by the directed emf method generally drops out of the solution. At the same time, this component has a significant value for the electrically short antennas.

The purpose of this work is to determine the input impedance of a system made of N symmetrical vibrators 2L long and d in diameter which intersect at the power point at angle ϕ_1 and which are suspended at altitude h above the surface of homogeneous ground with permeability ε and conductance σ using the Hansen-Bekerly method. The input impedance of a single vibrator is found in a particular case.

The Hansen-Bekerly method has already been used to determine the input impedance of a single vibrator, however, the analysis either did not take into consideration the most significant induction component of losses [5] or was limited to the case of a low-conducting ground [6],

Statement of the Task

We will examine an idealized system made of 2N flat current sectors with radius L located at altitude h (fig. 1). We assume that the average width of the sector equals the diameter of the vibrator ($d=\phi_0 L$). We make an axis of the cylindrical coordinate system ρ, ϕ and z through the intersection point of the sectors.

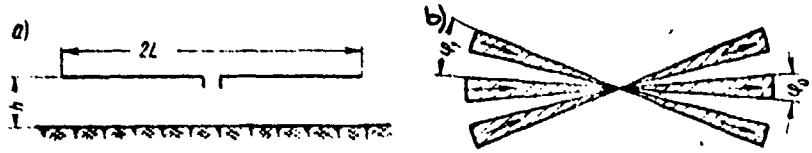

Figure 1.

It is known [7] that the stream of active power which passes through the plan located above the emitter with assigned current distribution, precisely equals

$$P_1 = 60\pi^2 k \sum_{s=2}^{3} \sum_{n=-\infty}^{\infty} \int_0^k [|f_{sn}^+|^2 + |\alpha_s f_{sn}|^2 + 2\mathrm{Re}(\alpha_s f_{sn}^- f_{sn}^{+*})] \frac{I^2 dl}{m} = R_1 I_0^2. \quad (1)$$

The stream of active power that passes through the plane which is located below the emitter, but above the earth's surface:

$$P_2 = 60\pi^2 k \sum_{s=2}^{3} \sum_{n=-\infty}^{\infty} \left[\int_0^k (1 - |\alpha_s|^2) |f_{sn}^-|^2 \frac{I^2 dl}{m} + \int_k^{\infty} \mathrm{Im}\, \alpha_s |f_{sn}^-|^2 \frac{I^2 dl}{\sqrt{l^2 - k^2}} \right] = R_n I_0^2. \quad (2)$$

In these expressions

$$f_{sn}^{\pm} = \frac{1}{2\pi I^2} \int \vec{i} \vec{A}_{sn}^{\pm *} \rho \, d\rho \, d\varphi \, dz. \quad (3)$$

--coefficients of expansion of the vector potential of the assigned distribution of the current density vector $\dot{i}$ in the system of orthogonal vector functions $A^{\pm}_{sn}$ which form a discrete spectrum of azimuth harmonics with different n and noncontinuous spectrum of waves with different angles ϑ=arc cos l/k (including the complex with l > k) between the wave perpendicular and the plane of the horizon. The remaining designations have the following meaning:

$$z_1 = \frac{m - m_1}{m + m_1}, \quad z_2 = \frac{\bar{\varepsilon} m - m_1}{\bar{\varepsilon} m + m_1}, \tag{4}$$

$$m = \sqrt{k^2 - l^2}, \quad m_1 = \sqrt{\bar{\varepsilon} k^2 - l^2}, \quad \bar{\varepsilon} = \varepsilon + i\beta,$$

$$\beta = 60\sigma\lambda, \quad k = 2\pi/\lambda,$$

λ--wavelength.

We assume that the vector of current density has only a radial projection which is assigned by the product of two functions

$$i_\rho = I_0 f_1(\rho) f_2(\varphi), \tag{5}$$

where I_0--effective value of the current at the inlet of the emitting system.

Since $i_\phi = i_z = 0$, then we need the projections $\dot{A}_{sn}$ only on the ρ axis:

$$A^{\pm}_{2n\rho} = \frac{in}{\rho} J_n(l\rho)\, e^{\pm imz}\, e^{\pm in\varphi}, \tag{6}$$

$$A^{\pm}_{3n\rho} = \pm \frac{im}{k} \frac{d}{d\rho} J_n(l\rho)\, e^{\pm imz}\, e^{in\varphi}. \tag{7}$$

Then the coefficients f_{sn} can be written as follows:

$$f^{\pm}_{2n} = -in \frac{e^{\pm imh}}{2\pi l^2} \Phi_n T_{2n} I_0, \tag{8}$$

$$f_{3n} = \pm \frac{im}{k} \frac{e^{\pm imh}}{2\pi l^2} \Phi_n T_{3n} I_0, \tag{9}$$

where

$$\Phi_n = \int_0^{2\pi} f_{2n}(\varphi)\, e^{-in\varphi}\, d\varphi, \tag{10}$$

$$T_{2n} = \int_0^{l} f_1(\rho) J_n(l\rho)\, d\rho, \tag{11}$$

$$T_{3n} = \int_0^{l} f_1(\rho) \frac{d}{d\rho} J_n(l\rho)\, \rho\, d\rho. \tag{12}$$

We further assume that the normed distribution of ...ent density along the vibrators has the appearance of a standing wave:

$$f_1(\rho) = \frac{1}{\rho} \frac{\sin k_1 (L - \rho)}{\sin k_1 L}, \qquad (13)$$

where $k_1 = \eta k$, η--shortening of the vibrator.

This case does not take into consideration the non-inphase nature and damping of the amplitude of current distribution along the vibrator which are associated with radiation. However, these effects are comparatively small for electrically short vibrators.

Normed azimuth distribution of the current density for an odd number of vibrators is assigned in the form

$$f_2(\varphi) = \begin{cases} +1/N \varphi_0 \text{ with } \varphi_{i1} < \varphi < \varphi_{i2}, \\ -1/N \varphi_0 \text{ with } \pi + \varphi_{i1} < \varphi < \pi + \varphi_{i2}, \\ 0 \qquad \text{outside current vectors} \end{cases}$$

where $$\varphi_{i1} = i\varphi_1 - \varphi_0/2, \quad \varphi_{i2} = i\varphi_1 + \varphi_0/2, \qquad (14)$$

i--number of vibrator.

In computing (10) with regard for (14) we have for odd azimuth harmonics

$$\Phi_n = \frac{4}{n\varphi_0 N} \sin \frac{n\varphi_0}{2} \frac{\sin Nn\varphi_1/2}{\sin n\varphi_1/2}. \qquad (15)$$

For n even $\Phi_n = 0$.

It can be shown that (15) is correct even for an even number of vibrators.

In order to compute T_{2n} we use the presentation of Besselian functions through the producer

$$e^{(W - 1/W)z/2} = \sum_{k=-\infty}^{\infty} J_k(z) W^k. \qquad (16)$$

Assuming the argument of the producer function $W = e^{i\chi}$, we have the known correlation

$$\sin(z \sin \psi) = 2 \sum_{i=0}^{\infty} J_i(z) \sin(2i + 1)\psi, \qquad (17)$$

while assuming $W=ie^{\chi}$;

$$\sin(z\operatorname{ch}\chi) = 2\sum_{i=0}^{\infty}(-1)^i J_{2i+1}(z)\operatorname{ch}(2i+1)\chi. \qquad (18)$$

By transforming the numerator of (13) with $1>k_1$ with the help of (17), and with $1>k_1$ with the help of (18), and by using the known formula

$$\int_0^a J_n(x)\,J_m(a-x)\,\frac{dx}{x} = \frac{1}{n}\,J_{n+m}(a), \qquad (19)$$

we obtain the following series for T_{2n}:

$$T_{2n} = \frac{2}{n}\sum_{i=0}^{\infty} t_{2i+1}\,J_{n+2i+1}(lL), \qquad (20)$$

where $t_{2i+1} = \sin(2i+1)\psi$, $\psi = \arcsin k_1/l$, if $1>k_1$ and $t_{2i+1} = (-1)^i \operatorname{ch}(2i+1)\chi$, $\chi = \ln\left[\frac{k_1}{l} + \sqrt{\left(\frac{k_1}{l}\right)^2 - 1}\right]$, if $1<k_1$.

We similarily obtain

$$T_{2n} = 2\frac{k_1}{l}\left[\sum_{i=0}^{\infty}(-1)^i J_{n+2i+1}(lL) + 2\sum_{j=1}^{\infty} u_{2j} \times \right.$$
$$\left. \times \sum_{i=0}^{\infty}(-1)^i J_{n+2j+2i+1}(lL)\right], \qquad (21)$$

where $u_{2j}=\cos 2j\psi$ with $1>k_1$ and $u_{2j}=(-1)^j \operatorname{ch} 2j$ with $1<k_1$.

The substitution of (20) and (21) into (8) and (9) and further in (1)-(2) provides an accurate solution to the set task in the form of the sum of single integrals which can be numerically found.

We now obtain the calculated ratios after making certain permissible approximations.

Radiation Impedance

In computing R_{Σ}, the integration variable 1 does not exceed k. If the electric length of the vibrator $k_1 l$ is not more than 115°, then the argument of the Besselian functions in (20) and (21) does not exceed 2. Following [5,6] we replace $J_n(lL)$ with the first term in the exponential series expansion:

$$J_n(lL) = \left(\frac{lL}{2}\right)^n \cdot \frac{1}{n!}. \qquad (22)$$

In addition, since in the region which is important for the integration, $k_1 l = ch\ x >> 1$, then the approximation is permissible

$$ch\, jx \approx 2^{l-1}(ch\, x)^l. \qquad (23)$$

By using (22) and (23), we have

$$|f_{21}| = |f_{2,-1}| = q_1 \frac{L}{4\pi l}, \quad |f_{31}| = |f_{3,-1}| = \frac{ml}{k}|f_{21}|,$$

where
$$q_1 = \frac{\Phi_1}{2} \frac{k_1 L}{\sin k_1 L}\left[1 - \frac{(k_1 L)^2}{12} + \frac{(k_1 L)^4}{360} - \ldots\right], \qquad (24)$$

and, taking into consideration only the terms with $|n|=1$, we obtain for the radiation impedance

$$R_\Sigma = 10q^2k^2L^2\left\{1 + \frac{3}{4}\int_0^1\left[|\alpha_2|^2 + 2\cos 2mh\, \mathrm{Re}\,\alpha_2 - 2\sin 2mh\, \mathrm{Im}\,\alpha_2 + \right.\right.$$
$$\left.\left. + \frac{m^2}{k^2}(|\alpha_3|^2 - 2\cos 2mh\, \mathrm{Re}\,\alpha_3 + 2\sin mh\, \mathrm{Im}\,\alpha_3)\right] d\left(\frac{m}{k}\right)\right\}. \qquad (25)$$

We will also present the reflection coefficients in the form of a series

$$\alpha_2 = -1 + \frac{2r}{1!}\frac{m}{k} - \frac{4r^2}{2!}\left(\frac{m}{k}\right)^2 + \frac{6r^3}{3!}\left(\frac{m}{k}\right)^3 - \frac{30r^5}{5!}\left(\frac{m}{k}\right)^5 + \ldots, \qquad (26)$$

$$\alpha_3 = \frac{\sqrt{\varepsilon - 1}}{\sqrt{\varepsilon + 1}}\left[1 + \frac{2}{\sqrt{\varepsilon}}\left(\frac{m}{k} - 1\right) - \ldots\right], \qquad (27)$$

where $r = p + iq = 1 / \sqrt{\varepsilon - 1}$.

In computing the radiation impedance, one can be limited to two terms in (26) and one in (27). Then computation (25) yields

$$R_\Sigma = 10q_1k^2L^2\left\{\frac{1}{|\sqrt{\varepsilon} - 1|} + \left(\frac{1 + \mathrm{Re}\sqrt{\varepsilon}}{|\sqrt{\varepsilon}| + 1 + 2\mathrm{Re}\sqrt{\varepsilon}}\right)^2 + \frac{3}{2}\left[1 - \frac{\sin\xi}{\xi} + \right.\right.$$
$$+ 2p\left(\frac{\sin\xi}{\xi} + \frac{\cos\xi - 1}{\xi^2} - \frac{1}{2}\right) - 2q\left(\frac{\sin\xi}{\xi^2} - \frac{\cos\xi}{\xi}\right) +$$
$$\left.\left. + \mathrm{Re}\frac{\sqrt{\varepsilon - 1}}{\sqrt{\varepsilon + 1}}\left(\frac{1}{3} - 2\frac{\cos\xi}{\xi^2} - \frac{\sin\xi}{\xi^2} + 2\frac{\sin\xi}{\xi^3}\right)\right]\right\}. \qquad (28)$$

where $\xi = 2kh$.

If $|\bar{\varepsilon}| \gg 1$, then with height of the suspension approaching zero, (28) becomes

$$R_\Sigma = 20 q_1^2 k^2 L^2 / |\bar{\varepsilon}|, \qquad (29)$$

i.e., for short $\left(k_1 L < \frac{\pi}{8}\right)$ and thin ($q_1 \to 8$) vibrators, formula (29) has the appearance of Rudenberg's formula with a numerical coefficient that is reduced because of the influence of the ground.

In another extreme case, with $h \to \infty$ and $\bar{\varepsilon} \gg 1$

$$R_\Sigma = 18{,}3 q_1^2 k^2 L^2. \qquad (30)$$

In particular, for a thin half-wave vibrator $R_\Sigma = 73.5$ Ohm.

Consideration for the subsequent terms in the series (22), (23), (26) and (27), as well as the terms with $|n| > 1$ yields multipole components of radiation resistance which are proportional to $(kL)^4$, (kL^6)..., whose quantity is small for short vibrators.

Loss Impedance

The dipole component of losses for radiation into the ground of waves which have in the ground an angle of inclination of the wave perpendicular in limits from $\vartheta = 90°$ to $\vartheta_1 = \arccos |\bar{\varepsilon}|^{-\frac{1}{2}}$ is determined by the terms with $|n| = 1$ in the first term of (2). By computing under the same conditions, as in the computation of R_Σ, we have

$$R_l = 10 q_1^2 k^2 L^2 \left[\frac{3}{2} \operatorname{Re} \frac{1}{\sqrt{\bar{\varepsilon} - 1}} - \frac{1}{|\bar{\varepsilon} - 1|} + \frac{1}{4} \left(1 - \left| \frac{\bar{\varepsilon} - 1}{\bar{\varepsilon} + 1} \right| \right) \right]. \qquad (31)$$

The results of the computation according to formula (31) coincide with the results obtained in [5] by numerical integration.

For ground with $|\bar{\varepsilon}| \gg 1$, formula (31) becomes

$$R_l = 21{,}7 q_1^2 k^2 L^2 |\bar{\varepsilon}|^{-1/2}. \qquad (32)$$

The losses associated with the dipole waves are emitted into the ground with slipping angles in the ground from $\vartheta = \vartheta_1$ to $\vartheta = 0$. They are determined by the terms with $|n| = 1$ in the second term (2) in the

interval of integration $k<l<k\sqrt{\varepsilon}$:

$$R_{II} = 240\pi^2 k^4 \int_k^{k\sqrt{\varepsilon}} (|f_{21}|^2 \operatorname{Im} \alpha_2 + |f_{31}|^2 \operatorname{Im} \alpha_3) \frac{l^3\,dl}{l^2 - k^2}. \qquad (33)$$

Since in this case $l>k$, then a larger number of terms is needed in the series (26) to approximate α_2. In the interval $0<\nu<\sqrt{\varepsilon-1}$ four terms provide sufficient accuracy:

$$\operatorname{Im} \alpha_2 = 2p\nu + 2pq\nu^2 - (p^3 + 3pq^2)\nu^3, \qquad (34)$$

where $\nu = \sqrt{l^2-k^2}/k$.

For $\operatorname{Im}\alpha_3$ in the interval $0<\nu<|\varepsilon-1|^{-\frac{1}{2}}$, the following expression yields satisfactory accuracy:

$$\operatorname{Im} \alpha_3 = 2\nu \operatorname{Re}\left(\varepsilon / \sqrt{\varepsilon - 1}\right), \qquad (35)$$

and in the interval $|\varepsilon-1|^{-1/2} < \nu < |\varepsilon-1|$ —

$$\operatorname{Im} \alpha_3 = 0{,}8 / \nu |\sqrt{\varepsilon - 1}|. \qquad (36)$$

To simplify the computations, we assume that (36) is correct for the entire interval $0-1\sqrt{\varepsilon-1}$, which yields a result which is exaggerated by several percentages. Computation of (33) with regard for (34) and (36), bearing in mind that

$$|f_{21}| = q_1 \frac{L}{2\pi l} e^{-t\nu}, \quad |f_{31}| = \nu |f_{21}|, \qquad (37)$$

yields

$$\begin{aligned} R_{II} = 15 q_1^2 k^4 L^2 \{ & (2p + 0{,}8|\varepsilon - 1|^{-1/2}) [1 - (1 + t) e^{-t}] \xi^{-3} + \\ & + 2pq [2 - (2 + 2t + t^2) e^{-t}] \xi^{-4} - (p^3 - 3pq^2) \times \\ & \times [6 - (6 + 6t + 3t^2) e^{-t}] \xi^{-5} \}, \end{aligned} \qquad (38)$$

where $t = \xi\sqrt{\varepsilon-1}$.

In contrast to the expression obtained in [6], expression (38) yields a final result even with $h \to 0$. The difference is explained by the fact that the approximation adopted in [6] $\operatorname{Im}\alpha_3$ with $l=k$ yields a

divergent result, while in reality $\mathrm{Im}\alpha_3 \to 0$ with $l \to k$.

For a short vibrator located on the surface of the ground without losses, on the condition that $\varepsilon \gg 1$, formula (38) becomes

$$R_{II} = 17{,}3k^2L^2 \left| \frac{}{} - 1. \right. \qquad (39)$$

A similar formula was obtained in [3] for the input impedance of an infinitely small dipole lying on the interface of the dielectric and the air. The numerical coefficient in [3] is larger than in (39), as a result of the fact that the current distribution is assumed to be rectangular, as here, and not sinusoidal.

For low-conducting ground, the component R_{II} mainly determines the input impedance. However, in the case of a semi-conducting ground, the induction losses are dominant. They are determined by the remaining part of the second term in (2).

We will designate

$$R_{III} = 240\pi^2 k \sum_{n=1}^{\infty} \int_k^{\infty} |f_{2n}^-|^2 \operatorname{Im} z_2 \frac{l^3 dl}{\sqrt{l^2 - k^2}}, \qquad (40)$$

$$R_{IV} = 240\pi^2 k \sum_{n=1}^{\infty} \int_k^{\infty} |f_{3n}^-|^2 \operatorname{Im} z_3 \frac{l^3 dl}{\sqrt{l^2 - k^2}}. \qquad (41)$$

As is apparent from (20) and (21), the value of any of the functions T_{sn} is negligible until the argument lL exceeds the least of the indices of the Besselian functions which are included in the formulas. In the transition of the argument through the value $lL=n$, the value of the function drastically rises, and with a further rise in the argument, it fluctuates around a certain average value.

By using the threshold nature of change in the functions T_{sn}, we replace them by exponential functions equal to zero at $lL<n$, and with $lL> n$, equal to the average value of T_{sn} during the period of change in $I_n(lL)$:

$$T_{1n} \approx \frac{1}{n} - \frac{q_2}{lL}, \quad T_{3n} \approx \frac{q_2}{lL} + \frac{\kappa_1^2 n}{l^3}, \qquad (42)$$

where $q_2 = k_1 L \operatorname{ctg} k_1 L$.

The rapidly changing function $|\phi_n|^2$ is also approximately replaced by its average value, equal to 4 in the interval $0<n<\pi/2N\phi_1$, equal to $4/N$ in the interval $n_1<n<n_2=2/\phi_0$ and close to 0 with $n>n_1$.

For $\mathrm{Im}\alpha_2$ the relative error on the order of 5% is yielded for the semi-conducting ground by the approximation:

$$\mathrm{Im}\,\alpha_2 \approx e^{-1.43/|\sqrt{\varepsilon}|} - e^{-3.2/|\sqrt{\varepsilon}|}. \qquad (43)$$

For the approximation $\mathrm{Im}\alpha_3$ we use the asymptotic value:

$$\mathrm{Im} = \frac{2\beta}{(\varepsilon+1)^2+\beta^2}. \qquad (44)$$

Since the terms in the sum in (40)-(41) differ little from each other, we will replace the summation by an integration according to the formula

$$\sum_{a}^{\infty} f(x) = \frac{1}{H}\int_{a-H/2}^{\infty} f(x)\,dx, \qquad (45)$$

where H--summation spacing equal in our case to two. We will further change the order of integration

$$R_{III} = 240k\left[\frac{N-1}{N}\int_{1/L}^{n_0/L} dl\int_{0}^{lL} f(n,\ l)\,dn + \frac{1}{N}\int_{1/N}^{n_0/L} dl\int_{0}^{lL} f(n,\ l)\,dn\right], \qquad (46)$$

where

$$f(n,\ l) = \left(e^{-akv} - e^{-bkv}\right)\left(1 - \frac{nq_2}{lL}\right)\frac{1}{\sqrt{1+v^2}},$$

$$a = 2h + 0{,}226\lambda_3,\ b = 2h + 0{,}495\lambda_3,\ \lambda_3 = \lambda/|\sqrt{\varepsilon}|.$$

In the expression $\sqrt{1+v^2}$, we ignore the 1 which yields a slight error for short vibrators (kL<1) since the lower limit of integration for l is considerably greater than k. For longer vibrators, this ignoring yields a somewhat exaggerated value of the losses. Finally,

$$R_{III} = 120kLq_3\left\{\frac{N-1}{N}\left[\mathrm{Ei}\left(-\frac{\pi a}{2ND}\right) - \mathrm{Ei}\left(-\frac{\pi b}{2ND}\right) - \right.\right.$$
$$- \mathrm{Ei}\left(-\frac{a}{L}\right) + \mathrm{Ei}\left(-\frac{b}{L}\right)\Big] + \frac{1}{N}\left[\mathrm{Ei}\left(-2\,\frac{a}{d}\right) - \right.$$
$$\left.\left. - \mathrm{Ei}\left(-2\,\frac{b}{d}\right) - \mathrm{Ei}\left(-\frac{a}{L}\right) + \mathrm{Ei}\left(-\frac{b}{L}\right)\right]\right\}. \qquad (47)$$

where $q_3 = 1 - q_2 + q_2^2/3$.

The component R_{IV} is found in exactly the same way:

$$R_{IV} = \frac{120 q_4}{kL} \frac{\beta}{(\varepsilon+1)^2+\beta^2} \left\{ \frac{N-1}{N} \left[\mathrm{Ei}\left(-\frac{\pi h}{2ND}\right) - \mathrm{Ei}\left(-\frac{2h}{L}\right) \right] + \right.$$
$$\left. + \frac{1}{N} \left[\mathrm{Ei}\left(-\frac{4h}{d}\right) - \mathrm{Ei}\left(-\frac{2h}{L}\right) \right] \right\}. \qquad (48)$$

where $q_4 = q_2^2 + (k_1 L)^2 q_3 + (k_1 L)^4/3$.

Discusssion of Results

The component R_{III} is negligble for a single vibrator shorter than λ_3 and also if the height of its suspension significantly exceeds λ_3. If the length of the vibrator is much greater than the wavelength in the ground, then, assuming that L>>b, and by using the approximation Ei(-x)=ln 1.78x, we find

$$R_{III} = 592 \frac{L}{\lambda} q_3 \left\{ 1 + 1{,}275 \left[\mathrm{Ei}\left(-\frac{0{,}45\lambda_3 + 4h}{d}\right) - \mathrm{Ei}\left(-\frac{\lambda_3 + 4h}{d}\right) \right] \right\}. \qquad (49)$$

For a thin vibrator, whose height of the suspension and the diameter (width) are much smaller than λ_3, formula (50) can be simplified even more:

$$R_{III} = 2Lq_3 \frac{296}{\lambda}. \qquad (50)$$

The last cofactor in (50) is the linear impedance of successive losses of the conductor of infinite length. Consequently, the component R_{III} is mainly determined by the successive losses of the vibrator.

The cofactor q_3 depends on the shape of the current distribution. For a short vibrator with triangular distribution, $q_3 = 1/3$. For a half-wave vibrator, $q_3 = 1$.

The component R_{IV} for a single vibrator with $\beta >> \varepsilon$ and $h \to 0$:

$$R_{IV} = \frac{2}{\pi \sigma L} q_4 \ln \frac{2L}{d} \qquad (51)$$

and is known from the theory of grounding electrodes as the impedance of spreading for a dipole made of uninsulated conductors placed on the surface of the ground. With $\beta >> \varepsilon$ and $k_1 L << 1$, this component does

not depend on the frequency, and consequently, is a constant component of losses.

Thus, all the components of the input impedance of the vibrator are found by a single method. In this case, in contrast to those known in the literature, dependences are obtained for all the components on the height of the suspension, the width of the vibrator and its length which are also correct for the limiting values of these parameters.

The components R_Σ and R_1 for low-set antennas are generally smaller than the others.

The component R_{II} prevails when the length of the vibrator is smaller than the length of the wave in the ground. If the length of the vibrator is considerably greater than λ_3 then the component R_{III} becomes dominant. The component R_{IV} has a noticeable value where the height of the suspension is commensurate with the width of the dipole even above dry ground when ε and β have one order. Generally, with an increase in the height of the suspension, the constant component diminishes considerably faster than the others.

The components R_Σ, R_I and R_{II} depend on the width of the vibrator as $\Phi_1^2 \cdot (2L/d)^2 \sin^2 d/2L$, i.e., very weakly. The dependence of R_{III} on the vibrator width has a completely different nature.

Calculations according to formula (49) show that the input impedance of a fairly long vibrator drops as its width increases as if it consisted of N mutually isolated vibrators. The number N is determined by the number of half-waves in the ground which is laid along the width in the middle of the vibrator arm.

The fact that parallel, low-set vibrators, separated by a half-wave in the ground, can be considered isolated, is known. Such an assertion is proved for vibrators which intersect at one point with the help of formula (47) with $N \neq 1$.

In fact, for vibrators with length much greater than λ_3, the component R_{III} dominates. Then the dependence of the input impedance on the distance between the ends of the dipoles, computed according to formula (47) with $h \ll \lambda_3$ has the appearance shown in fig. 2.

It is apparent in fig. 2 that the vibrators can be considered completely isolated, then $D/\lambda_3 > 3$. In this case, the input impedance of the system $R_{вх\ N}$ is N times smaller than the impedance of a single

vibrator $R_{вх\ 1}$.

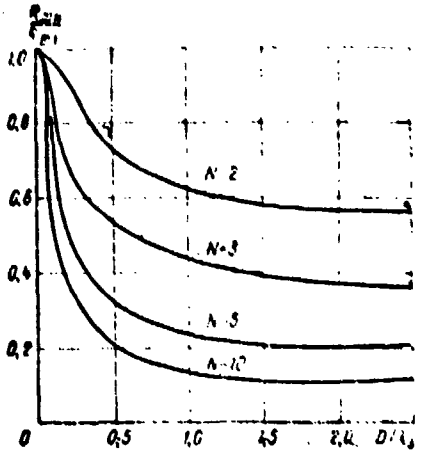

Figure 2.

If the distance between the ends of the vibrators equals the length of the wave in the ground, then the input impedance of the system roughly equals

$$R_{вхN} = \frac{R_{вх1}}{N}\left(1 + 0{,}4\,\frac{N-1}{N}\right). \qquad (52)$$

The presence of a second term in the parentheses is explained by the coupling impedance. For the case of two intersecting vibrators, whose ends are separated by $\lambda_з$, the coupling impedance increases the input impedance by 20% as compared to the case of complete isolation.

With an increase in the number of vibrators, the coupling impedance increases somewhat, and as a result, the input impedance of the array made of a large number of vibrators whose ends are separated by $\lambda_з$ is roughly equal to $R_{вхN} = 1.4\ R_{вх1}/N$.

The condition $D \geq \lambda_з$ can be considered a criterion for designing the array made of intersecting low-set vibrators above semiconducting ground.

Examples

We will take as the first example the dependence already examined in [4] and [6] of the input impedance of a single half-wave vibrator on the height of the suspension with $\lambda = 5$ m.

In figure 3, curves 1 and 2 show the calaculated dependences which

were taken from [4]. Curve 1 is calculated by the method of directed emf for ground with $\varepsilon=10$, $\sigma=10^{-2}$ mho/m. Curve 2 was computed by the Hansen-Bekerly method [6] for ground with $\varepsilon=7$, $\sigma=2.8 \times 10^{-2}$ mho/m, but without consideration for the R_{III} and R_{IV} components. Curve 3 was

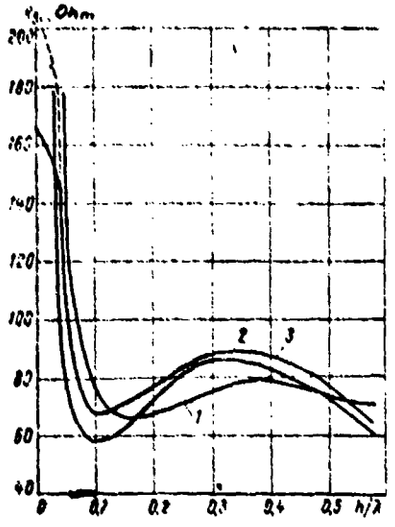

Figure 3.

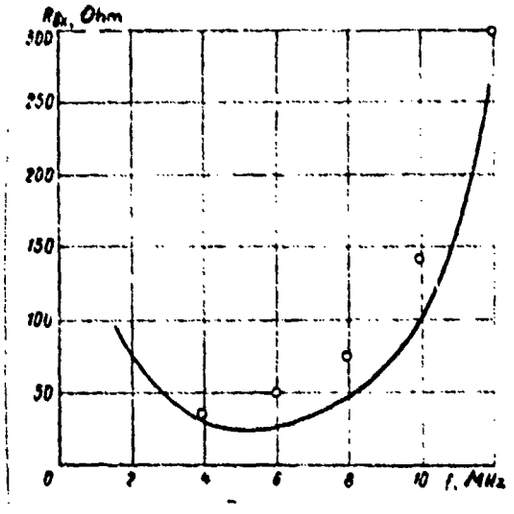

Figure 4.

computed with the help of formula (28), (31), (38), (47) and (48) for ground with $\varepsilon=10$ and $\sigma=10^{-2}$ mho/m. The shortening was determined by

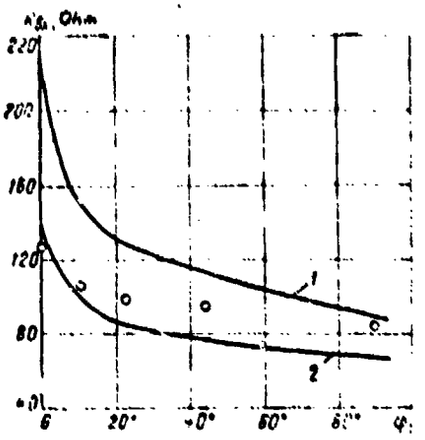

Figure 5.

the technique presented in [2]. The dotted line shows the calculated curve obtained on the assumption that $\eta=1$.

Comparison shows that with $h>0,1\lambda$, the course of all the curves is roughly the same, and curves 1 and 3 almost coincide. However, with low heights of the suspension, the curves significantly differ, and calculation by the formulas presented here yields finite values of the input impedance. This really occurs in practice.

We will examine as a second example the dependence on the frequency of the input impedance of a three-beam antenna (N=3) located on the surface of the ground with $\varepsilon=5$, $\sigma=10^{-4}$. The calculation was made according to the five formulas indicated above for the case h=0. The length of the vibrator arm L=4.2 m, diameter of the conductor d=10 mm. Shortening was assumed to be equal to $\eta=|\sqrt{\varepsilon}|$. The aperture angle between the extreme beams is $2\phi_1=60°$.

In figure 4, the solid line shows the calculated dependence of the input impedance on the frequency in the range 2-12 MHz. The points on fig. 4 show the values of the input impedance measured in the summer. The prototype was made from RK-3 cable placed on the surface of the ground (dry sand) and slightly sprinkled with sand from above.

As the last example we will examine the dependence of the input impedance of a two-beam antenna on the angle between the vibrators ϕ_1.

The calculation was made for the system made of two vibrators 2L= 2 x 150 m long placed at a height of 10 mm above the ground with

frequency of 360 kHz.

Shortening according to the experimental data was assumed to be equal to $n=1.37$. The calculation results are shown in fig. 5. Curve 1 was obtained for ground $\varepsilon=7$, $\sigma=10^{-3}$ moh/m, curve 2 for ground $\varepsilon=10$, $\sigma=10^{-3}$ moh/m.

The points show the measured values. The vibrators were made of BPVL conductor 2.5 mm^2, freely placed on the surface of the ground. The measurements were made in winter.

We note that the dependence $R_{вх}=j(\phi_1)$ can be used to measure the conductance of the ground in the medium wavelength region.

Conclusions

The Hansen-Bekerly method makes it possible to obtain all components of the input impedance of low-set vibrators without exception. In contrast to others, this method yields a final result which agrees with the experiment even for heights of the suspension close to zero.

Mutual impedance between the intersecting low-set dipoles is low if the distance between their ends exceeds the wavelength in the ground.

Bibliography

1. Kontorovich, M. I. "Equivalent Parameters of a Conductor," Trudy VETAS, No. 6, 1944.

2. Braude, B. V. "Electromagnetic Field of a Conductor Located on the Axis of a Cylindrical Cavity in a Semiconducting Medium," Byulleten' elektropromyshlennosti Leningrada, No. 9-10, 1946.

3. Wait, J. R. "Impedance of Radiation of a Dipole Located on the Interface of Two Dielectrics," Can. J. of Ph., 1, 34, No. 1, 1956.

4. Lavrov, G. A.; and Knyazev, A. S. Prizemnyye i podzemnyye antenny ["Near-earth and Underground Antennas"], Izd-vo Sovetskoye radio, 1965.

5. Istrashkin, A. D. "Calculation of Antenna Impedance with Regard for Electrical Parameters of the Ground," Trudy VETAS, No. 12, 1946.

6. Baranov, M. M. "Impedance of Radiation of Horizontal Vibrator Located on the Surface of the Ground," Izvestiya KPI, Vol. 16, 1954.

7. Braude, B. V. "Method of Calculating Complete Active Impedance of Antenna with Regard for Finite Conductance of the Ground," Radiotekhnika, Vol. 1, No. 5, 1946.